ALERT Geomaterials

Alliance of laboratories in Europe for Research and Technology
Aussois, September 29 – October 01, 2025

36th ALERT Workshop / POSTER SESSION

Booklet of abstracts

Editors: Nadia Benahmed
Antoine Wautier
(INRAE, France)

ALERT Geomaterials

The Alliance of Laboratories in Europe for Education, Research and Technology

36th ALERT Workshop

Poster Session

Aussois 2025

Editors:

Nadia Benahmed
Antoine Wautier

(INRAE, Aix-en-Provence – France)

ISBN: 978-2-9584769-5-3

Dear colleagues,

We are pleased to welcome you to Aussois and to our 36th ALERT Workshop and School.

As always, it is an exciting time for us to continue to meet and bring together inspired people for fruitful days with interesting, stimulating discussions, exchange of knowledge and experience on Geomechanics. Presentations of recent advances offer the chance to get up-to-date and to remain at the cutting edge.

We would like to express our thanks to all of you who contributed to the success of this poster session. The number of received posters this year is growing year by year with 59 contributions this year gathering contributors from 19 countries (Czech Republic, Finland, France, Belgium, Germany, Austria, Australia, Canada, Italia, Japan, Spain, The Netherlands, Chile, China, Colombia, Norway, Switzerland, UK, USA) and belonging to 56 different research institutions. They are summarized in the histogram below together with the corresponding number of posters (>1).

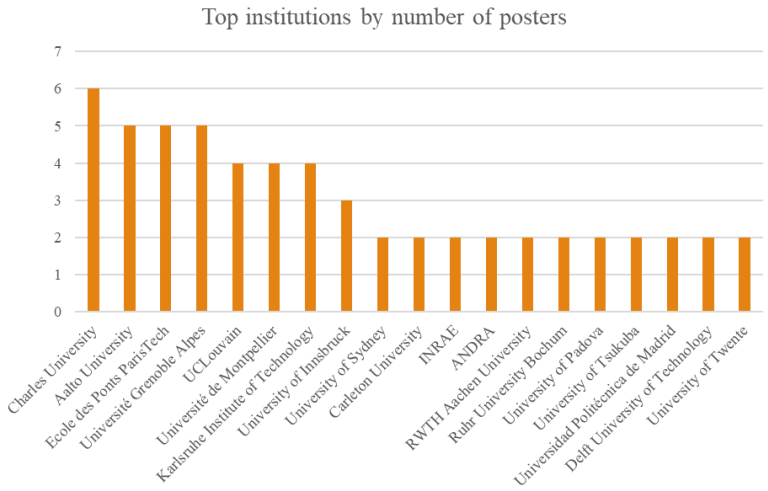

The posters cover numerical, experimental and analytical approaches and mostly consider sand clays or rock material with the following repartition.

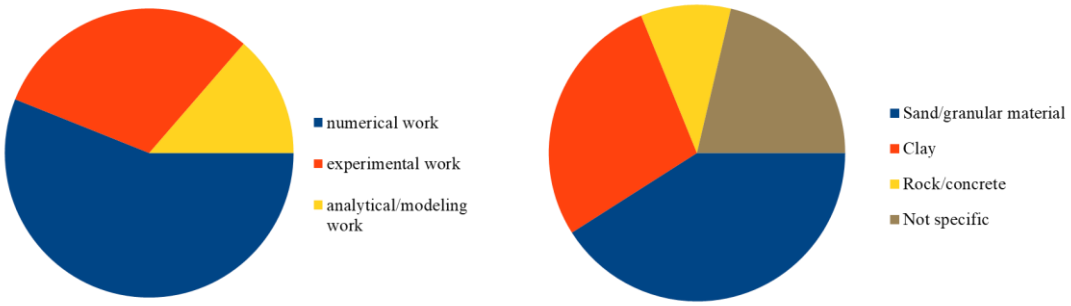

Eventually, we can propose the following analysis, gathering the abstracts by selected (but necessarily biased) key words. This gives an idea of the current hot topics in geomechanics.

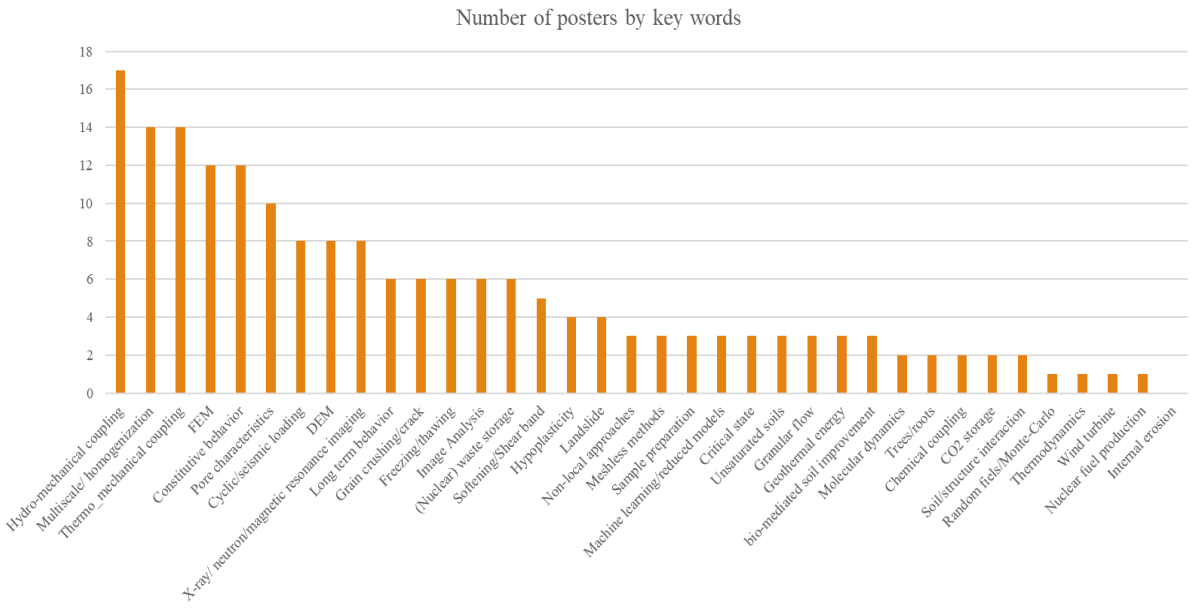

28 posters were eligible for the poster competition 2025. The Poster Prize was granted to:

Jungfeng REN (ENPC) & Retief LUBBE (University of Twente)

for their posters entitled respectively

"Laboratory and numerical investigation on the poro-elasto-visco plastic behaviour of in-situ heated Callovo-Oxfordian claystone"

And

"A Physically Consistent Unification of Critical State Soil Mechanics and the μ(I)-φ(I) rheologies"

Congratulation also to the third nominee, ***Max WINKELMANN (University of Twente, The University of Edinburgh)*** *for his poster of excellent quality.*

Looking forward to see you next year in Aussois!

Kind regards,

Nadia Benahmed and Antoine Wautier.

Table of contents

Improving Bearing Capacity of a Model Foundation Using Microbially Induced Calcite Precipitation

Hanieh Babaeizad, Wiebke Baille, Torsten Wichtmann

Ruhr University Bochum, Universitätsstr. 150, 44801, Bochum, Germany

hanieh.babaeizad@rub.de, wiebke.baille@rub.de, torsten.wichtmann@rub.de

Keywords: Microbially Induced Calcite Precipitation (MICP), bio-mediated soil improvement, Sporosarcina pasteurii, cementation solution, model foundations

Abstract

Microbially Induced Calcite Precipitation (MICP) through the hydrolysis of urea is a promising bio-mediated soil improvement method with applications in different geotechnical areas. The method has the potential to enhance the mechanical properties of sandy soils with different characteristics through the formation of calcite bridges between the soil grains. Although previous studies have demonstrated the success of MICP in significantly enhancing the stiffness and shear strength of sandy soils at small scales, some challenges remain regarding its application under different field conditions.

This study focuses on preliminary model tests to assess strategies to efficiently improve the bearing capacity of a foundation using the MICP method. The model experiment was performed in a 56 × 36 × 30 cm box filled with fine sand, with a 4 × 4 × 1.5 cm model foundation placed at the surface. The soil was treated with the injection of the bacterial strain Sporosarcina pasteurii, followed by three injection cycles of a cementation solution, composed of urea, calcium chloride, and ammonium chloride. Each cycle involved the application of 1.2 pore volumes of solution at 24-hour time intervals. The injection and extraction of bacterial and cementation solutions were carried out under three different conditions to identify the most effective treatment strategy.

The stiffness changes were determined non-destructively during each treatment through shear wave velocity measurements via bender elements installed at two different depths below the foundation. Moreover, pH was monitored on aqueous samples from the pore fluid before and after each injection to confirm successful urea hydrolysis. The load-settlement curves of the model foundation on both uncemented and cemented soil were measured using a load press (Fig.1 (a-b)) and a displacement transducer. The impact of cementation on the bearing capacity was investigated by a comparison between the model test results from the uncemented and cemented soils.

Results showed that MICP could enhance the bearing capacity of the model foundation considerably (Fig. 2) even at low cementation levels. A direct correlation was observed between shear wave velocity and post-treatment calcite content, with an approximate increase up to a shear wave velocity of 280 m/s for 9% calcite content. Additionally, pH levels during the cementation cycles dropped to approximately 7.5 after injection and rose to around 8.7 by the end of the retention period, confirming effective carbonate precipitation in soil pores.

The obtained results generally demonstrate the potential of the MICP method for larger scale geotechnical applications, including the improvement of foundations. However, further optimizations regarding the material usage, minimizing byproducts, and consideration of more challenging field conditions will be crucial in future larger scale trials.

Figures

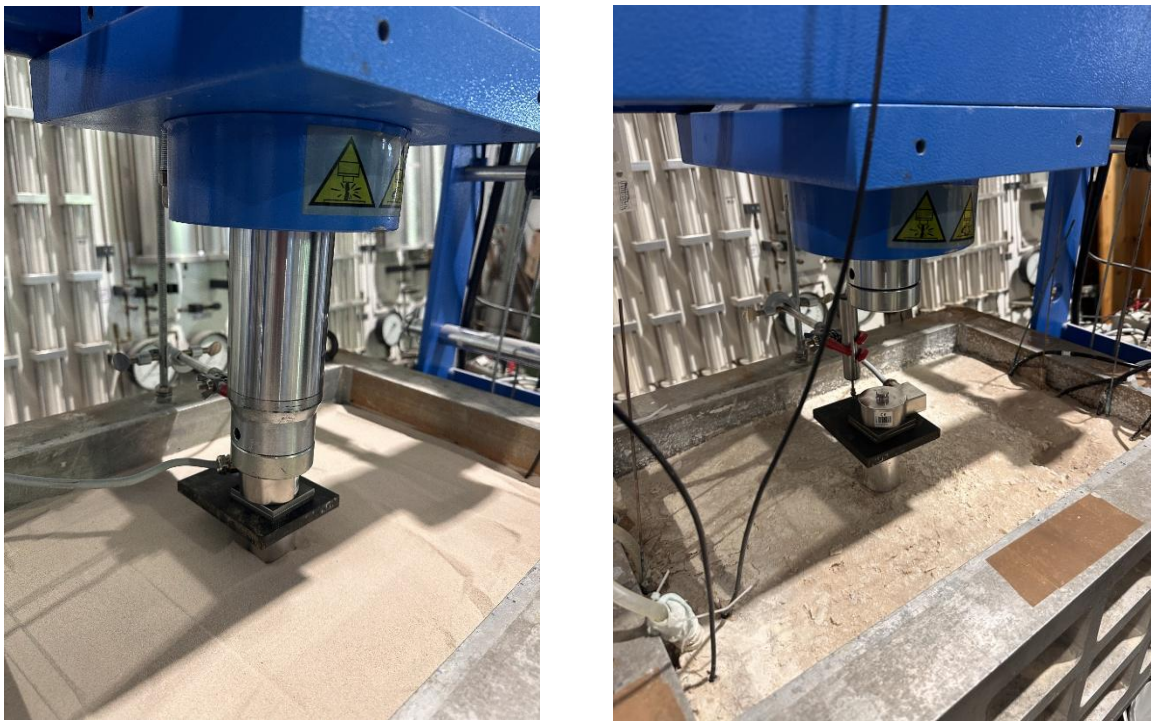

Figure 1: *Measurement of load-settlement curves for the model foundation on (a) uncemented, and (b) cemented sand.*

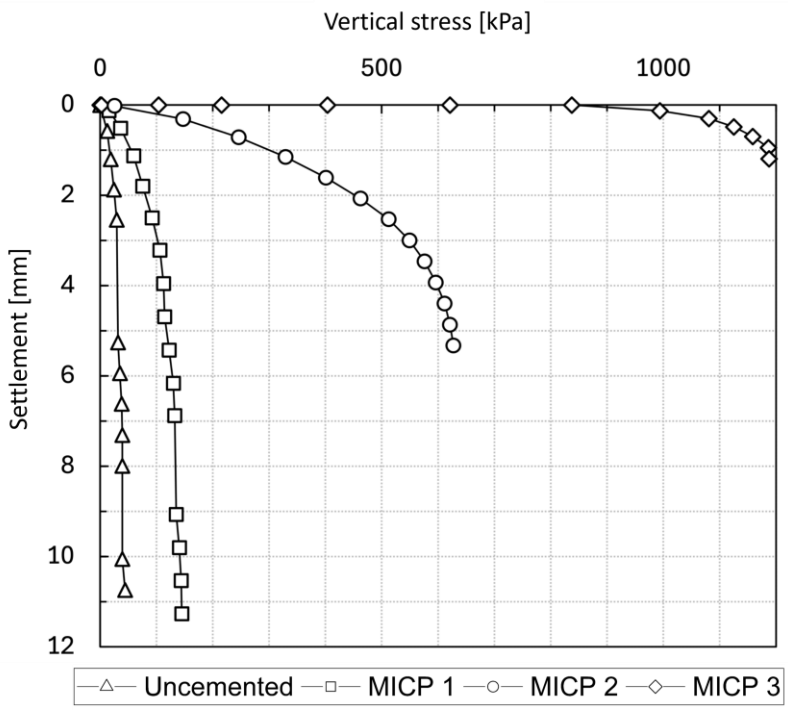

Figure 2: *Load-settlement curves of uncemented and cemented soils (tests MICP 1, MICP 2, MICP3)*

"Zhulong" Multi-Source Fast CT System and the In-situ Experimental Devices for Geomaterials

Ji-peng Wang, Mengchen Li, Shaohan Wang, Ji-yuan Luan

School of Civil Engineering and Hydraulic Engineering, Shandong University

17923 Jingshi Road, Jinan, China

ji-peng.wang@sdu.edu.cn, li_mcc@outlook.com, shao-han.wang@mail.sdu.edu.cn, jasperluan@outlook.com

Keywords: Geomaterials, Micro-structure, Fast CT system, CT image analysis, Hydro-mechanical properties

Abstract

Multiphase geomaterials often face complex challenges related to seepage and mechanical properties in engineering practice. CT three-dimensional imaging is an essential microscopic research tool for clarifying their intricate mechanisms. However, conventional single-source single-detector CT systems suffer from several technical limitations: a trade-off between projection acquisition efficiency and image quality, incompatibility between dynamic loading devices and micro-CT scanners, and difficulty in correlating microscopic structural changes with macroscopic stress-strain behavior. These limitations make it challenging to capture the dynamic evolution of geomaterials. Our research team successfully developed the "Zhulong", a triple-source and triple-detector rapid micro-CT scanning system, which reduces the scanning time to one-third of that of traditional CT systems while maintaining the same image quality [1].

The configuration of the triple-source and triple-detector system is shown in Figure 1. Three X-ray sources and three detectors are arranged 120° apart, and the sample is placed on a central rotating stage. By rotating the stage only 120°, the system can acquire a full set of projections equivalent to a 360° rotation in traditional single-source CT systems. To evaluate the performance of this system, we scanned the same unsaturated sand specimen using both the triple-source and conventional single-source modes under the same parameters. As shown in Figure 2, the grayscale distribution and particle size distribution are highly consistent between the two methods. Under the same field of view and resolution, the measurement errors in porosity and degree of saturation between the two scanning modes were both within 3%.

Furthermore, to meet the demands of non-destructive investigation of multiphase materials under coupled fields, we developed two CT-compatible in-situ mini devices for the mechanical [2] and seepage tests [3]. Based on the triple-source and triple-detector rapid micro-CT scanning system, these two devices enable high-resolution, non-destructive 3D imaging of critical states during testing. As demonstrated in Figures 3 and 4, we successfully visualized the microscopic mechanisms of geomaterials under triaxial shear and multiphase seepage conditions. In conclusion. This system provides a novel experimental tool for investigating the microscopic dynamic evolution of multiphase geomaterials.

References

[1] Gao X G, Sha J F, Luan J Y, et al. A triple-source CT system for micro-scale investigation of geological materials: A simulation study. Applied Radiation and Isotopes, 2022, 190: 110510.

[2] Wang J P, Luan J Y, Gao X G, et al. A micro-investigation of unsaturated sand in mini-triaxial compression based on micro-CT image analysis. Acta Geotechnica, 2022, 17(11): 4799-4821.

[3] Wang J P, Liu T H, Wang S H, et al. Investigation of porosity variation on water retention behaviour of unsaturated granular media by using pore scale Micro-CT and lattice Boltzmann method. Journal of Hydrology, 2023, 626: 130161.

Figures

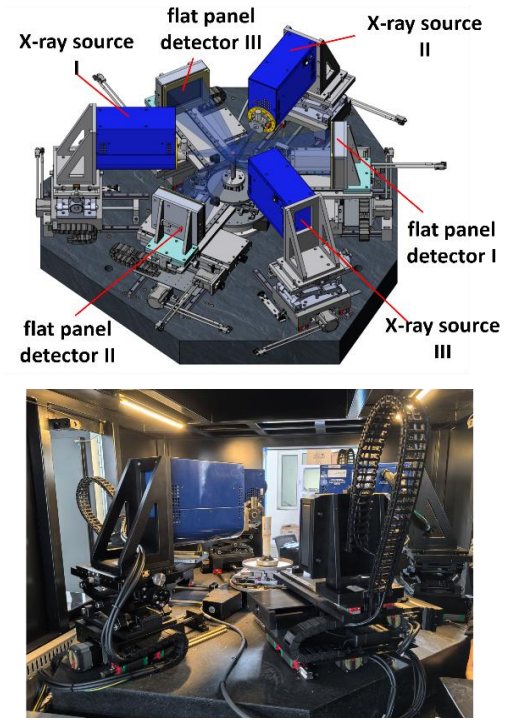

Figure 1. *A triple-source and triple-detector rapid micro-CT scanning system: "Zhulong"*

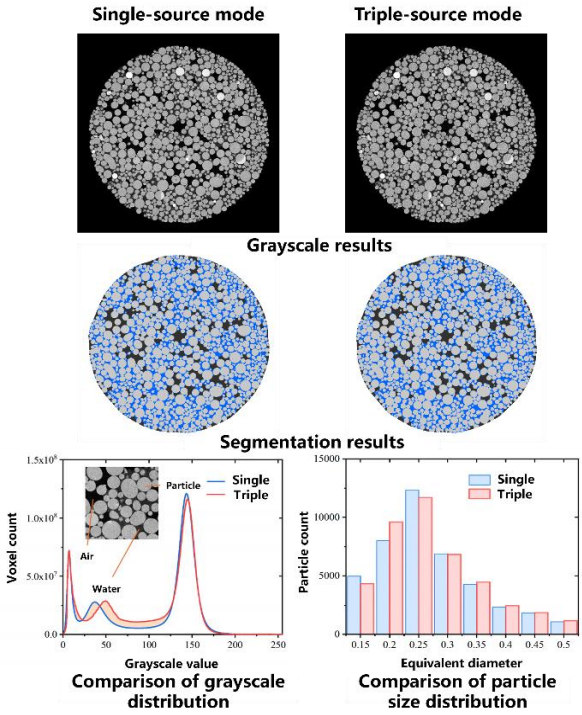

Figure 2. *Comparison of results between single-source and triple-source modes*

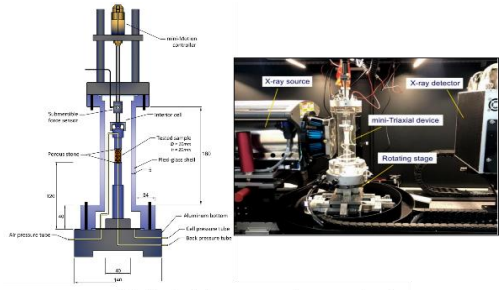

Mini triaxial compression test device

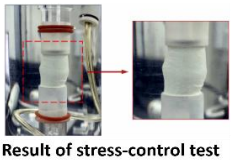

Result of stress-control test

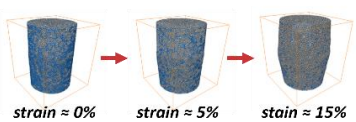

3D reconstruction model of mechanical test

Figure 3. *Mini multi-phase triaxial shear test with in-situ X-ray tomography*

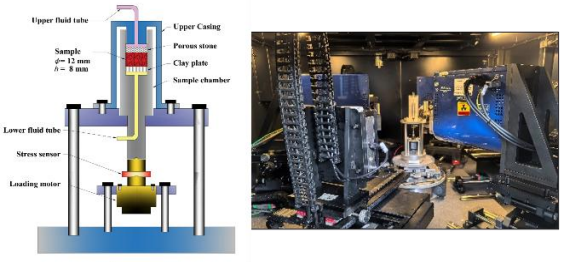

Mini multi-phase seepage test device

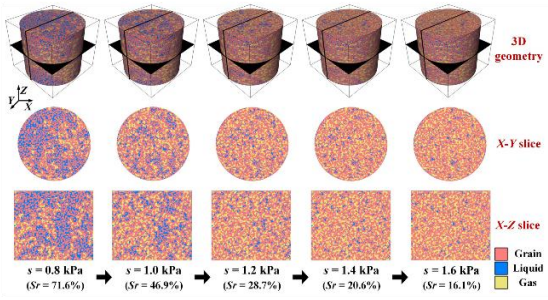

3D reconstruction model of seepage test

Figure 4. *Mini multi-phase seepage test with in-situ X-ray tomography*

Hypoplastic Predictions of Sandy Silt Tailings Behaviour under General Loading Conditions

Gertraud Medicus[1], Riccardo Fanni[2], David Reid[3], Andy Fourie[4]

[1]University of Innsbruck, Austria

[2]C2WSP, Australia

[3]Red Earth Engineering, Australia

[4]The University of Western Australia

gertraud.medicus@uibk.ac.at

Keywords: hypoplasticity, sandy silt tailings, stress paths, constitutive modelling

Abstract

Stress conditions in geotechnical applications, such as those within slopes, often differ from the simplified, axisymmetric conditions that are typically used to calibrate and validate constitutive models. Applications often involve stress paths that include varying deviatoric directions, as well as principal stress rotation. Assessing the reliability of model predictions therefore requires evaluation of predictive capability under such loading conditions.

This study investigates the hypoplastic model by von Wolffersdorff (1996), calibrated for sandy silt gold tailings using conventional drained and undrained triaxial compression tests (Fanni et al., 2025) following the calibration procedure of Herle (1997). Validation is then carried out using additional loading paths from Fanni et al. (2025; in print), including:

- drained and undrained simple shear tests, including constant shear drained loading, performed in the torsional shear hollow cylinder (TSHC) device,
- drained and undrained triaxial extension tests, and
- TSHC tests under drained and undrained conditions at constant, non-axisymmetric stress Lode angle θ and constant principal stress direction α.

These paths cover both consolidation and failure stages, including peak and critical states. The results show that hypoplasticity is able to predict trends of the behaviour of sandy silt tailings across a wide range of loading paths; an example of undrained simple shear on initially loose samples is shown in Figure 1.

Acknowledgement

This research was funded in part by the Austrian Science Fund (FWF) 10.55776/V918. G.M. is funded by the FWF. For open access purposes, the author has applied a CC BY public copyright license to any author accepted manuscript version arising from this submission. In addition, G.M. is supported by *Le Pôle interdisciplinaire d'études françaises de l'Université d'Innsbruck (Frankreich-Schwerpunkt der Universität Innsbruck).*

References

Fanni, R., Reid, D., & Fourie, A. (in print). Drained simple shear tests on a sandy silt gold tailings using a torsional shear hollow cylinder apparatus. Soils and Foundations.

Fanni, R., Reid, D., & Fourie, A. (2025). Drained and undrained behaviour of a sandy silt gold tailings under general multiaxial conditions. Géotechnique, 1–20.

Herle, I. (1997). Hypoplastizität und Granulometrie einfacher Korngerüste. PhD thesis. Veröffentlichungen des Institutes für Bodenmechanik und Felsmechanik der Universität Karlsruhe, No. 142.

von Wolffersdorff, P.-A. (1996). A hypoplastic relation for granular materials with a predefined limit state surface. Mechanics of Cohesive-Frictional Materials, 1(1), 251–271.

Figures

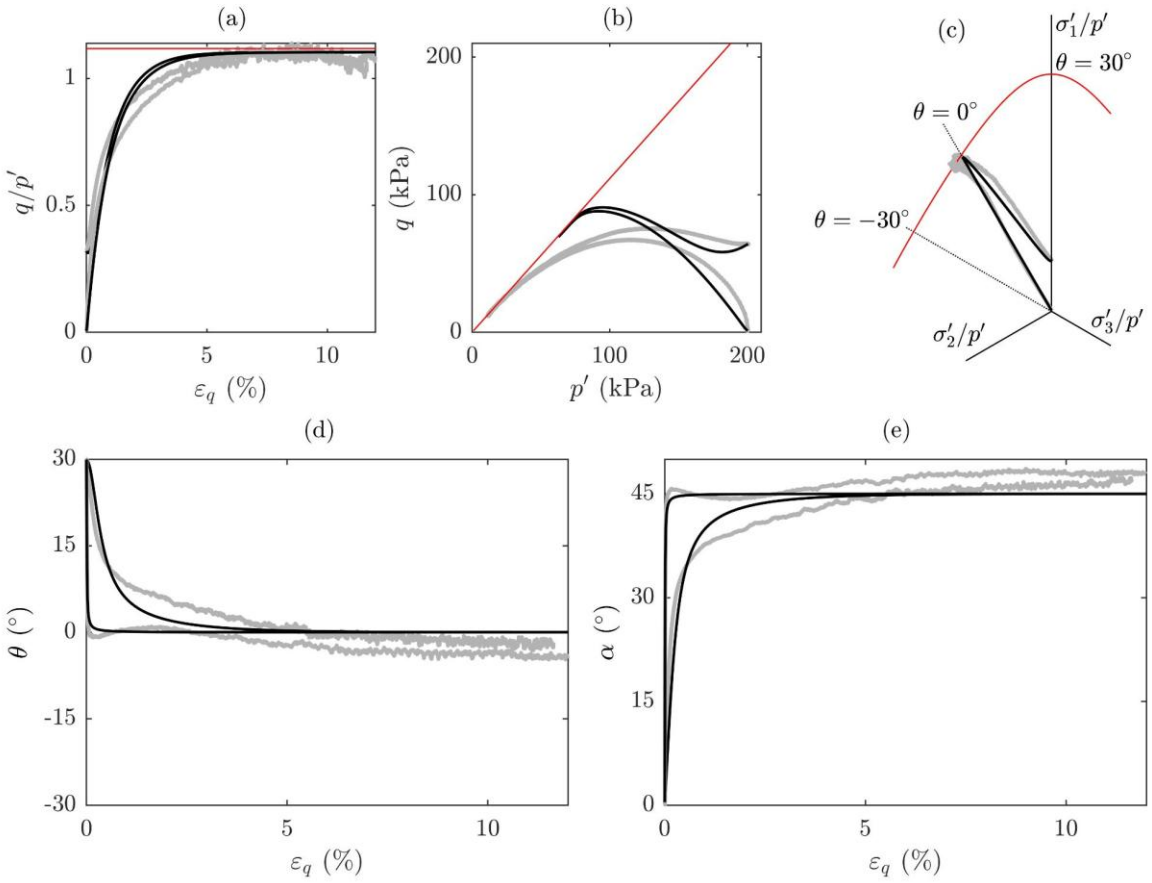

***Figure 1**: Hypoplastic predictions (black) of undrained simple shear tests of initially loose samples. Experimental data (grey) were obtained by Fanni et al. (2025) using a TSHC device. The red lines in (a) and (b) indicate Matsuoka-Nakai critical stress states for a Lode angle of θ = 0°. The Matsuoka-Nakai critical stress surface is shown in the deviatoric plane in (c), with the stress paths added. Hypoplasticity predicts θ = 0° at critical state and follows the experimental trend in (d). The angle of principal stress rotation α reaches 45° in the simulations at critical state and is also close to the experimental results in (e).*

Numerical Prediction of Mode I Fracture in the Pseudo-Compact Tension Test Using Phase-Field Models

L. Piñeiro Martínez, M. Martín Stickle, A. Yagüe, N. Tarque, P. Navas, D. Manzanal

ETS de Ingenieros de Caminos, Canales y Puertos, Universidad Politécnica de Madrid

leire.pmartinez@alumnos.upm.es, miguel.martins@upm.es, d.manzanal@upm.es

Keywords: Phase-field fracture, Mode I fracture, pseudo-Compact Tension (pCT), geomaterials, finite element method, CO_2 geological storage, Griffith energy, crack propagation

Abstract

The prediction of crack initiation and propagation is central in civil engineering, particularly in evaluating the integrity of subsurface reservoirs for geological storage of greenhouse gases (GHG). In this context, fractures and discontinuities in caprock or host formations can lead to leakage and system failure. Therefore, a precise numerical modeling framework is required to assess tensile failure mechanisms in geomaterials (Cajuhi et al. 2018). This study focuses on simulating the Mode I fracture response of geomaterials subjected to the pseudo-Compact Tension (pCT) test using a phase-field model of fracture. This model is integrated within the finite element method (FEM) and provides a continuous, regularized approach to simulating crack nucleation, growth, and post-peak behavior.

The model was developed and implemented as a phase-field fracture model for Mode I tensile failure in geomaterials within an in-house FEM code, aiming to apply it to the evaluation of the pseudo-Compact Tension (pCT) test, a newly developed method for geomaterials. The model is based on the variational formulation of Griffith's fracture theory (1921), regularised via a scalar damage-like field (phase field, φ). The total energy functional combines the elastic strain energy, fracture energy (via a crack surface density function $\gamma_l(\varphi)$), and external mechanical work. The AT2 phase-field formulation is adopted, which requires a critical energy release rate (Gc), a regularisation length scale (l) and the elastic parameters (E, ν). Coupled PDEs are derived and solved using a staggered finite element scheme, alternately updating displacement and phase-field variables. The model was validated with a direct tension test: a notched square specimen, a pure shear test: cracked panel under lateral shear and a three-point bending: standard beam geometry. Each case showed excellent agreement with benchmark data from Miehe et al. (2010) (Figure 1).

The validated model was applied to the pseudo-Compact Tension (pCT) test, designed to measure tensile fracture resistance of geomaterials like rock and cemented soils. Results show realistic crack paths from the notch tip, reaction-displacement curves consistent with experiments and post-peak damage zones concentrated along expected fracture lines (Figure 2). This test provides a more direct alternative to indirect tensile tests (e.g., Brazilian test), better suited to modeling fracture under gas injection conditions in geological reservoirs. The proposed phase-field framework, predicts tensile fracture in geomaterials with high fidelity, avoids remeshing or crack-tracking complexities and enables modeling of complex fracture patterns including branching and coalescence.

References

Cajuhi, T., Sanavia, L., & De Lorenzis, L. (2018). Phase field modeling of fracture in variably saturated porous media. Computational Mechanics, 61(3), 299–318.

Griffith, A. A. (1921). The phenomena of rupture and flow in solids. Philosophical Transactions of the Royal Society A: Mathematical, Physical and Engineering Sciences, 221(582–593), 163–198.

Miehe, C., Hofäcker, M., & Welschinger, F. (2010a). A phase field model for rate-independent crack propagation: Robust algorithmic implementation based on operator splits. Computer Methods in Applied Mechanics and Engineering, 199(45 48), 2765–2778.

Figures

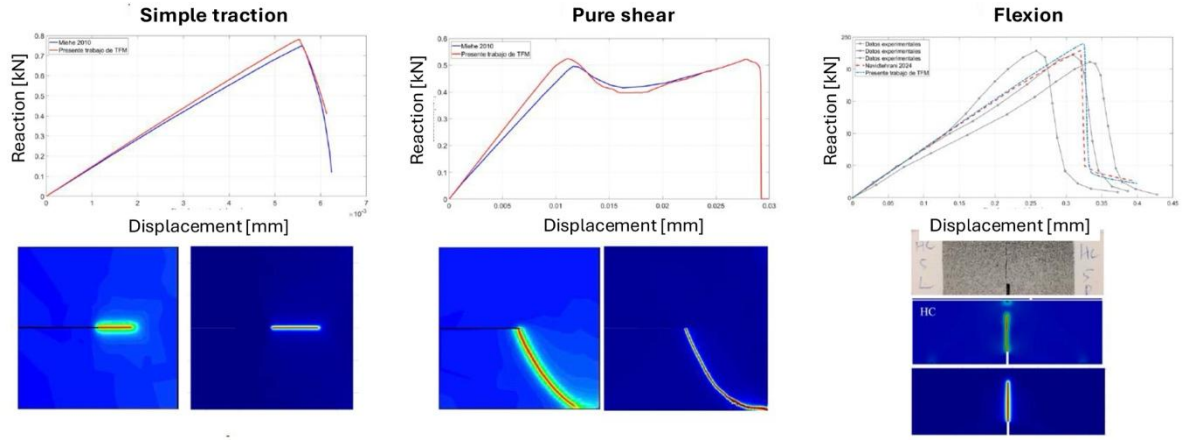

Figure 1: *Validation of the PF-FEM implementation*

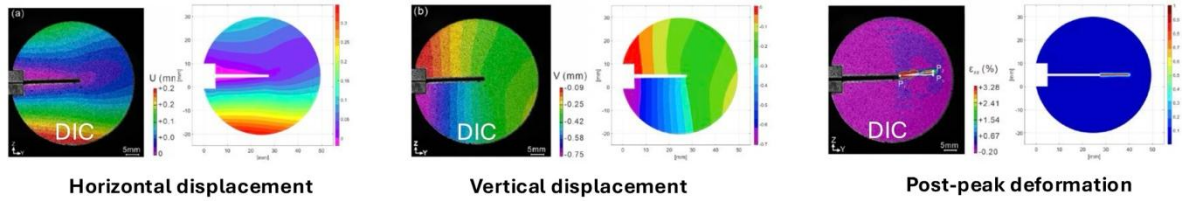

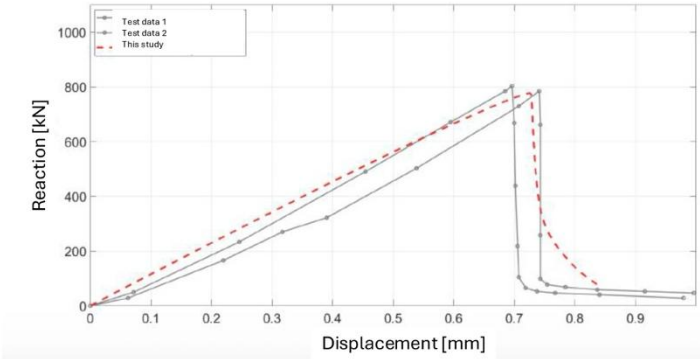

Figure 2: *PF-FEM modelling of pseudo-Compact Tension (pCT) test*

Experimental and numerical assessment of Salamanca Formation as CO2 underground storage

C. Laskowski[1,2], D. Manzanal[1], S. Orlandi[2], M. Muñiz-Menéndez[3] , M. Martín Stickle[1] & J. Allard[2]

[1]Universidad Politécnica de Madrid,

[2]Universidad Nacional de la Patagonia San Juan Bosco,

[3]Laboratorio de Geotecnia del CEDEX

ceciliabelen.las@alumnos.upm.es, d.manzanal@upm.es

Keywords: CO2 storage, numerical simulations, direct shear test, sandstone

Abstract

During the past few years, researchers have studied feasible alternatives for climate change mitigation. One of the practical options is CO2 capture and storage, which takes advantage of the empty space left behind oil and gas exploitation. Before proposing a Formation as possible CO2 storage, it is necessary to consider the reservoir's integrity (Hawkes et al. 2004). In this context, leakage and earthquake related events should be studied in detail. The mentioned events are mainly related to different types of discontinuities present in underground reservoirs (Cornet et al. 2007 and Hawkes et al. 2004).

Although several authors have analyzed how discontinuities change with CO2 exposure (Cerasi et al. 2015, Jahanbakhsh et al. 2021 and Casagrande et al. 2022), few focused on mechanical and dilatant behavioral changes. The current study analyzes natural discontinuities present in the Banco Verde sandstone (Salamanca Formation, Argentinian Patagonia). The mechanical and dilatant changes resulting from the exposure of the rock were investigated carrying out direct shear tests over pristine and 30-day CO2 exposed specimens. With the aim of studying the reservoir-scale behavior of CO2 storage, long-term simulations were conducted, using the experimental results obtained.

The direct shear tests performed on both pristine and 30-day CO2 exposed specimens were carried out with axial stresses ranging from 10MPa to 30MPa with the aim of covering the possible pressures reached at reservoir depth. In Figure 1, the results obtained from direct shear tests performed with a 20MPa axial stress are shown. As it might be observed, there is a reduction in the shear strength of the discontinuity, which is more pronounced in the peak than in the residual shear strength. This is a generalized behavior for the tests performed, which means that there is a reduction in the mechanical strength of the discontinuity due to its exposure to CO2.

Numerical simulations were performed using COMSOL Multiphysics software, coupling hydraulic and mechanical phenomena. The design was based on experimental results previously obtained (Figure 2a). From coupled simulations results, it was possible to analyze, the shear stress distribution and slip relative displacement along the fault (Figure 2b and c). Both the greatest slip relative displacement and peak shear stress occur in the interface between the reservoir rock (Banco Verde) and the underlying caprock (Fragmentosa), which is the usual fault reactivation point (Urpi et al. 2015).

All in all, this study seeks to show the importance of accurately determining the properties of the materials as well as the discontinuities present in the geometrical model to be numerically simulated. The effect CO2 has over the mechanical behavior of the natural discontinuities

studied was shown. From the numerical results obtained, it was possible to verify that the fault reactivation in Salamanca Formation occurs as in the interface between the reservoir rock and the underlying caprock.

Acknowledgement

The principal author thanks Fundación José Entrecanales Ibarra for funding her Ph.D. Thesis. The authors acknowledge the financial support provided by the European Commission (MSCA-RISE 2020 Project DISCO2-STORE, Grant Agreement No 101007851), the 'Ministerio de Ciencia y Innovación' under Grant Number PID2023-149658NB-I00, the UNPSJB (Project PI1983), and FONTAR from Argentina (PICT 2020–0288).

References

Casagrande, C.; Piqué, T. M.; Gómez, J. L.; Epele, B.; Sánchez, M.; & Manzanal, D. 2022. Characterization of mechanical discontinuities using triaxial shear tests under high confining pressure. Proceedings 56th U.S. Rock Mechanics/Geomechanics Symposium, 26th-29th june 2022, Santa Fe, United States.

Cerasi, P.; & Stroisz, A. 2015. Experimental Investigation of Cement to Rock Bonding. Proceedings 49th U.S. Rock Mechanics/Geomechanics Symposium, June 2015, San Francisco, California, United States.

Cornet, H., Bérard, T., Bourouis, S. (2007) How close to failure is a granite rock mass at a 5km depth? International Journal of Rock Mechanics and Mining Sciences, Volume 44, Issue 1, 47-66.

Hawkes, C.; Mclellan, P.; & Bachu, S. 2004. Geomechanical factors affecting geological storage of CO2 in depleted oil and gas reservoirs. Journal of Canadian Petroleum Technology 44 (10).

Jahanbakhsh, A.; Liu, Q.; Mosleh, M. H.; Agrawal, H.; Farooqui, N. M.; Buckman, J.; Recasens, M.; Maroto-Valer, M.; Korre, A.; & Durucan, S. 2021. An Investigation into CO2–Brine–Cement–Reservoir Rock Interactions for Wellbore Integrity in CO2 Geological Storage. Energies 14 (5033).

Urpi, L., Rinaldi, A. P., & Wassing, B. 2015. Modelling fault reactivation and velocity dependent friction with tough-flac. Proceeding of the TOUGH Symposium 2015, Lawrence Berkeley National Laboratory, Berkeley.

Figures

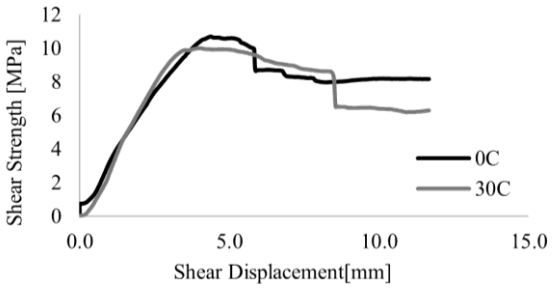

Figure 1: *Results from direct shear tests performed for pristine (0C) and 30-day CO2 exposed (30C) specimens.*

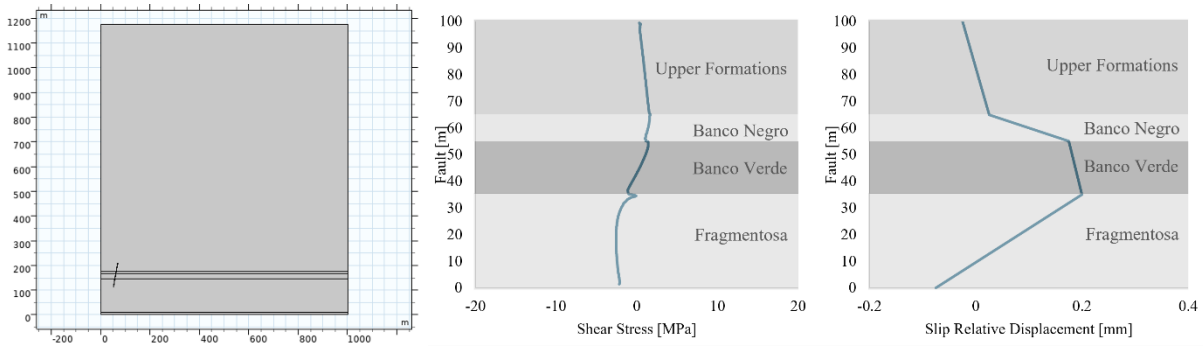

Figure 2: a. *Underground geometrical design.* ***b.*** *Shear stress and,* ***c.*** *slip relative displacement along the fault.*

Hypoplasticity for sand enhanced for modelling cyclic and fabric effects

L. Mugele[1], H. H. Stutz[1], Z. X. Yang[2]

[1]Institute of Soil Mechanics and Rock Mechanics, Karlsruhe Institute of Technology, Germany

[2]Department of Civil Engineering, Zhejiang University, Hangzhou, 310058, China

Luis.mugele@kit.edu

Keywords: hypoplasticity, overshooting, anisotropic critical state theory, cyclic behavior, liquefaction

Abstract

A recently published hypoplastic constitutive model is presented that combines novel and already established advanced constitutive theories to realistically capture the mechanical behaviour of sands under monotonic and cyclic loading. The proposed model, published in [1] and further called HP+GIS+ACST, is based on the hypoplastic formulation after von Wolffersdorff (HP) [2] and motivated by Yang et al. [3]. It integrates two major theoretical extensions: (A) the Generalized Intergranular Strain (GIS) concept [4] for capturing cyclic and strain accumulation effects, and (B) the Anisotropic Critical State Theory (ACST) [5] to account for an evolving anisotropic fabric and its impact on the conventional measurable macroscopic soil behaviour. The model uses six internal state variables, including the effective stress, the void ratio, a fabric tensor, the intergranular strain tensor, and two scalar variables memorizing the cyclic and dilative preloading.

To validate the model's predictive capabilities, element simulations are performed and compared against experimental results from cyclic and monotonic tests on Karlsruhe fine sand (KFS) [6, 7] and Fraser River sand [8]. To demonstrate the prediction quality of the HP+GIS+ACST, additional comparisons with the widely used hypoplasticity after von Wolffersdorff [2] with the Intergranular Strain extension [9] (HP+IS) are presented. The novel HP+GIS+ACST resolves key limitations of earlier hypoplastic models. Figure 1 shows, as an example, the eliminated issue of the so-called overshooting of the Asymptotic State Boundary Surface (ASBS) due to an un- and reloading using a drained triaxial test. Additionally, as shown in Figure 2, the HP+GIS+ACST reproduces cyclic soil liquefaction in undrained triaxial experiments in loose and dense sands. Simulations with the widely used HP+IS model show qualitatively and quantitatively inaccurate curves.

This contribution illustrates how integrating established theoretical concepts into the hypoplastic framework can substantially improve our ability to model realistic soil behavior under challenging loading conditions. The resulting HP+GIS+ACST represents a next step in the evolution of hypoplastic constitutive models. Note that implementations (umat.for and udsm.dll) are available from the author.

References

[1] Mugele, L., Stutz, H. H., & Yang, Z. X. (2025). Accounting for cyclic and fabric effects in an enhanced hypoplastic model for sand. Computers and Geotechnics, 187, 107462.

[2] von Wolffersdorff, P. A. (1996). A hypoplastic relation for granular materials with a predefined limit state surface. Mechanics of Cohesive-frictional Materials: An International Journal on Experiments, Modelling and Computation of Materials and Structures, 1(3), 251-271.

[3] Yang, Z., Liao, D., & Xu, T. (2020). A hypoplastic model for granular soils incorporating anisotropic critical state theory. International Journal for Numerical and Analytical Methods in Geomechanics, 44(6), 723-748.

[4] Mugele, L., Stutz, H. H., & Mašín, D. (2024). Generalized intergranular strain concept and its application to hypoplastic models. Computers and Geotechnics, 173, 106480.

[5] Li, X. S., & Dafalias, Y. F. (2012). Anisotropic critical state theory: role of fabric. Journal of engineering mechanics, 138(3), 263-275.

[6] Wichtmann, T., & Triantafyllidis, T. (2016). An experimental database for the development, calibration and verification of constitutive models for sand with focus to cyclic loading: part I—tests with monotonic loading and stress cycles. Acta Geotechnica, 11(4), 739-761.

[7] Wichtmann, T., & Triantafyllidis, T. (2016). An experimental database for the development, calibration and verification of constitutive models for sand with focus to cyclic loading: part II—tests with strain cycles and combined loading. Acta Geotechnica, 11(4), 763-774.

[8] Uthayakumar, M., & Vaid, Y. P. (1998). Static liquefaction of sands under multiaxial loading. Canadian Geotechnical Journal, 35(2), 273-283.

[9] Niemunis, A., & Herle, I. (1997). Hypoplastic model for cohesionless soils with elastic strain range. Mechanics of Cohesive-frictional Materials: An International Journal on Experiments, Modelling and Computation of Materials and Structures, 2(4), 279-299.

Figures

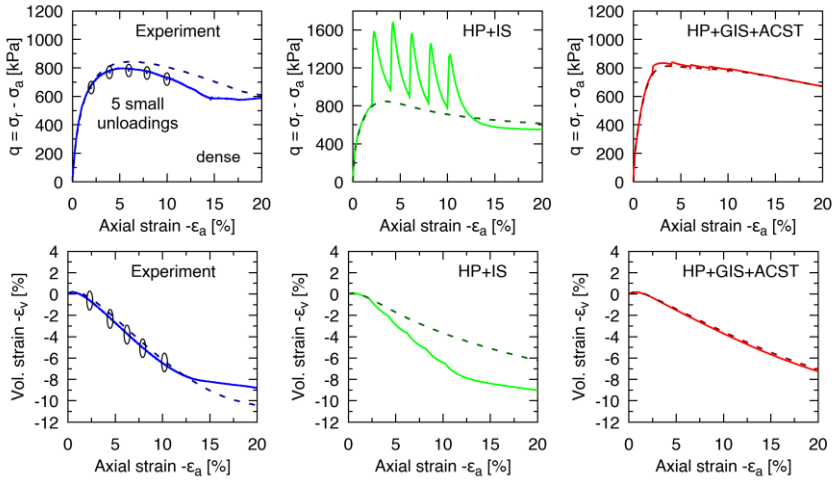

Figure 1: *A comparison between experimental results (drained triaxial tests) and simulations using HP+IS and HP+GIS+ACST shows that the HP+GIS+ACST prevents overshooting.*

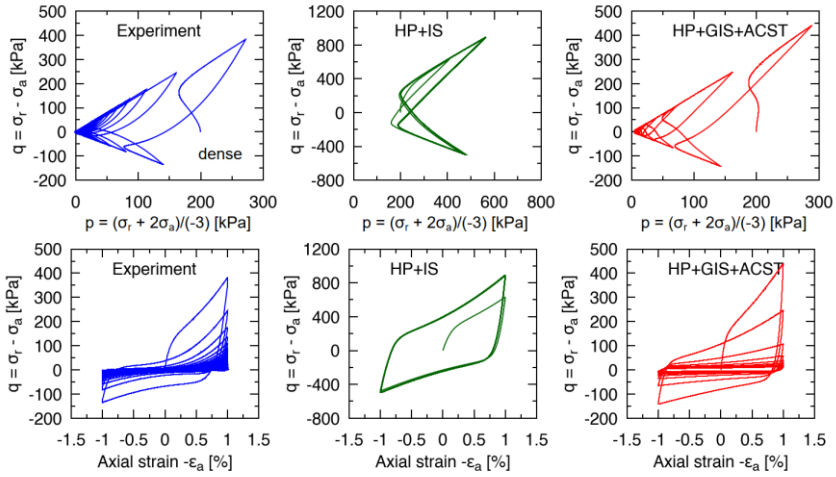

Figure 2: *A comparison between experimental results (undrained triaxial test) and simulations using HP+IS and HP+GIS+ACST shows that the HP+GIS+ACST reproduces cyclic liquefaction in dense sands.*

Micropolar Theory for Granular Media: More Than Just Rotations?

Max Winkelmann*,†, Vanessa Magnanimo*, Stefanos-Aldo Papanicolopulos†, and Stefan Luding*

**Faculty of Engineering Technology, University of Twente, PO Box 217, 7500 AE Enschede, Netherlands*

† School of Engineering, Institute for Infrastructure and Environment, University of Edinburgh, Edinburgh EH9 3FG, UK

m.winkelmann@utwente.nl

Keywords: Micro-to-macro, micropolar, contact friction, particle shape, rotations

Abstract

In granular materials, friction and shape at the particle scale [1] influence the bulk response—particularly the material's rotational behaviour. It has been shown that contact friction and particle shape affect how grains rotate and interact [2, 3].

Using discrete-to-continuum (D2C) upscaling methods, discrete particle data such as particle mass, particle velocity and contact forces can be mapped onto continuous fields like density, velocity, and contact stress. Building on the approach by Goldhirsch [4] and Weinhart [5, 6], we develop a D2C method to transform rotation-related particle properties—angular velocity, angular momentum, tangential forces, and contact torque—into non-classical micropolar fields: relative rotation, curvature, skew-symmetric stress, and couple stress. In classic continuum mechanics, the work-conjugate pair of symmetric stress and strain causes plastic dissipation. These additional micropolar fields form their own work-conjugate pairs, revealing two further dissipation mechanisms associated with rotational behaviour.

We demonstrate this using a DEM simulation of a planar split-bottom shear cell. Bulk shear induces microscale rotation, which is captured in the corresponding micropolar fields. A parameter study with spherical particles shows that rolling friction has the strongest impact on quantities such as skew-symmetric stress and relative rotation. This suggests a dominant role of shape in generating micropolar effects. And indeed, particle shape affects rotationally-induced macroscopic fields, which localise in regions of large deformation, such as shear bands. These fields align in position, width, and qualitative shape with the zone of failure.

While the natural next step is constitutive modelling with the multitude of micropolar effects, this work also points to a larger potential in micropolar theory. In particular, the moment of inertia production term—included in the balance laws of micropolar theory [7]—has yet to be fully explored. Could it model changes in particles, such as breakage or agglomeration? If so, micropolar theory may offer more than a refined kinematic framework; it may help to predict granular evolution rooted in microstructure.

This poster presents our recent findings, but also invites discussion: Can micropolar theory offer a more complete framework for understanding the rotational physics of granular materials?

References

[1] S. Luding. Cohesive, frictional powders: contact models for tension. Granular Matter, 10:235-246, 2008.

[2] R. Rorato et al. Linking shape and rotation of grains during triaxial compression of sand. Granular Matter, 22(4):88-109, 2020.

[3] U. Ali et al. Systematic effect of particle roundness/angularity on macro- and microscopic behavior of granular materials, Granular Matter, 25(3):51-67, 2023.

[4] I. Goldhirsch. Stress, stress asymmetry and couple stress: From discrete particles to continuous fields. Granular Matter, 12(3):239-252, 2010.

[5] T. Weinhart et al. Coarse-grained local and objective continuum description of three-dimensional granular flows down an inclined surface, Physics of Fluids, 25(7):070605, 2013.

[6] T. Weinhart et al. Influence of coarse-graining parameters on the analysis of DEM simulations of silo flow. Powder Technology, 293:138-148, 2016.

[7] W. H. Müller et al. Micropolar Theory with Production of Rotational Inertia: A Farwell to Material Description. Physical Mesomechanics, 20:250-262, 2017.

Engineering approaches to tree stability assessment: a Geotechnical perspective

Marrazzo Giacomo, Galli Andrea

Politecnico di Milano, Italy

giacomo.marrazzo@polimi.it, andrea.galli@polimi.it

Keywords: stability of trees, shallow foundations, pulling tests, cyclic behaviour, soil-root interaction

Abstract

Tree stability assessment is nowadays a relevant component of risk management strategies in urban environments, where the issue of falling trees (Figure 1) is exacerbated by ongoing climate change effects. Within this context, soil mechanics and geotechnical engineering can provide a significant contribution in the evaluation of tree toppling resistance against uprooting, trying to clarify important aspects that govern the complex hydro-mechanical interaction between the root system and the surrounding soil. From an engineering point of view, this can indeed be considered as a particularly complex example of a soil-structure interaction problem (SSI), where the tree can be assimilated to a "living" structure and the root-plate plays the role of shallow foundation for the system (Galli et al., 2024; Marrazzo et al., 2024).

Starting from this framework, the aim of this contribution is to exhibit preliminary results obtained from on-site tests on trees and to highlight geotechnical aspects that could represent possible (new?) fields of research and application addressing the topic of tree stability assessment. This latter is typically performed by professional agronomists and one of the most common non-destructive tests they adopt in practice is the so called "pulling test" (Figure 2). This test consists in the application of a transversal load to a tree stem by means of a pulling rope and a manual winch. A loading cell, put along the pulling rope, and an inclinometer, installed at the base of the trunk, record the applied load and the rotation of the stem collar, respectively. The standard testing procedure involve the estimation of a representative secant stiffness of the moment-rotation curve at 0.25° that is empirically linked to the ultimate resisting moment according to the procedure proposed by Wessolly and Erb (1998). The possible influence of several aspects such as the chosen loading path, the loading rate dependency and seasonal effects (e.g. soil moisture variation) are not systematically considered in the agronomic practice. To explore these possible effects, not yet fully investigated in geotechnical research literature, several pulling tests were performed on the same sample tree in different periods by considering different loading rates (e.g. Figure 3a). For example, Figure 3b reports the moment rotation curves of cyclic tests showing a good reproducibility of the cycles (reversible regime) but a significant difference in the average secant stiffness K of the cycles, attributed to both loading rate effects and seasonal environmental factors.

The contribution would explore those geotechnical fields needed to more accurately interpret pulling tests and to better understand the phenomenon of complete root-plate overturning, such as (i) the description of the mechanical interaction of roots with highly deformable loose soils, (ii) the effect of soil partial saturation, (iii) the mechanical characterization of vegetated soils at low burial depth (thus at low confining stresses, (iv) the response to complex and combined environmental loads (e.g. wind actions and watering/dewatering effects). A deeper

investigation of these aspects is fundamental for developing more reliable predictive models. These topics will be briefly explained during the poster presentation.

References

Galli, A., Sala, C., Castellanza, R., Marsiglia, A., & Ciantia, M. O. (2024). Lesson learnt from static pulling tests on trees: an experimental study on toppling behaviour of complex foundations. Acta Geotechnica, 19(3), 1477-1494.

Marrazzo, G., Ciantia, M. O., Riccio, T., Knappett, J. A., & Galli, A. (2024, October). Multi-axis loading tests on a small-scale tree roots model. In ECPMG 2024: 5th European Conference on Physical Modelling in Geotechnics. International Society for Soil Mechanics and Geotechnical Engineering.

Wessolly, L, and M. Erb. (1998). Handbuch der Baumstatik und Baumkontrolle. Patzer, Berlin.

Figures

Figure 1: *Tree failures in urban areas due to root-plate overturning.*

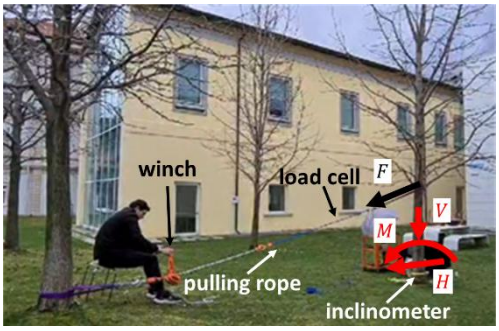

Figure 2: *Execution of a pulling test with a manual winch at the Lecco Campus (Politecnico di Milano).*

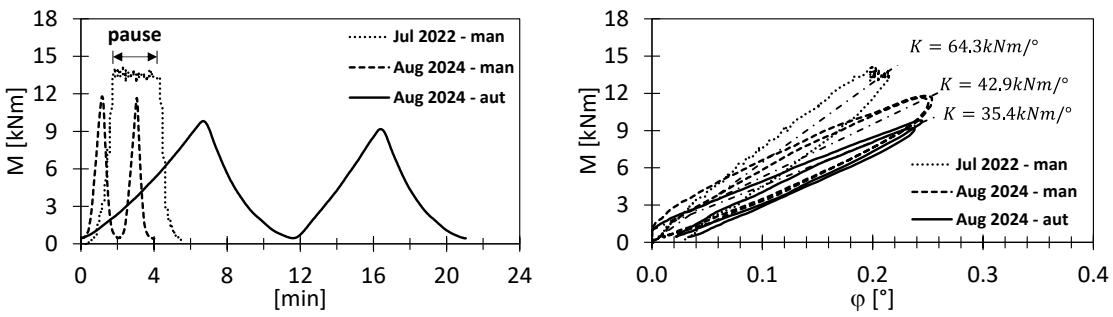

Figure 3: *(a) loading history imposed during the pulling tests; (b) moment-rotation curves.*

Effective stress in bentonite membranes

J. C. Walter, L. Mugele, H. H. Stutz

Institute of Soil Mechanics and Rock Mechanics, Karlsruhe Institute of Technology, Karlsruhe, Germany

jonathan.walter@kit.edu

Keywords: Bentonite, Suspension, Filtercake, Membrane

Abstract

Bentonite suspension is used in geotechnical engineering e. g. to support boreholes, open diaphragm walls or to the face stability of tunnels. Support of the soil is provided by forming an im-permeable membrane on the interface on the interface of the suspension and soil. To investigate the formation and properties of such bentonite membranes under high pressures, a novel test device was developed that allows pressures of up to 4 MPa to be studied (see Figure 1). To conduct the tests, the pressure in the pipe is increased to the desired pressure. Afterwards the lower outlet valve is opened, thereby activating the pressure gradient. The outflowing water is collected in a container placed on a scale and its mass is measured. The pressure inside the pressure tube is also measured. In addition, the configuration of the test (see Figure 1) allows to investigate the for-mation of two membranes (Walter et al. 2025).

Tests show that an almost impermeable membrane forms within seconds. Initially, this membrane is only a few millimetres thick, but becomes thicker over time. The water content was measured by cutting out a piece of the membrane, then scraping off the material layer by layer across the height of the membrane and determining the water content of each layer. It was measured, that the wa-ter content decreasing from the sand surface as the thickness increases. However, test showed that the water content at the sand surface remains constant over time. The effective stress in the sand corresponds to the total applied pressure. Therefore, the total pressure must become effec-tive stresses over the height of the membrane.

A comparison of a test in the pressure pipe with an applied pressure of 400 kPa and an oedometric compression test on suspension shows that the void ratio of the membrane at the sand surface corresponds to the void ratio measured in the oedometer at the same load. The oedometric compression test shows a linear relationship between stress and void ratio in the double logarithmic stress-void ratio diagram (Figure 2 left). Therefore, a compression relation after Butterfield is modi-fied which provides a sufficiently accurate approximation for the large void ratio changes (Butter-field 1979). Figure 2 (right) shows the void ratio across the thickness of the membrane. It can be seen that this is lowest at the sand surface (h=0) and continues to increase asymptotically to the void ratio of the suspension with the thickness. Using these two tests, it is now possible to calculate the effective stresses across the height of the membrane (Figure 3) from the void ratio of the oe-dometer test and the void ratio across the height of the membrane.

References

Walter, J. C., Mugele, L., Gudehus, G., H. H., Stutz (2025). Underground energy storage by means of injected bentonite double membranes. International Conference on Energy Geotechnics.

Butterfield, R. (1979). A natural compression law for soils (an advance on e–log p′). Géotechnique, 29(4), 469-480.

Figures

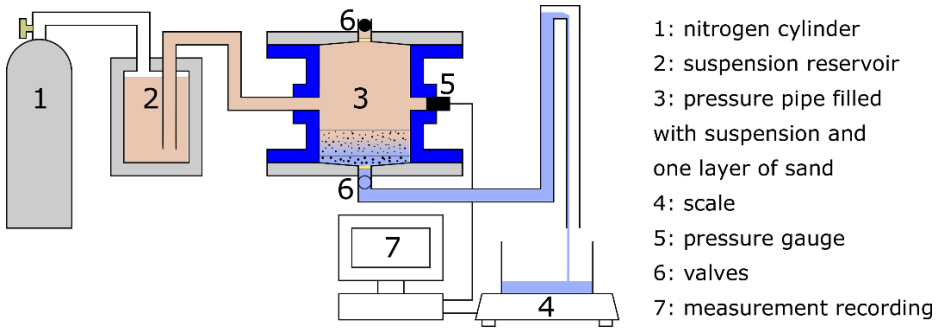

Figure 1: *Test device (Walter et al.2025)*

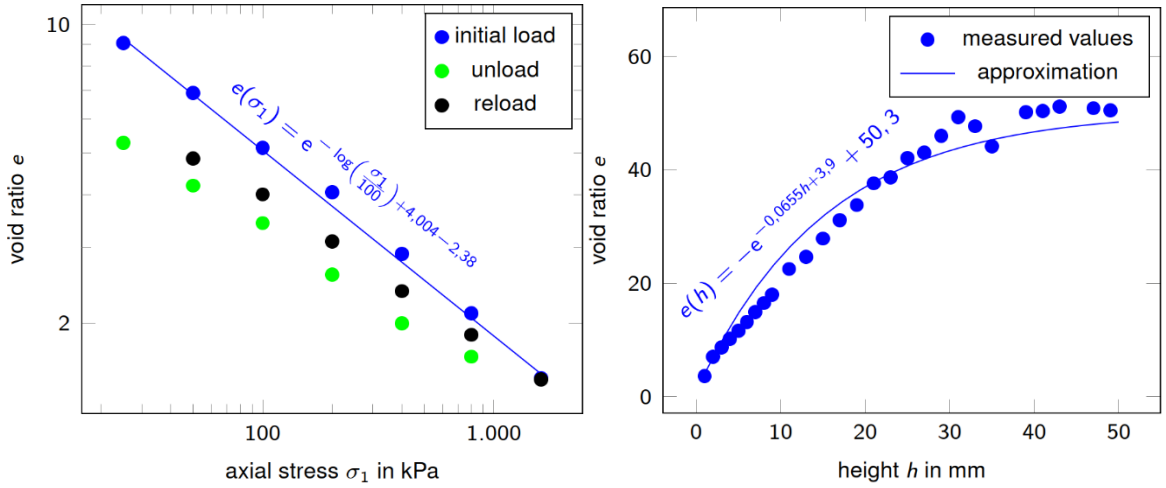

Figure 2: *Left: results of an oedometric test on suspension; right: void ratio over the height of the membrane*

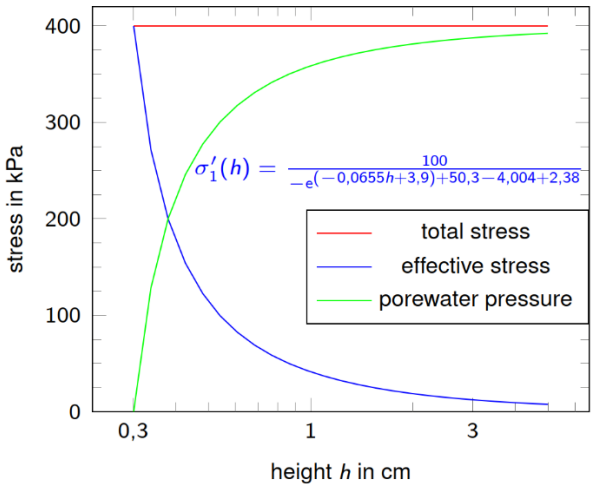

Figure 3: *Calculated function of the effective stress over the height of the membrane*

On the homogeneity and reproducibility of specimens prepared using dry air pluviation

H.H. Stutz[1], L. Mugele[1], J.D. Arroyo Lopez[1], J. Zürn[1]

[1]Institute of Soil Mechanics and Rock Mechanics, Karlsruhe Institute of Technology, Germany

Luis.mugele@kit.edu

Keywords: specimen preparation, sand, homogeneity, dry air pluviation

Abstract

Experimental results in soil mechanics depend crucially on the chosen specimen preparation method and the quality of the preparation process itself [1, 2]. A widely used preparation method is the dry air pluviation (AP) technique, which is intended to imitate the natural sedimentation process through the air of granular material. Besides replicating the soil genesis, the specimen preparation method should also ensure two other important aspects: (A) reproducibility and (B) homogeneity. Reproducibility means that specimens produced sequentially should have comparable properties, for example, a comparable average density. Only if the specimens fulfil the reproducibility criteria can one anticipate that the tests carried out on them will be repeatable. Homogeneity means that the state of the prepared specimen (e.g., density) is approximately identical throughout the whole specimen and does not contain any significant variations. The homogeneity of the state of a specimen is essential to fulfil the frequently made assumption of an experimental element test and the resulting interpretation of the experimental data.

To investigate the quality of manually prepared AP specimens, the local density distribution in cylindrical specimens (10 × 20 cm) was measured using a segmented mould consisting of ten PVC rings, each 2 cm in height. The dry mass of the used Karlsruhe sand (KS) was determined in each of these rings. A total of 12 specimens were prepared by three individuals with varying levels of experience (beginner, intermediate, expert) using two different nozzle diameters. The resulting relative density distributions are shown in Figure 1 (left). Large deviations were observed: the mean relative density varied up to $\Delta I_D = |\overline{I_{(D,2)}} - \overline{I_{(D,1)}}| \approx 0.09$, and within individual specimens, coefficients of variation of the locally measured relative density reached up to 11%. These findings show that both the homogeneity and reproducibility of manually prepared AP specimens are unsatisfactory, regardless of the technician's level of experience.

To overcome the issues of manual specimen preparation (MSP), the so-called Robotic Automated Specimen Preparation (RASP) method for the AP technique was recently developed [3]. The device, shown in Figure 2, is based on a conventional collaborative robot (cobot) with a modified tool end. Using the cobot, a well-defined three-dimensional path can be applied to the nozzle. The density distributions for four RASP AP-specimens (two with different nozzle diameters) are shown in Figure 1 (right). Both homogeneity and reproducibility are significantly improved compared to hand-made specimens. The achieved density can be controlled precisely, for example, by the nozzle diameter (shown) or the fall height (not shown). Interestingly, both manual and RASP AP-specimens show a reduced density at the bottom of the specimen, which is likely due to the interaction of the falling grains and the base plate of the mould.

In summary, it can be concluded that large inhomogeneities are to be expected in conventional manual AP-specimen preparation, which are additionally not reproducible. This issue can be resolved using the RASP method proposed in [3], which generates reproducible and more homogeneous specimens.

References

[1] Wichtmann, T., Steller, K., & Triantafyllidis, T. (2020). On the influence of the sample preparation method on strain accumulation in sand under high-cyclic loading. Soil Dynamics and Earthquake Engineering, 131, 106028.

[2] Yang, Z. X., Li, X. S., & Yang, J. (2008). Quantifying and modelling fabric anisotropy of granular soils. Géotechnique, 58(4), 237-248.

[3] Mugele, L., Arroyo Lopez, J. D., Zürn, J., & Stutz, H. H. (2025). Robotic Automated Specimen Preparation (RASP): Applied to Air pluviation. Acta Geotechnica (submitted).

Figures

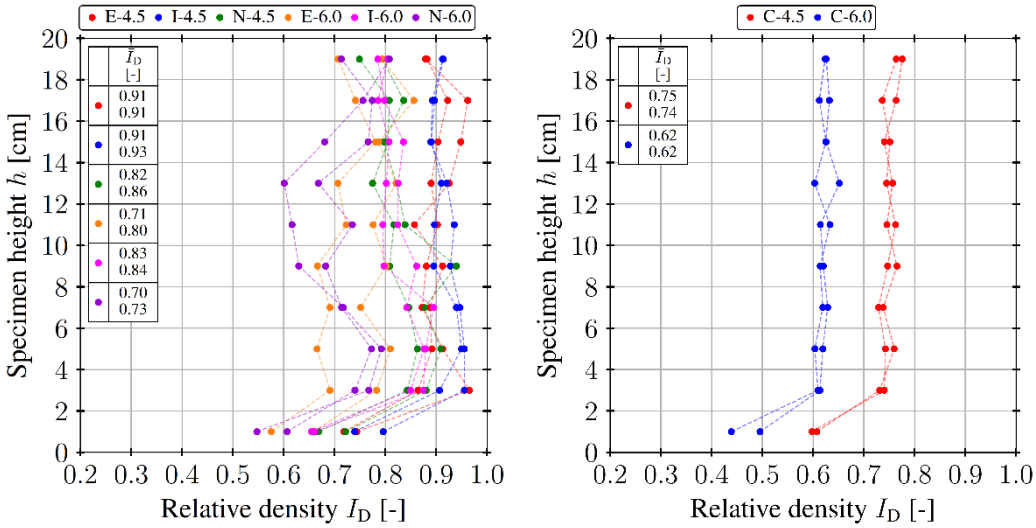

Figure 1: *Relative density distribution across the height of the specimen: manual specimen preparation (left) and automated specimen preparation (right) [1]*

Figure 2: *Robotic Automated Specimen Preparation (RASP) device using a conventional collaborative robot*

Settlement of submarine power cables on soft structured clay seabed

Reza Khalili, Wojciech T. Solowski

Department of Civil Engineering, Aalto University, Espoo, Finland

Reza.1.khalili@aalto.fi

Keywords: Settlements, Berm construction, Submarine power cable, Backfill

Abstract

Submarine power cables installed on soft seabed are prone to environmental damage caused by fishing gear, anchors, and seabed erosion. To mitigate these risks, the paper investigates a protective berm constructed over the cable and its settlements. we examine two berm geometries (Figure 1), as well as staged construction, and the influence of the pre-consolidation of backfill before berm placement.

Despite numerous studies on submarine power cables that investigated variations in burial depth [e.g., 1-3], cable failure [e.g., 4-6], and thermal performance of cables [e.g., 7,8] in a variety of seabed conditions, there are no studies which are relevant for soft clays in the Gulf of Bothnia, which would investigate the interaction between the cable, berm, and structured clay seabed and their long-term settlement.

This research aims to estimate the long-term settlement of submarine power cables in the Gulf of Bothnia. The calculations account for creep and destructuration of the clay during the consolidation process. The research analyses the effects of berm geometry adjustments, pre-consolidation of backfill, and backfill width on the settlements and consolidation of the seabed.

Results indicate that using pre-consolidation of backfill can lead to smaller settlements. A smaller berm geometry also decreases settlement, although in practice it may not provide sufficient protection. Finally, the influence of backfill extension was assessed, and it was found to have only a negligible effect on the final settlement (Figure 2).

References

[1] Wagner, E. (1995). Submarine cables and protections provided by the law of the sea. Marine Poficy, 19(2), 127–136.

[2] Allan, P. G. (1998). Selecting Appropriate Cable Burial Depths-A Methodology IBC Conference on Submarine Communications. The Future of Network Infrastructure. In The Future of Network Infrastructure (Ed.), In A Methodology IBC conference on Submarine Communication. (pp. 1–12).

[3] Ahn, S. H., & Kim, D. S. (2009). Submarine Cable Installation and Protection Methods according as Characteristics of Ocean Environment. Journal of the Korean Society of Marine Environment & Safety, 15(1), 25–32.

[4] Van Maanen, B., Plet, C., Van Der Wielen, P., Meijer, S., De Wild, F., & Steennis, F. (2015). Failures in underground power cables–return of experience. IEEE Int. Conf. Insulated Power Cables, 1–5.

[5] Bawart, M., Marzinotto, M., & Mazzanti, G. (2016). Diagnosis and Location of Faults in Submarine Power Cables. IEEE Electrical Insulation Magazine, 32(4), 24–37.

[6] Wang, W., Yan, X., Li, S., Zhang, L., Ouyang, J., & Ni, X. (2021). Failure of submarine cables used in high-voltage power transmission: Characteristics, mechanisms, key issues and prospects. IET Generation, Transmission & Distribution, 15(9), 1387–1402.

[7] Hughes, T. J., Henstock, T. J., Pilgrim, J. A., Dix, J. K., Gernon, T. M., & Thompson, C. E. L. (2015). Effect of sediment properties on the thermal performance of submarine HV cables. IEEE Transactions on Power Delivery, 30(6), 2443–2450.

[8] Chen, Y., Wang, S., Hao, Y., Yao, K., Li, H., Jia, F., Yue, D., Shi, Q., Cheng, Y., & Huang, X. (2021). Temperature monitoring for 500 kV oil-filled submarine cable based on BOTDA distributed optical fiber sensing technology: Method and application. IEEE Transactions on Instrumentation and Measurement, 71, 1–10.

Figures

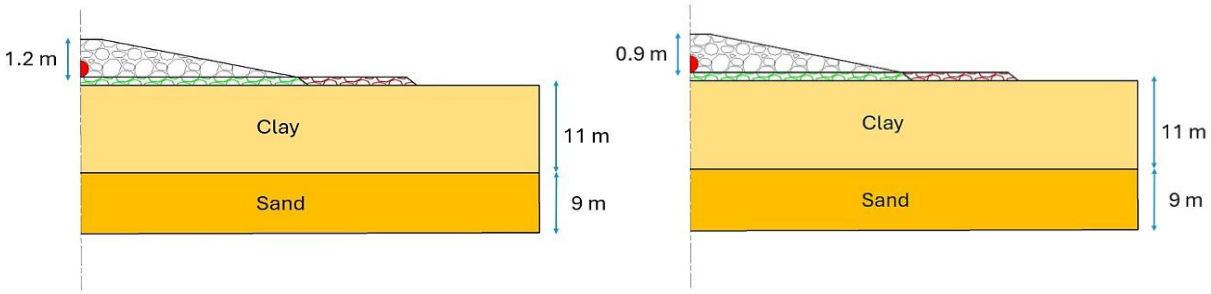

Figure 1: *Berm geometries*

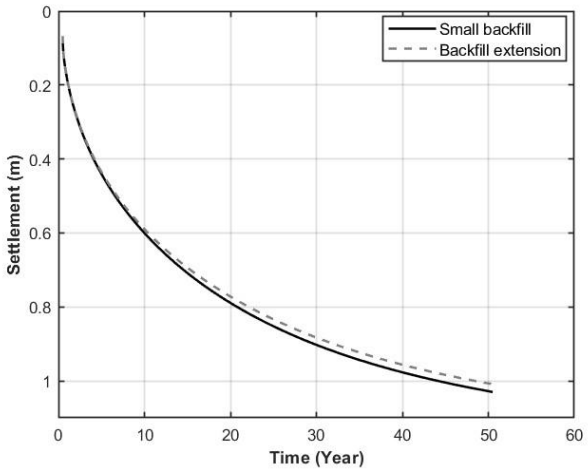

Figure 2: *The final settlement for different widths of backfills*

Thaw-Induced Ground Subsidence at a Radar Site in Arctic Canada

Zachary MacDonald-Ducharme, Victor Pozsgay, Mehdi Pouragha, Stephan Gruber

Carleton University, Canada

zacharymacdonaldduch@cmail.carleton.ca

Keywords: ground subsidence, permafrost degradation, frost heave, thermokarst, thermo-hydro-mechanical modelling

Abstract

Permafrost degradation is a well-documented process with considerable impact on infrastructure in Arctic regions. Thaw subsidence poses a particular challenge to the stability of pile foundations as the once stable frozen soil degrades in strength and stiffness. In this study we investigate a radar site in northern Canada, where ongoing permafrost degradation threatens the integrity of pile-supported structures. This site was selected due to visible evidence of large subsidence (up to 3 m, with 0.20–0.25 m observed in the past year, see Figure 1a), the formation of ponds (Figure 1b), its strategic importance, and the availability of geotechnical and climatic data. The first stage of the study will be to characterize soil parameters required for thaw consolidation analysis.

Preliminary site investigations revealed the stratigraphy of ~0.20m of topsoil/organic mat, underlain by at least 1 to 1.5m of diamict composed of clayey silt, with increasing gravel content at depth. The active layer in the undisturbed tundra is very shallow, in many cases being immediately beneath the organic cover; in all test holes, soil samples with more than 50% ice by volume were observed. The stratigraphy is consistent with general records; defined as till-blanket, with surficial depth likely falling in between 2 – 10m based on available borehole data [1] and generally fine-grained [1, 2]. Buried ground ice and ice wedges are expected [3].

Climate analysis, based on reanalysis data [4, 5, 6] (Figure 2), supported by intermittent local weather observations on site indicates an increase in mean annual air temperature from -10.5oC in 1948 to -7.2oC in 2024 (Figure 3, equivalent to 3-4oC/century). A series of 15 near-surface thermistors were installed in five areas to record ground temperatures, to be later compared with simulated temperatures at the ground surface boundary.

Together, soil characterization and ground temperature records form the foundation for our numerical simulations. The thaw consolidation theory of Morgenstern and Nixon [7] offers a first-order model, while 2D THM FEM simulations are planned to improve projections of future ground response under warming climate scenarios.

References

[1] S.L. Smith, M.M. Burgess, J. Chartrand, and D.E. Lawrence. Digital borehole geotechnical database for the Mackenzie Valley/Delta region. Tech. Rep. 4924, 2005.

[2] G.S. Hanna. Surficial geology of Canada, 2014. Can. Geosci. Map 195 (conv. of Map 1880A), 1:5,000,000, 2014.

[3] Mines Canada. Dept. of Energy and Resources. Topographic Map MCR 4177, 1:50,000, 1972.

[4] H. Hersbach, B. Bell, P. Berrisford, et al. ERA5 hourly data on pressure levels (1940–present). C3S CDS, 2023. DOI:10.24381/cds.bd0915c6 (accessed 19-Aug-2025).

Figures

a) b)

Figure 1: *a) Effects of ground subsidence on piles and b) Thermokarst pond at a radar site near Inuvik, Canada*

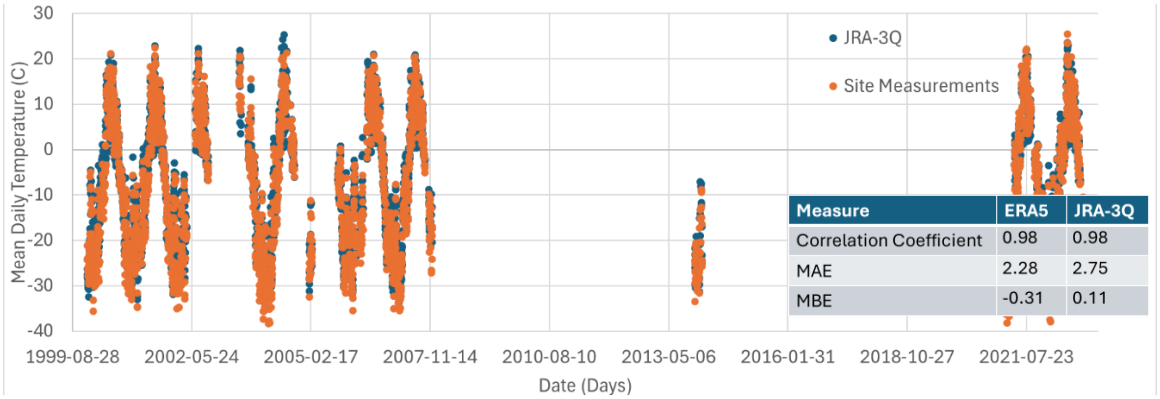

Measure	ERA5	JRA-3Q
Correlation Coefficient	0.98	0.98
MAE	2.28	2.75
MBE	-0.31	0.11

Figure 2: *Comparison of JRA-3Q reanalysis with site measurements from weather observation station*

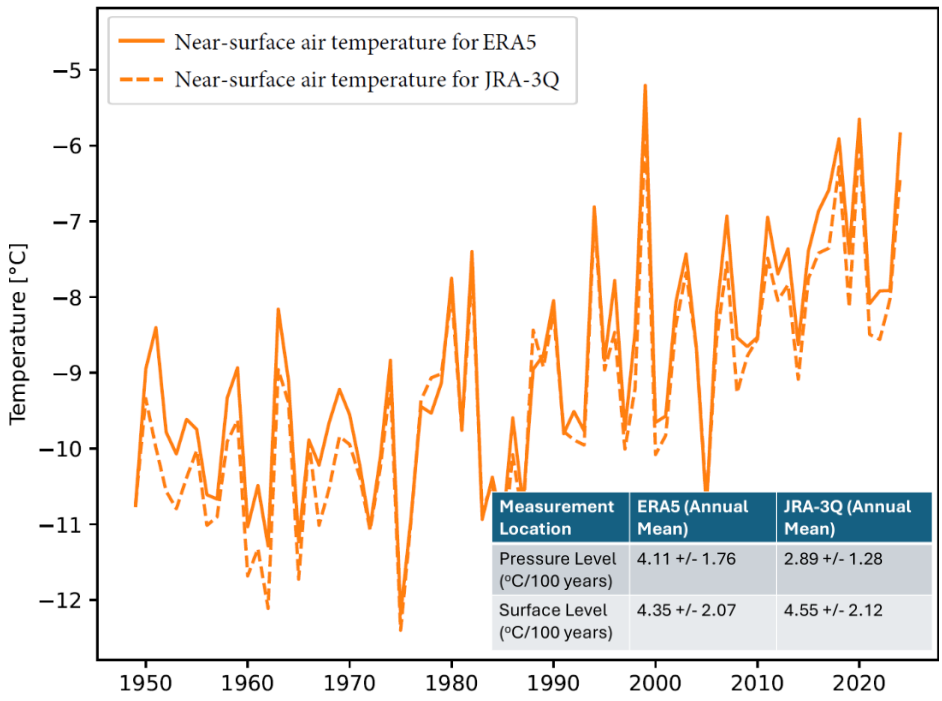

Measurement Location	ERA5 (Annual Mean)	JRA-3Q (Annual Mean)
Pressure Level (°C/100 years)	4.11 +/- 1.76	2.89 +/- 1.28
Surface Level (°C/100 years)	4.35 +/- 2.07	4.55 +/- 2.12

Figure 3: *Reanalysis from ERA5 and JRA-3Q climate models at near-surface level [4, 5, 6]*

A Two-System Heat Transfer Approach to Soil Freezing

Chenjie Ruan, Wojciech T. Solowski

Department of Civil Engineering, Aalto University, Rakentajanaukio 4 A, 02150 Espoo, Finland

chenjie.ruan@aalto.fi, wojciech.solowski@aalto.fi

Keywords: Ground freezing, Numerical modelling, Pore structures, Hydrothermal conditions

Abstract

Since the early 20th century, the frozen soil problem has attracted a lot of attentions, and many theoretical and numerical models on soil freezing have been proposed, including the contributions from Miller (1978), Nishimura et al. (2009) and Gao et al. (2022). These models assume that the temperature of the soil skeleton and water is the same. However, local thermal equilibrium conditions impose many limitations (see, for example, Kaviany (2012) and Roshan et al. (2014)). Furthermore, most of these models assume the existence of a continuous unfrozen water film around soil particles during freezing, while recently Jia et al. (2019) have shown that when sand freezes, the water on the surface of the soil particles freezes first, see Figure 1.

We proposed a new thermo-hydraulic framework for soil freezing, which assumes that soil particles and water surrounding them may have different temperatures (Ruan et al., 2025). The proposed framework is suitable for low-clay-content soils. Based on the particle size distribution, which is the main input for the model, the framework estimates pore size distribution. Based on the estimated pore size distribution, we model the changes in the pore sizes during freezing and associated changes in the soil permeability. The model replicates phase transition, water migration, the existence of the frozen fringe, and the evolution of frost-heave in time.

The framework is implemented in MATLAB by using the finite difference method. The calculation results demonstrate a good agreement between simulations and experimental observations (see Figure 2). Therefore, it seems that the proposed framework, which uses the particle size distribution as an input, can be used for the assessment of frost heave evolution in soils where the amount of clay is small. Currently, we are working on extending the model so it includes mechanical coupling, as the external stress significantly affects the amount of the frost heave and its evolution.

References

Gao, H., Ghoreishian Amiri, S. A., Kjelstrup, S., Grimstad, G., Loranger, B., & Scibilia, E. (2022). Formation and growth of multiple, distinct ice lenses in frost heave. International Journal for Numerical and Analytical Methods in Geomechanics. https://doi.org/10.1002/nag.3461

Jia, H., Ding, S., Wang, Y., Zi, F., Sun, Q., & Yang, G. (2019). An NMR-based investigation of pore water freezing process in sandstone. Cold Regions Science and Technology, 168, 102893.

Kaviany, M. (2012). Principles of heat transfer in porous media. Springer Science & Business Media.

Konrad, J.-M., & Morgenstern, N. R. (1980). A mechanistic theory of ice lens formation in fine-grained soils. Canadian Geotechnical Journal, 17(4), 473–486.

Lyu, C., Grimstad, G., Nishimura, S., Singh, P., & Singh, D. N. (2024). Pore pressure coefficient in frozen soils. Géotechnique, 0(0), 1–4. https://doi.org/10.1680/jgeot.24.00100

Miller, R. D. (1978). Frost heaving in non-colloidal soils. Proceedings, 3rd International Conference on Permafrost, 1978.

Nishimura, S., Gens, A., Olivella, S., & Jardine, R. J. (2009). THM-coupled finite element analysis of frozen soil: formulation and application. Géotechnique, 59(3), 159–171.

Roshan, H., Cuthbert, M. O., Andersen, M. S., & Acworth, R. I. (2014). Local thermal non-equilibrium in sediments: Implications for temperature dynamics and the use of heat as a tracer. Advances in Water Resources, 73, 176–184. https://doi.org/https://doi.org/10.1016/j.advwatres.2014.08.002

Ruan, C., A. Gupta, & Sołowski, W. T. (2025). A Two-System Heat Transfer Approach to Soil Freezing: Numerical simulation of frost heave considering local thermal non-equilibrium effects [Manuscript submitted for publication]. Department of civil engineering, Aalto univeristy.

Figures

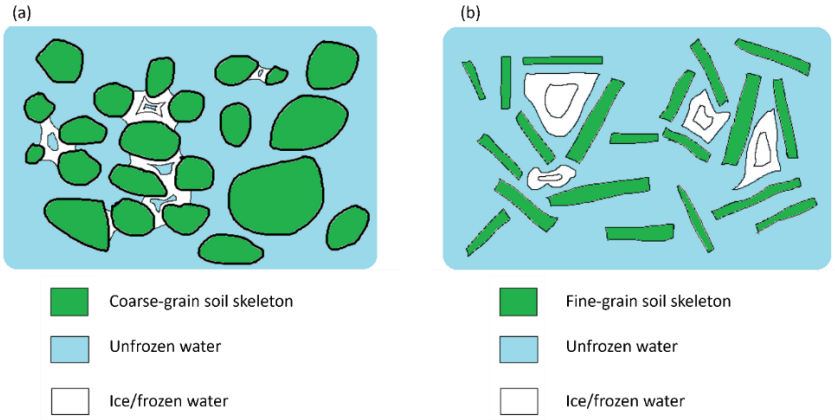

Figure 1: *Illustration of ice formation in pores during freezing in (a) coarse-grain and (b) fine-grain soil skeleton adapted from Lyu et al. (2024)*

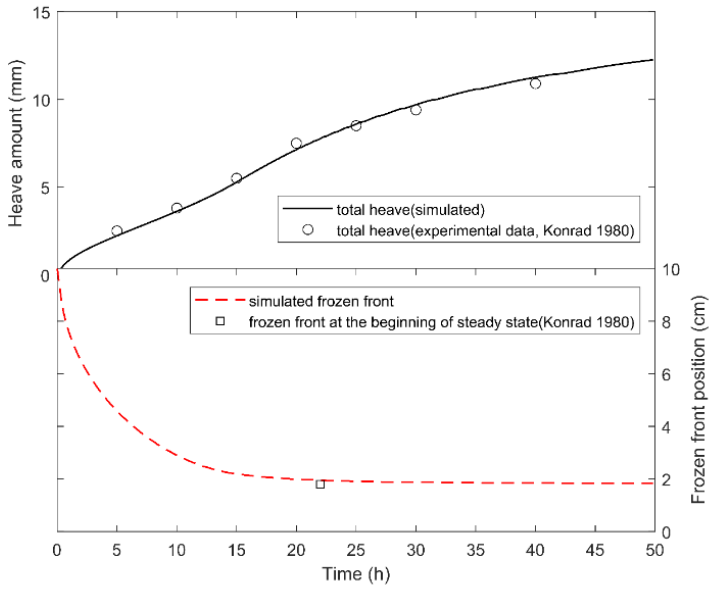

Figure 2: *Heave amount and frozen front during freezing in NS-5 conducted by Konrad & Morgenstern (1980)*

Estimating vibrations induced by dynamic compaction using the finite element method

Naum Shpata, Wojciech T. Sołowski

Department of Civil Engineering, Aalto University, Rakentajanaukio 4 A, 02150 Espoo, Finland

naum.shpata@aalto.fi, wojciech.solowski@aalto.fi

Keywords: dynamic compaction, vibrations, FEM, impact

Abstract

Dynamic compaction is a soil improvement method in which a heavy tamper is repeatedly dropped onto the ground. When the tamper hits the ground, it induces strong vibrations that may be harmful to nearby structures. The research aim is to numerically simulate the impact of the tamper and replicate the amount of vibration caused by the dynamic compaction at a distance. However, a key challenge arises: the recorded acceleration signal from the tamper (see Shpata, 2024) cannot be used directly in Plaxis software, which does not accommodate initial velocity and deceleration. To overcome this, we derived velocity and displacement signals from the measured acceleration to serve as input for the simulations (Fig. 1) (Shpata et al., 2025). This raises the central research question: which of these derived signals provides the most reliable prediction of ground vibrations?

In addition to defining the input, accurately modelling the soil response was essential. We developed a custom constitutive model for soil that accounts for shear strain–dependent stiffness degradation at small strains and implemented it in PLAXIS 2D. The model requires only two parameters (Shpata, 2024) and is coupled with Rayleigh damping, with damping ratios adjusted based on an empirical curve linking the damping ratio to the shear strain (Darendeli, 2001).

The two input signals, velocity and displacement, produced different outputs in terms of particle velocity (Fig. 2) and vertical acceleration (Fig. 3). Comparison with field tests revealed that neither signal was universally superior: the velocity input provided a better prediction of peak vertical acceleration, while the displacement input yielded more accurate estimates of peak particle velocity. These results raise questions about which approach should be trusted, highlighting the importance of engineering judgment. Moreover, we now explore alternative numerical methods, such as the Material Point Method, which may offer a more robust solution for simulating the impact process.

References

Darendeli, M. B. (2001). Development of a new family of normalized modulus reduction and material damping curves. The University of Texas at Austin.

Shpata, N. (2024). Numerical replication of vibrations caused by dynamic compaction (Master's thesis). Aalto University, Espoo, Finland.

Shpata, N., Kanty, P., & Sołowski, W. T. (2025). A simple framework to predict vibrations due to dynamic compaction [Manuscript submitted for publication]. Soil Dynamics and Earthquake Engineering.

Figures

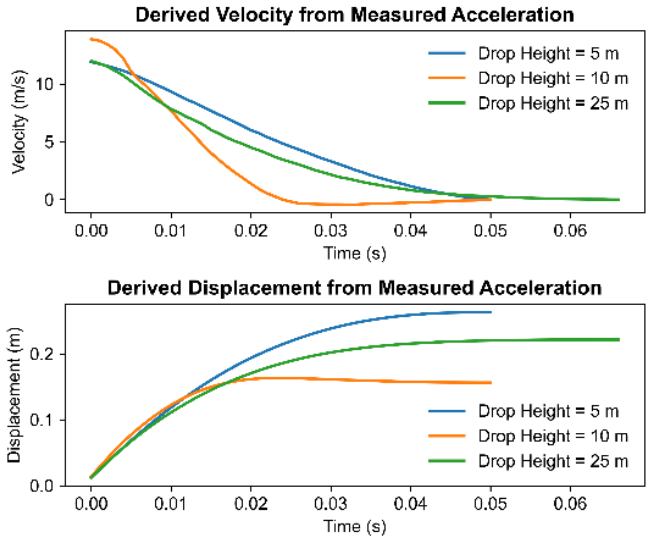

Figure 1: *Derived input signal (Shpata et al., 2025).*

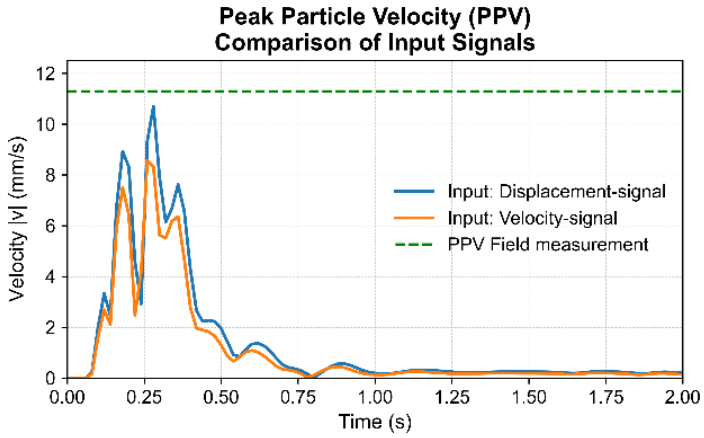

Figure 2: *Estimation of the peak particle velocity (Shpata et al., 2025).*

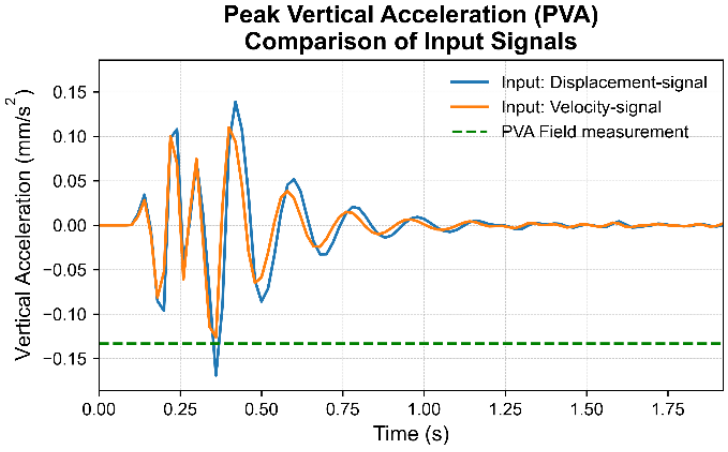

Figure 3: *Estimation of the peak vertical acceleration (Shpata et al., 2025).*

Numerical Simulation of Soil Mixing Using the Generalized Interpolation Material Point Method

Ying Ma, Wojciech T. Sołowski

Department of Civil Engineering, Aalto University, Rakentajanaukio 4 A, 02150 Espoo, Finland

ying.1.ma@aalto.fi, wojciech.solowski@aalto.fi

Keywords: Soil Mixing, Ground Improvement, Material Point Method, Generalized Interpolation Material Point Method

Abstract

Deep soil mixing has become one of the most widely used ground improvement techniques. It is an in-situ admixture stabilisation method, developed and put into practice in Japan and Nordic countries in the 1970s for the stabilisation of deep soil using cement and/or lime (Kitazume & Terashi, 2013). In the Nordic countries, soil mixing is particularly often used to improve the shear strength and stiffness of soft clays.

Numerical simulation of the mixing process is challenging due to the extreme shear deformations involved. Traditional approaches, such as the Finite Element Method are often unsuitable due to severe mesh distortion that occurs under large deformations. The Material Point Method is one of the few continuum-mechanics-based methods that can simulate the process, as the material points move across a fixed computational grid, thereby avoiding mesh distortion (Sulsky et al., 1994). This research uses the Generalized Interpolation Material Point Method, which introduces weighting functions (also known as shape functions or interpolation functions) and gradient weighting functions with a higher degree of smoothness, thereby preventing abrupt stress changes when material points cross cell boundaries (Bardenhagen & Kober, 2004; Kiriyama & Higo, 2020; Sołowski et al., 2021).

Moreover, most existing research has focused on the strength properties of soil after mixing (Bouassida & Porbaha, 2004; Wonglert et al., 2018), whereas the efficiency of the mixing process has received limited attention.

In this research, a simplified soil mixing process in Malmi clay—a typical Finnish clay with high plasticity and low shear strength, was numerically replicated using the GIMP implemented in the Uintah software (http://uintah.utah.edu). In the simulation, the soil was modelled with Mohr–Coulomb constitutive model to capture its plastic behaviour, while the rotating blade was represented as a rigid body.

To evaluate the mixing performance, the evolution of soil deformation and particle distribution during the simulated process was analysed, and the Lacey mixing index (Lacey, 1954) was applied to quantitatively assess the mixing efficiency. The results reveal highly heterogeneous mixing, with regions located beyond approximately 1.3 times the blade radius exhibiting poor mixing. Furtherer, the mixing efficiency reaches a stable level after only a few blade rotations.

References

Bardenhagen, S. G., & Kober, E. M. (2004). The generalized interpolation material point method. Computer Modeling in Engineering and Sciences, 5(6), 477-496.

Bouassida, M., & Porbaha, A. (2004). Ultimate bearing capacity of soft clays reinforced by a group of columns—application to a deep mixing technique. Soils and foundations, 44(3), 91-101.

Kitazume, M., & Terashi, M. (2013). The deep mixing method (Vol. 21). London: CRC press.

Kiriyama, T., & Higo, Y. (2020). Arbitrary particle domain interpolation method and application to problems of geomaterial deformation. Soils and Foundations, 60(6), 1422-1439.

Lacey, P. M. C. (1954). Developments in the theory of particle mixing. Journal of applied chemistry, 4(5), 257-268.

Sołowski, W. T., Berzins, M., Coombs, W. M., Guilkey, J. E., Möller, M., Tran, Q. A., ... & Soga, K. (2021). Material point method: overview and challenges ahead. Advances in Applied Mechanics, 54, 113-204.

Sulsky, D., Chen, Z., & Schreyer, H. L. (1994). A particle method for history-dependent materials. Computer methods in applied mechanics and engineering, 118(1-2), 179-196.

Wonglert, A., Jongpradist, P., Jamsawang, P., & Larsson, S. (2018). Bearing capacity and failure behaviors of floating stiffened deep cement mixing columns under axial load. Soils and Foundations, 58(2), 446-461.

Figures

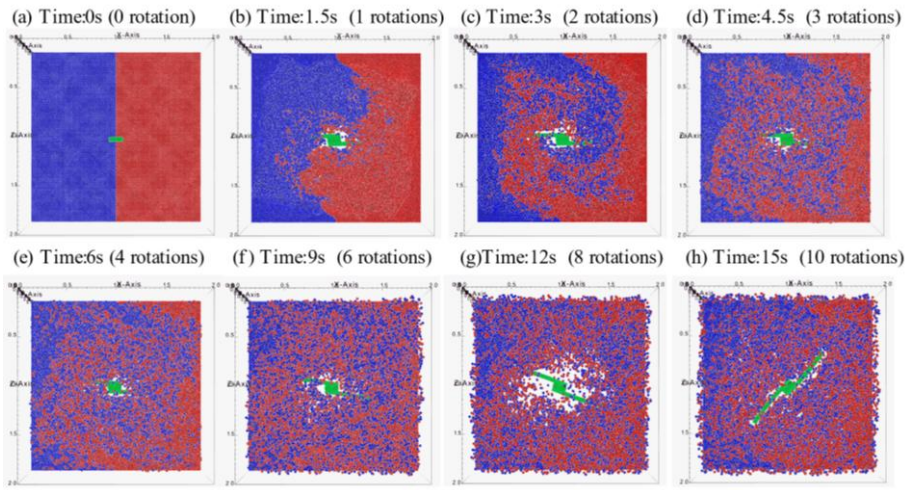

Figure 1: *Top view of blue and red material points at eight different times. The blade rotates in a clockwise direction at speeds of 40rpm.*

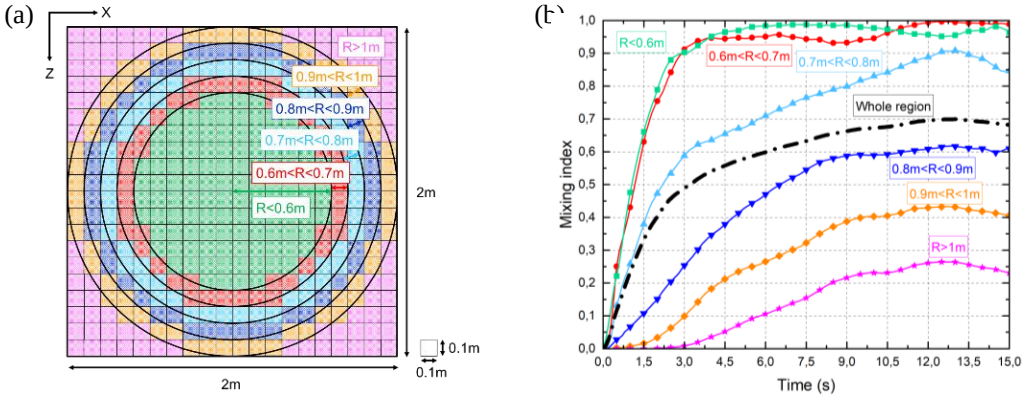

Figure 2: *(a) Top views of various calculation regions. (b) relationship between Lacey mixing index, M, over time in the indicated regions.*

Laboratory and numerical investigation on the poro-elasto-visco-plastic behaviour of in-situ heated Callovo-Oxfordian claystone

Junfeng Ren[1], Philipp Braun[1,*], Siavash Ghabezloo[1], Carlos Plúa[2], and Minh Ngoc Vu[2]

[1]Navier Laboratory, 6-8 avenue Blaise Pascal, Champs-sur-Marne, France

[2]ANDRA, Châtenay-Malabry, France

[*]philipp.braun@enpc.fr

Keywords: Callovo-Oxfordian Claystone, deviatoric testing, poro-mechanics, viscoplasticity

Abstract

The Callovo–Oxfordian (COx) claystone has been selected by the French National Radioactive Waste Management Agency (Andra, 2005) as the potential host rock for the future deep geological repository for high-level radioactive waste. During operation, the COx formation may experience thermal loading up to 90 °C due to the decay heat of radioactive nuclides. While its thermo-hydro-mechanical (THM) behaviour under natural conditions is well documented (Menaceur et al., 2015; Belmokhtar et al., 2018; Braun et al., 2021), potential changes in hydro-mechanical properties after thermal cycling remain less explored.

This study investigates the transversely isotropic poro-elasto-visco-plastic behaviour of COx claystone after in-situ heating–cooling experiments conducted by Andra (Plúa et al., 2024). Six deviatoric tests were performed on resaturated samples, loaded either parallel or perpendicular to bedding along different stress paths until failure (Figure 1a). Drained and undrained poro-elastic behaviours were characterised via rapid unloading and drainage phases. Elastic and plastic strains were decomposed with loading cycles (Figure 1b). A set of stress dependent elastic parameters was calibrated using drained elastic strains. Plastic strain analysis identified the onset of plasticity and plastic flow direction. Failure characteristics were similar to natural samples, and stress path variations showed no significant influence on the critical state (Figure 2a). The permeability parallel to the bedding plane was calibrated with poro-elastic unloading steps and showed no significant effect of in-situ heating tests.

To reproduce the observed behaviour, an anisotropic poro-elasto-visco-plastic constitutive model was developed using MFront (Helfer et al., 2015) based on the Asymmetric Cam-Clay (ACC) formulation (Samudio, 2017), extended with non-uniform scaling for anisotropic plasticity (Mánica et al., 2016) and an overstress concept for viscoplasticity (Perzyna, 1966). Implemented in FEniCSx (Scroggs et al., 2022), this model was calibrated with the laboratory results and simulations successfully reproduced the viscoplastic behaviour (Figure 2b).

These findings indicated that the COx claystone is likely to preserve its favourable barrier properties as the host rock of repository after thermal cycling.

References

Andra, “Evaluation of the feasibility of a geological repository in an argillaceous formation,” Andra, Chatenay-Malabry, France, 2005.

H. Menaceur, P. Delage, A.-M. Tang, and N. Conil, “The thermo-mechanical behaviour of the callovo-oxfordian claystone,” International Journal of Rock Mechanics and Mining Sciences, vol. 78, pp. 290–303, 2015.

M. Belmokhtar, P. Delage, S. Ghabezloo, and N. Conil, "Drained Triaxial Tests in Low-Permeability Shales: Application to the Callovo-Oxfordian Claystone," Rock Mechanics and Rock Engineering, vol. 51, no. 7, pp. 1979–1993, Jul. 2018.

P. Braun, S. Ghabezloo, P. Delage, J. Sulem, and N. Conil, "Transversely Isotropic Poroelastic Behaviour of the Callovo-Oxfordian Claystone: A Set of Stress-Dependent Parameters," Rock Mechanics and Rock Engineering, vol. 54, no. 1, pp. 377–396, Jan. 2021.

M. Mánica, A. Gens, J. Vaunat, and D. F. Ruiz, "A cross-anisotropic formulation for elasto-plastic models," Géotechnique Letters, vol. 6, no. 2, pp. 156–162, 2016.

C. Plúa, M. N. Vu, R. de La Vaissière, and G. Armand, "In situ thermal hydrofracturing behavior of the callovo-oxfo2015rdian claystone within the context of the deep geological disposal of radioactive waste in france," Rock Mechanics and Rock Engineering, vol. 57, no. 6, pp. 4265–4283, 2024.

T. Helfer, B. Michel, J.-M. Proix, M. Salvo, J. Sercombe, and M. Casella, "Introducing the open-source mfront code generator: Application to mechanical behaviours and material knowledge management within the pleiades fuel element modelling platform," Computers & Mathematics with Applications, vol. 70, no. 5, pp. 994–1023, 2015.

M. Samudio, "Modelling of an oil well cement paste from early age to hardened state: hydration kinetics and poromechanical behaviour," Ph.D. dissertation, Université Paris-Est, 2017.

P. Perzyna, "Fundamental problems in viscoplasticity," Advances in applied mechanics, vol. 9, pp. 243–377, 1966.

M. W. Scroggs, I. A. Baratta, C. N. Richardson, and G. N. Wells, "Basix: a runtime finite element basis evaluation library," Journal of Open Source Software, vol. 7, no. 73, p. 3982, 2022.

Figures

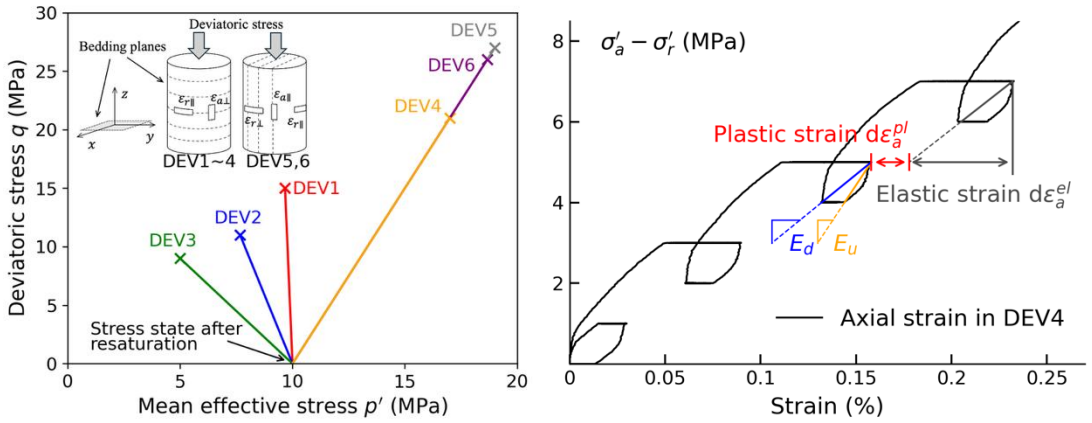

Figure 1: *Presentation of stress paths (left) and decomposition of measured strains (right) of deviatoric tests.*

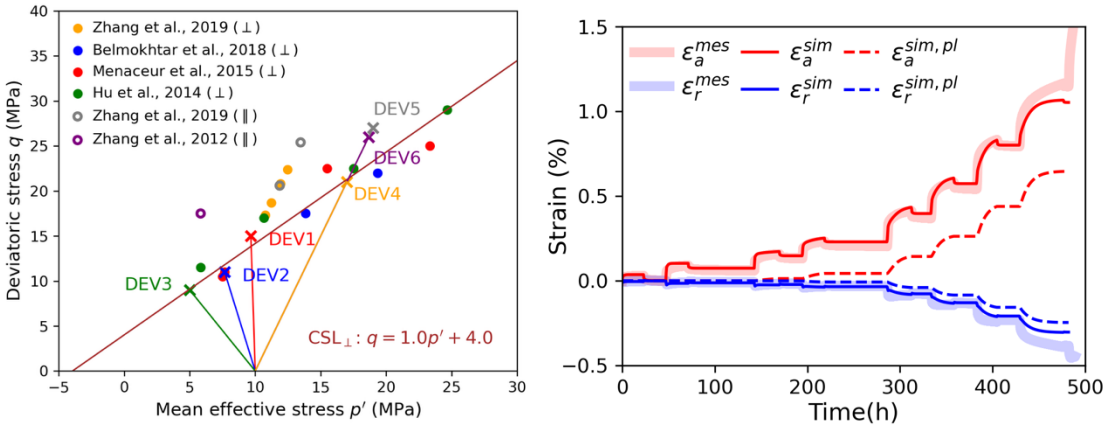

Figure 2: *Critical state of tests (left) and the reproduction of test DEV4 (right).*

Measurement of internal dynamics in continuously flowing granular media

Andrés Escobar[1,2], James Baker[3], François Guillard[2], Thierry Faug[1] and Itai Einav[2,*]

[1]Université Grenoble Alpes, CNRS, INRAE, IRD, Grenoble INP, IGE, Grenoble, France.

[2]School of Civil Engineering, University of Sydney, Sydney, NSW, Australia.

[3]School of Computer Science and Mathematics, Liverpool John Moores University, Liverpool, UK.

** Itai.Einav@sydney.edu.au*

Keywords: Granular flows, Secondary flows, X-ray radiography

Abstract

In mountain regions, geophysical flows such as avalanches, landslides, and rockfalls pose a recurring threat to people and infrastructure. When little water is present, these flows can be treated as granular flows, made of thousands of particles colliding with each other as they move downhill. When such flows hit an obstacle, their mainly unidirectional internal motion can be disrupted, often producing 'secondary flows', which are internal displacements in directions other than the main one. Secondary flows often create changes in the free surface, such as undulations or dips. Examples of secondary flows in granular media can be found in Couette cells [1] and even in Martian avalanches [2].

Most studies of secondary flows in granular materials use simulations or experimental setups to study the internal dynamics indirectly, either by inferring them from free surface deformations [1] or by using CT scans of flows in the quasi-static regime (where the flow is arrested during imaging [3]). However, a direct measurement of secondary flows in faster flows remains elusive.

Here, we present an experimental setup to measure internal velocities in granular flows using x-ray radiography. The setup consists of an open channel ending in a perpendicular wall with a bottom gap for flow exit. The open channel sits above a conveyor belt that controls the granular flow speed as it displaces towards the perpendicular wall. Upon impact, the granular flow forms a heap against the wall. The height of the perpendicular wall is adjusted to balance the outgoing flow rate with the incoming flow rate from the reservoir, keeping the formed heap steady over time. The steady flow is measured using x-ray radiography from two orthogonal directions. A sketch of the experimental setup, with snapshots of the recorded radiographs in panels (a) and (b), is displayed in Fig.1.

From the radiographs, we reconstruct the time-averaged free surface by correlating the intensity from the top-view depth-averaged radiograph with the width-averaged height from the side-view radiograph. The measured free surface reveals a dip at the base of the heap in the centre of the flume, as shown in Fig.2a. This dip appears to be caused by secondary flows displacing from the side walls towards the centre before the heap begins. To investigate this, we perform a PIV analysis and implement the rheography algorithm [4]. This rheography algorithm connects the common velocity component between the radiographs. Next, by solving a deconvolution problem, it estimates the 3D velocity field in the main flow direction. These measurements confirm the presence of secondary flows. Furthermore, the velocity measurements enable us to estimate the local inertial number, revealing a flow that extends beyond the quasi-static regime around the dip, as shown in Fig.2b.

Finally, the experiments are complemented by a discrete element method (DEM) simulation, which reproduces the observed dip and secondary flows. These findings help bridge the gap between theoretical studies of secondary flows and experimental approximations by providing direct measurements of the internal velocity fields and free surface in continuously flowing granular flows.

References

[1] Krishnaraj, K. & Nott, P. R. A dilation-driven vortex flow in sheared granular materials explains a rheometric anomaly. Nat. Commun. 7,10630 (2016).

[2] Magnarini, G., Mitchell, T. M., Grindrod, P. M., Goren, L. & Schmitt, H. H. Longitudinal ridges imparted by high-speed granular flow flowmechanisms in martian landslides. Nat. Commun. 10, 4711 (2019).

[3] Wortel, G. et al. Heaping, secondary flows and broken symmetry inflows of elongated granular particles. Soft Matter 11, 2570–2576(2015).

[4] Baker, J., Guillard, F., Marks, B. & Einav, I. X-ray rheography uncovers planar granular flows despite non-planar walls. Nat. Commun. 9,5119 (2018).

[5] Escobar, A., Baker, J., Guillard, F. et al. Experimental confirmation of secondary flows within granular media. Nat Commun 16, 7446 (2025).

Figures

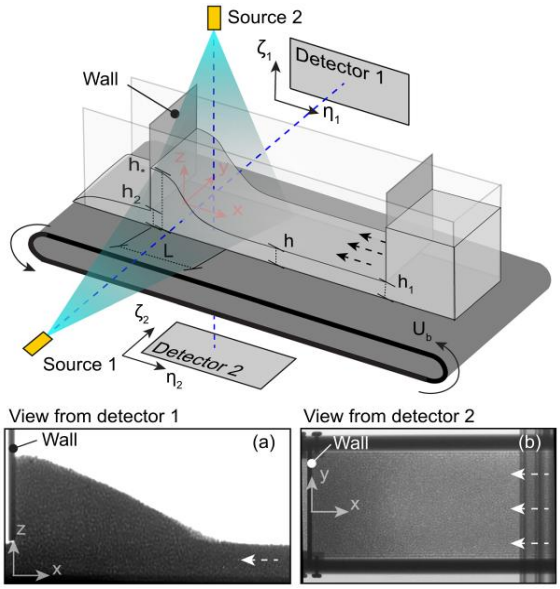

Figure 1: *Sketch of the experimental setup with the main dimensions highlighted. Panels (a) and (b) display the radiographs from detectors 1 and 2, respectively. Figure extracted from [5].*

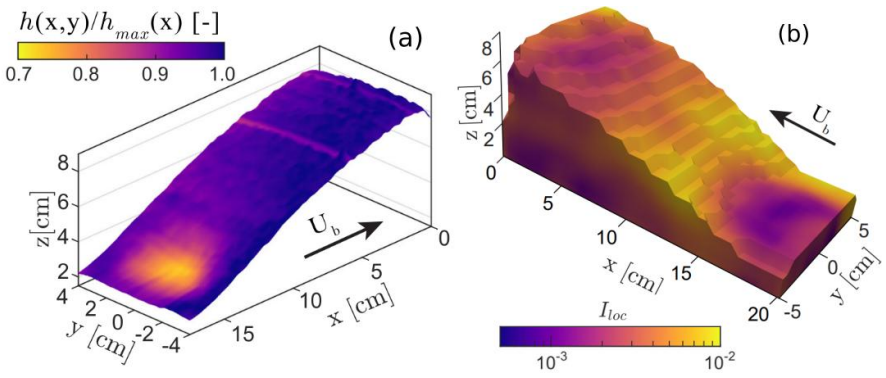

Figure 2: *Carried analysis from the recorded radiographs. Panel (a): Free surface, with colours displaying the relative height along the x-axis. Panel (b): Local inertial number I_{loc} . Figures extracted from [5].*

Numerical Modelling of granular flow dynamics utilizing Granular Generalized Interpolation Material Point Method

Hakimeh Koochi[1], Wojciech T. Solowski[1]

[1]Department of Civil Engineering, Aalto University, Rakentajanaukio 4 A, 02150 Espoo, Finland

hakimeh.koochi@aalto.fi

Keywords: Granular Material Point Method, Granular flow dynamics, Uintah-MPM software

Abstract

The aim of this work is to present the enhancements to the Granular Generalized Interpolation Material Point Method (GranularGIMP) initially developed by Seyedan and Solowski (2021, 2023). The optimized algorithm was implemented within the Uintah computational framework, an open-source, high-performance environment for simulating problems involving large deformations (Germain et. al. 2000).

At high mean stress and low void ratio, granular materials (e.g, sand) behave as solids. As deformation increases and mean stress decreases, grains may begin to flow. At sufficiently low mean stresses, inter-particle connections may be lost, and thus some grains move into a stress-free gas-like state (e.g., Kamrin 2008). While capturing all aspects of such a complex dynamic within a single numerical framework remains a major challenge, GranularGIMP proposes a more realistic numerical modelling of associated phase transitions.

Figure 1 compares the algorithms of the Generalized Interpolation Material Point Method (GIMP) by Bardenhagen and Kober (2004) and the GranularGIPM. In GIMP, granular materials are represented by material points cast over the background computational grid. Each material point is associated with a domain that governs the interpolation of data between nodes and points. GIMP relies on a global computational grid that considers all material points representing a granular material as a continuum body, independent of the inter-particle distances between the grains.

As shown in Figure 1(B), GranularGIMP uses the maximum size of a material point's domain, determined by the material's maximum void ratio, to capture the physical interactions and connections between the material points. Additionally, we employed Uintah's indexing scheme to form clusters of physically connected points, assigning them new material indices (e.g., mID = 0, 1, 2, 3). Over time, these clusters can merge into larger groups or break into smaller ones. Compared with Figure 1(A), this approach allows each material cluster to contribute individually to its own velocity field computations. Furthermore, by incorporating surface frictional contact, the contact model is applied only when the maximum domains of two material indices overlap, which enhances the accuracy of determining multi-malateral interfaces. The framework can also distinguish between self-contact (material points of the same material) and frictional surface contact with other materials (e.g., walls). Finally, upon material separation, the deformation gradient and volumetric changes are adjusted to address stress-free conditions (Seyedan and Soloweski, 2021; Kamrin, 2008).

Figure 2 shows the simulation results of a free-falling, initially densely packed dry sand (density ρ = 1477 kg/m³ - void ratio e = 0.8) held by an L-shaped elastic wall. Under gravity, the sand material points fall and deposit within the computational domain, with results shown at t = 0.8

s for both GIMP and GranularGIMP that is applied for maximum void ratio emax = 1.21. The sand is modelled as a cohesionless Mohr–Coulomb material with a shear modulus of G = 10 MPa, bulk modulus K = 13 MPa, and internal friction angle ϕ = 31°. Compared with GIMP, GranularGIMP reduces low-range velocities approximately 100 times, and slightly increases the maximum velocity. Additionally, GranularGIPM significantly eliminates unphysical gaps between deposited material points, producing a more natural sand pile.

References

Seyedan, S., & Sołowski, W. T. (2021). From solid to disconnected state and back: Continuum modelling of granular flows using material point method. Computers & Structures, 251, 106545.

Sołowski, W. T., & Seyedan, S. (2023). Granular Material Point Method: unsaturated soil mo-delling. Geomechanics for Energy and the Environment, 34, 100471.

Germain, J. D. D. S., McCorquodale, J., Parker, S. G., & Johnson, C. R. (2000, August). Uintah: A massively parallel problem solving environment. In Proceedings the Ninth International Symposium on High-Performance Distributed Computing (pp. 33-41). IEEE.

Kamrin, K. N. (2008). Stochastic and deterministic models for dense granular flow (Doctoral dissertation, Massachusetts Institute of technology).

Bardenhagen, S. G., & Kober, E. M. (2004). The generalized interpolation material point method. Computer Modeling in Engineering and Sciences, 5(6), 477-496.

Figures

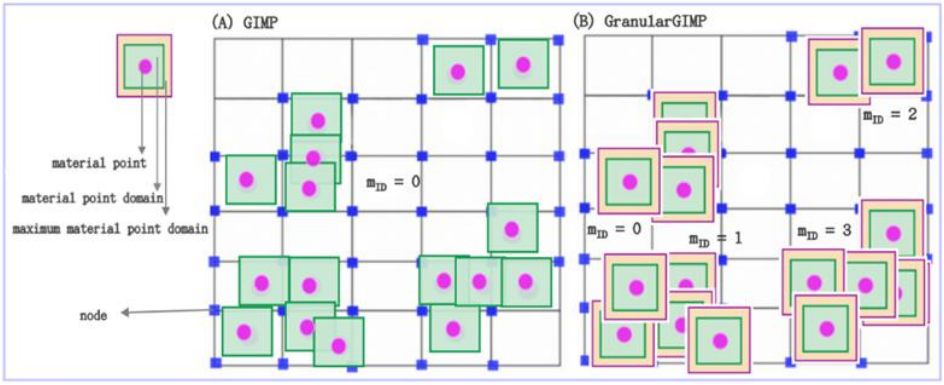

Figure 1: *Schematic of the Generalized Interpolation Material Point method (GIMP) (A), and Granular Generalized Interpolation Material Point method (GranularGIMP) (B).*

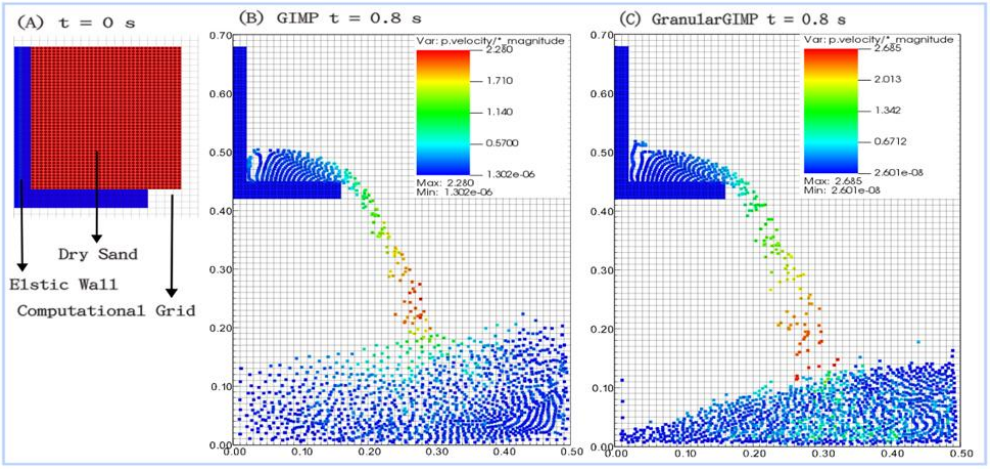

Figure 2: *Simulation of free-falling of densely packed dry sand initially held by an L-shaped elastic wall (A). The variation of free-falling material points representing the dry sand is shown at t = 0.8 s for GIMP (B) and GranularGIMP (C).*

Modelling the micro- and meso-scopic hydromechanical behaviour of damaged low-permeability sedimentary rock (Callovo-Oxfordian claystone)

Echeima Boubakeur, Benoît Pardoen

University of Lyon, ENTPE, LTDS, France

echeima.boubakeur@entpe.fr

Keywords: Micro to Meso-scale, hydromechanical behavior, numerical modelling, finite element method, Callovo-Oxfordian claystone

Abstract

The various orientations of countries towards new green energy productions highlight the need to study the energy transition. Within this context, the production of electricity from nuclear power remains a crucial debate regarding its possible environmental impact. In France, focus is on the deep geological nuclear waste repositories located at -490 meters in the sedimentary Callovo-Oxfordian clay rock, which serves as a natural barrier due to its low permeability, high retention capacity, and self-healing properties. Understanding its behaviour under loading is critical for evaluating the long-term safety of underground repositories.

Numerical modelling is carried out based on a fundamental theorical approach related to damage and cracking under deviatoric loading. It follows the objective of understanding and predicting the hydromechanical behaviour of this rock and to analyse the connection between damage, cracking, and permeability [1]. It is well known that material behaviour at the macroscopic scale is dependent on the material behaviour at smaller scales. A numerical double-scale approach is considered to represent both microscopic and mesoscopic material scales [2]. The research considers a representative elementary area (REA) in two dimensions (2D) based on the finite element method (FEM), with elastic mineral grains and damageable mineral contacts modelled by a cohesive law [2-3]. The REA is defined by micromechanical properties observed experimentally [4], and its mechanical and hydraulic responses are studied. Simulations under biaxial compression with deviatoric loading emphasise the mechanical response of deformable grains and cohesive interfaces, where shear and normal damage mechanisms dominate the observed failure.

The damage initiation in the pre-peak phase (Fig. 1.a) via the softening of mineral contacts (Fig. 2) leads to a loss of linearity of the material response (Fig. 1.a). After having reached the peak deviatoric stress, shear microcracks form a complete shear crack across the mesostructure, causing strain softening (Figs. 1-2). Then the evolution of this crack under an axial deviatoric loading led to a complete decohesion in the post-peak regime, inducing significant displacement between mineral grains and a global softening behaviour (fully damaged in Fig. 2).

The model enables the representation of microcracking induced by microdamage and to consider the relationship between material damage (cracking) and permeability evolution (Fig. 1.b and Fig. 2). In the model, crack openings at mineral grain contacts and through the clay matrix (between clay aggregates) define the crack hydraulic conductivity. The latter depends on the cube of the hydraulic aperture and a Poiseuille flow between parallel plates is assumed under saturated conditions of the cracks [2]. The mesoscale (REA) results in Fig. 1 (b) show an evolution of the hydraulic permeability (major permeability) of the claystone. This occurs during the development of the shear cracking (in

pre-peak regime) and a maximal permeability is reached when the crack fully develops across the mesostructure (in post-peak regime).

The obtained results demonstrate that the numerical model effectively simulates shear-induced cracking and damage at the microscopic and mesoscopic scales, revealing that tangential damage dominates over normal damage under deviatoric loading conditions. Furthermore, cracking implies an increase in the hydraulic permeability. These findings highlight the critical role of relative displacements and damage between mineral grains, at the microscale, in driving short-term permeability evolution in fractured zones. However, the model's hydraulic limitations necessitate refinements, including adjusting the hydraulic model law, considering the mesostructure in a 3D model, and better accounting for tangential displacements, to enable more comprehensive predictions of hydraulic behaviour. This will allow to model large-scale problem of gallery excavation as well as fractured and damaged zone [5].

References

[1] G. Armand, N. Conil, J. Talandier, Darius M. Seyedi. Fundamental aspects of the hydromechanical behaviour of Callovo–Oxfordian claystone: from experimental studies to model calibration and validation, Computers and Geotechnics 85, pp. 277-286, 2017.

[2] A.P. van den Eijnden, P. Bésuelle, F. Collin, R. Chambon. A FE² modelling approach to hydromechanical coupling in cracking-induced localization problems. International Journal of Solids and Structures, 97-98:475-488, 2016.

[3] B. Pardoen, P. Bésuelle, S. Dal Pont, P. Cosenza, J. Desrues. Accounting for Small-Scale Heterogeneity and Variability of Clay Rock in Homogenised Numerical Micromechanical Response and Microcracking, Rock Mechanics and Rock Engineering, 53:2727-2746, 2020.

[4] J-C. Robinet, P. Sardini, D. Coelho, J-C. Parneix, D. Prêt, S. Sammartino, E. Boller, S. Altmann. Effects of mineral distribution at mesoscopic scale on solute diffusion in a clay-rich rock: Example of the Callovo-Oxfordian mudstone (Bure, France), Water Resources Research, 48.5, 2012.

[5] C. Mourlas, B. Pardoen, P. Bésuelle. Large-scale failure prediction of clay rock from small-scale damage mechanisms of the rock medium using multiscale modelling. International Journal for Numerical and Analytical Methods in Geomechanics. 47(7):1254-1288, 2023.

Figures

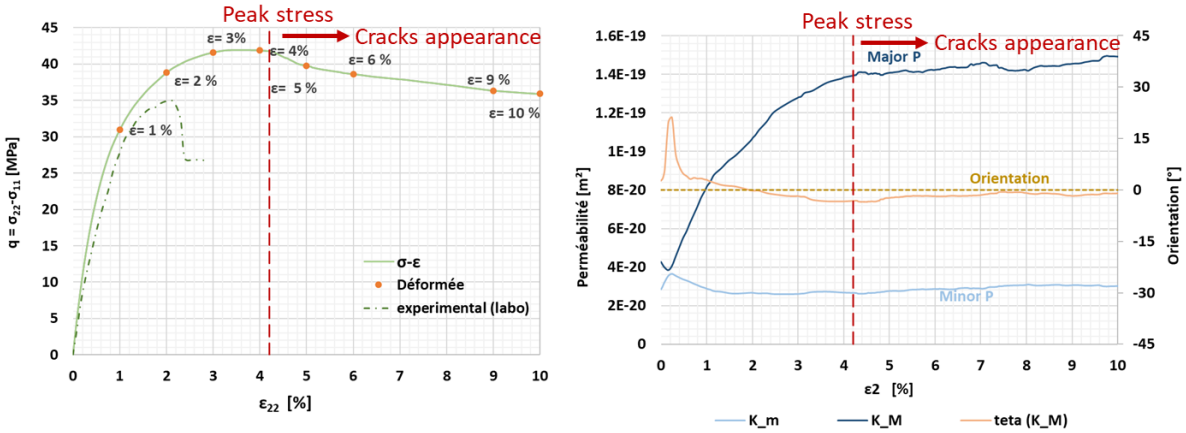

(a) ***(b)***

Figure 1: *Microscopic and mesoscopic hydromechanical clay rock behaviour: (a) material response and (b) permeability evolution.*

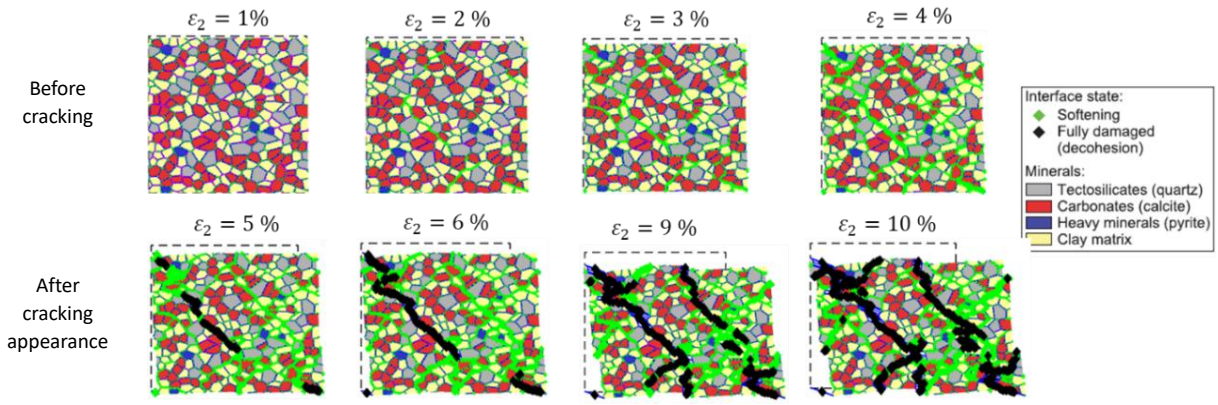

Figure 2: *Evolution of deformation and appearance of microcrack under deviatoric compression.*

A Physically Consistent Unification of Critical State Soil Mechanics and the μ(I)-φ(I) rheologies

Lubbe Retief, Hongyang Cheng, Stefan Luding, Vanessa Magnanimo

Faculty of Engineering Technology, University of Twente, PO Box 217, 7500 AE Enschede, Netherlands

r.lubbe@utwente.nl

Keywords: critical state soil mechanics, granular flow, thermomechanics, solid-fluid transition

Abstract

Granular materials exhibit both solid-like and fluid-like behaviour, which poses a challenge for continuum models of landslides. Current continuum models often cannot capture the full dynamics: from the onset of failure to the final deposition. Therefore, developing a unified framework for predicting granular the regime change has significant implications for the analyzing geohazards.

Critical State Soil Mechanics (CSSM) models, such as Cam Clay, excels at predicting quasi-static, history-dependent behaviour of soils [1, 2]. These models are systematically constructed from the thermomechanics framework [3, 4]. This framework can also derive rate-dependent viscoplasticity models [4]. However, it cannot yet describe rapid steady-state flows of granular materials.

The *μ(I)-φ(I)*-rheologies are highly effective for modelling steady-state flows of hard particles [5]. The generalized rheology framework [6] extends this by merging base models with product functions. These functions correct a shared asymptotic state to include additional effects like softness, gravity near the free surface, and cohesion. The next logical step is to apply this merging approach to more sophisticated models to describe transient and static states.

We unify both CSSM models and the *μ(I)-φ(I)*-rheologies using a thermomechanical approach. Inspired by generalized rheology, we use a product form hypothesis for granular constitutive models. Our model is thermodynamically consistent by construction and introduces no new parameters during the merging process.

This work shows the first numerical benchmarks of our unified model. A constant volume element test confirms that it can capture a rate-dependent steady state and a pressure response due to suppressed dilation. A Material Point Method boundary value problem confirms at a system level, it captures solid-like clogging and fluid-like rate-dependent friction.

References

1] A. N. Schofield and P. Wroth. Critical state soil mechanics. McGraw-hill, 1968.

[2] K. H. Roscoe and J. B. Burland. On the generalised stress-strain behaviour of 'wet' clay. Engineering Plasticity, pages 535-609, 1968.

[3] I. F. Collins and G. T. Houlsby. Application of thermomechanical principles to the modelling of geotechnical materials. Proceedings of the Royal Society of London. Series A, 453(1964):1975-2001, 1997.

[4] G. T. Houlsby and A. M. Puzrin. Rate-dependent plasticity models derived from potential functions. Journal of Rheology, 46(1):113-126, 2002.

[5] GDR MiDi. On dense granular flows. The European Physical Journal E, 14(4):341-365, 2004.

[6] S. Roy et al. A general (ized) local rheology for wet granular materials. New journal of physics, 19(4):043014, 2017.

Modelling Soil Water Content Response to Climate Forcing via Frequency-Domain Transfer Functions

A. Macías-Gutiérrez, Y. Vargas-Alzate, J. Vaunat

Department of Civil and Environmental Engineering, Technical University of Catalonia (UPC), Barcelo-na, Spain

andres.macias@upc.edu

Keywords: Soil moisture, transfer functions, diffusion, spectral analysis; slope stability, reduced-order modeling

Abstract

Soil water content plays a crucial role in slope stability, directly influencing pore pressure dynamics and effective stress states. Accurate, scalable modeling of its spatio-temporal evolution under climatic variability is vital for geotechnical risk assessments (Elia et al., 2017; Ng et al., 2016). Conventional numerical models are computationally expensive, especially for regional-scale or long-term predictions. To overcome this, this research explores Reduced-Order Models (ROMs) based on Transfer Functions (TFs) in the frequency domain. This study presents and compares two ROM strategies: a) Parametric Transfer Functions (PTFs), rooted in analytical diffusion equation. And b) Statistical Transfer Functions (STFs), based on spectral relationships between climatic inputs and soil moisture response.

The data needed for validation was obtained from the *Le Fauga* site (French Pyrenees, 2001–2007), comprising six atmospheric variables and volumetric water content measurements at 10 cm intervals down to 1 m depth. Spectral analysis using Fast Fourier Transforms revealed dominant harmonic modes (annual, diurnal) in climatic forcing, while rainfall and wind exhibited stochastic spectra. Soil moisture spectra showed depth-dependent attenuation and phase lag, consistent with diffusion-dominated processes.

PTFs are derived from analytical solutions of the 1D diffusion equation under harmonic boundary conditions (Carslaw & Jaeger, 1986). Assuming a constant diffusion coefficient κ, moisture content at any depth (θ) is reconstructed using amplitude and phase transfer functions, $TF_{A(z)}$, $TF_{\phi(z)}$, for dominant harmonics:

$$\theta_i = TF_{A_i} A_i \sum_{i=1}^{n} \sin\left(\omega_i t + TF_{\phi_i} + \phi_i + \frac{\pi}{2}\right) \qquad \text{Eqn. 1}$$

Calibration against observed profiles yielded an optimal $\kappa = 1\times10^{-7}$ m²s^{-1} and domain size L = 1.83 m. Using 100 harmonics, PTFs achieved excellent agreement (MSE = 0.0016) across depths, accurately reproducing amplitude decay and phase shifts. Even with only the top 10 harmonics, performance remained robust, particularly at depth, due to natural attenuation of high-frequency signals.

On the other hand, STFs model soil moisture as the output of a system driven by inputs variables, derived via direct Fourier amplitude ratios as established by many authors such as Vargas-Alzate et al., (2024):

$$TF_{i,j}(\omega) = \frac{f_{i,j}(\omega)}{g_j(\omega)} \quad \text{Eqn. 2}$$

where $f_{i.j(\omega)}$ is the Fourier amplitude spectrum of θ_i; $g_{j(\omega)}$ is the Fourier amplitude spectrum of the input variable g; subscripts i and j stand for a specific depth and a given input variable, respectively. The *TF* obtained through Equation 2 can be used to approximate the Fast Fourier Transform of the soil hydraulic response to another record, g_k. By means of the inverse Fourier transform the time evolution of soil water content is reconstructed from the estimated amplitud-frequency spectrum $f_{i,k}$.

$$f_{i,k} \approx TF_{i,j}(\omega) g_k(\omega) \quad \text{Eqn. 3}$$

Multivariate regression, combining temperature, solar radiation, and wind speed, enhanced correlation (R up to 0.64) and improved surface moisture content forecasting accuracy. Progressive layer-by-layer STFs further improved vertical resolution.

PTFs provide physically grounded, high-fidelity predictions, especially for depth-resolved applications. STFs excel in fast assessments, particularly when data or computational resources are limited. Combining both approaches offers a pathway toward hybrid models that leverage physical consistency and spectral efficiency for resilient geotechnical forecasting under climate variability.

References

1. Elia, G., Cotecchia, F., Pedone, G., Vaunat, J., Vardon, P. J., Pereira, C., ... & Osinski, P. (2017). Numerical modelling of slope–vegetation–atmosphere interaction: an over-view. Quarterly Journal of Engineering Geology and Hydrogeology, 50(3), 249-270.

2. Ng, C. W. W., Leung, A. K., & Zhang, L. M. (2016). Effects of surface cover on soil water regime and slope stability. Journal of Geotechnical and Geoenvironmental Engineering, 142(10), 04016053.

3. Carslaw, H. S., & Jaeger, J. C. (1986). Conduction of heat in solids (2nd ed.). Clarendon Press.

4. Vargas-Alzate, Y. F., Barbat, A. H., Pujades, L. G., Pinzón, L. A., Gonzalez, J. M., Ramirez, J., & Rastellini, F. (2024). Characterization of free-field seismic motions for soil-structure inte-raction analysis of nuclear structures using enhanced transfer functions. Soil Dynamics and Earthquake Engineering, 179, 108494.

Figures

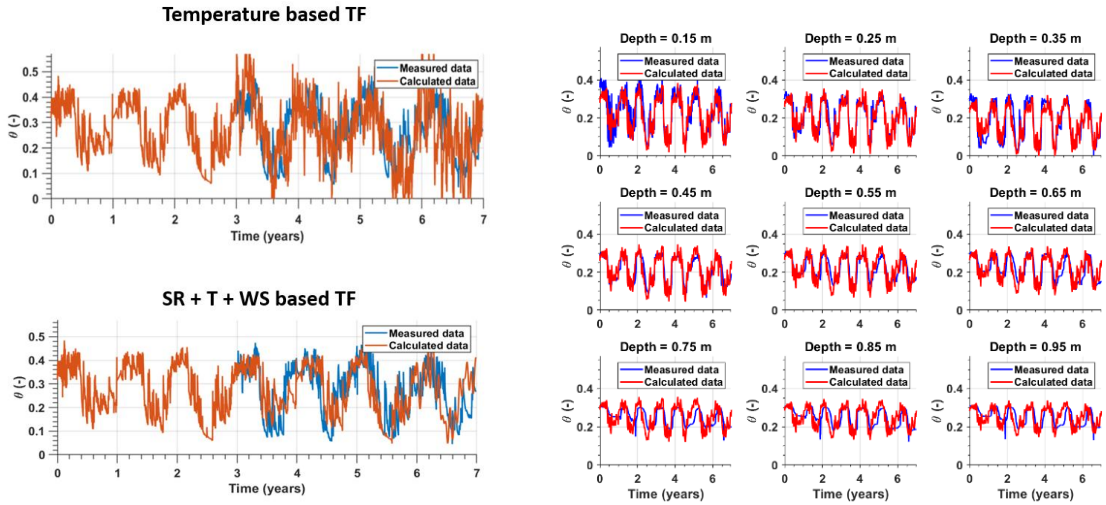

Figure 1: *Water content forecasting: Surface level with STFs based on temperature and multiregression models (MSE: 0.0084 – 0.0062) and subsurface with PTFs callibrated on field measurments (MSE: 0.0016).*

Experimental Study on a Hydraulic Gradient-Induced Failure Mechanism for Slurry Trench Cut-Off Walls

Ziteng Wang, Holger Reith, Andreas Bieberstein and Hans Henning Stutz

Karlsruhe Institute of Technology, Institute of Soil Mechanics and Rock Mechanics, Engler-Bunte-Ring 14, 76131 Karlsruhe, Germany

ziteng.wang@kit.edu

Keywords: Slurry trench cut-off wall, Self-hardening slurry, Single-phase method, Hydraulic gradient

Abstract

In geotechnical engineering, self-hardening slurry trench cut-off walls constructed using the single-phase technique can cause failure to meet the specified strength and permeability due to unknown reasons (e.g., Tillmanns, 2023).

To examine a failure mechanism, specifically failure due to hydraulic gradient acting in the wall depth direction (head difference per vertical seepage length), two slurries with identical densities but different yield strengths were initially produced for column tests as preliminary tests in this study. To obtain representative results, all slurries in this study were prepared in the laboratory, with density and yield strength controlled by varying the proportions of quartz and bentonite powder. After the preliminary tests, an apparatus (Figure 1) was developed as the main component of this study to measure the Darcy velocity of water seepage through slurries under different hydraulic gradients. Accordingly, four slurry types with different densities and yield strengths were prepared with reference to commercially available cut-off wall materials. Replicate specimens of each type were subsequently tested using the developed apparatus. This apparatus was inspired by the conventional triaxial permeameter to avoid sidewall leakage by applying cell pressure using a slurry.

The results from the column tests indicated that, in addition to the slurry density (as described in DIN 4126), the initial yield strength needs be considered to minimize the ingress of groundwater into slurry. Using the developed apparatus, the variation of representative Darcy velocity against hydraulic gradient was obtained for four slurry types (Figure 2a). The representative value was defined as the peak Darcy velocity of water seepage through slurry within two minutes after loading (Figure 2b). During loading, the representative velocity either diminished to an unmeasurable level or resulted in continuous seepage. Different levels of water seepage through the slurry were considered to represent different degrees of slurry deterioration through mechanisms such as dilution and erosion.

This study provided experimental evidence for an observed failure mechanism and introduced a methodological framework that includes slurry preparation based on density and yield strength, along with the development of an apparatus to investigate the hydraulic response of slurry trench cut-off walls under hydraulic gradients.

References

Tillmanns. M (2023). Ausführungssicherheit von Einphasendichtwänden. Institut für Bodenmechanik und Felsmechanik, Karlsruher Institut für Technologie.

Figures

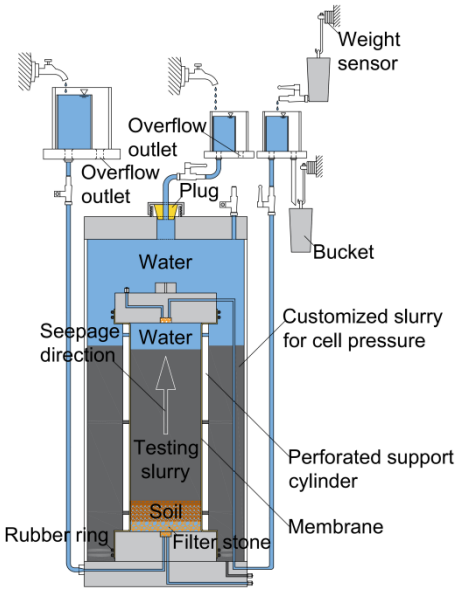

Figure 1: *Test apparatus for Darcy velocity of water seepage through cut-off wall slurry*

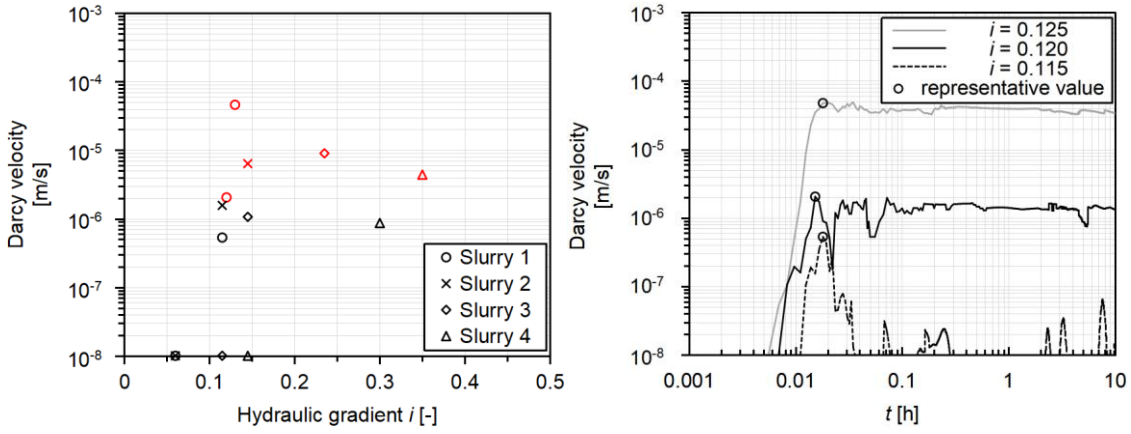

Figure 2: *(a) Variation of representative Darcy velocity against hydraulic gradient for four slurry types (continuous Darcy velocity was measured in the tests marked in red); (b) Darcy velocity of water seepage through slurry 1 over time under different hydraulic gradients (i)*

Comparison of Shear Band Thickness Measurements Using Digital Image and Volume Correlation

Shijin Li[a], Alexandre Sac-Moraneb[a], Jeroen Soetec[b], Hannes Claesd[c], Johan Vanhulste[b], Hadrien Rattez[a]

[a] *Institute of Mechanics, Materials and Civil Engineering, Université Catholique de Louvain, Louvain-la-Neuve, 1348, Belgium*

[b] *Department of Materials Engineering, Katholieke Universiteit Leuven, Belgium*

[c] *Department of Earth and Environmental Sciences, KU Leuven University, Celestijnenlaan 200E, 3001 Heverlee, Belgium*

shijin.li@uclouvain.be, alexandre.sac-morane@enpc.fr, jeroen.soete@kuleuven.be, hannes.claes1@kuleuven.be, johan.vanhulst@kuleuven.be, hadrien.rattez@uclouvain.be

Keywords: gap-graded soil, shear band, strain localization, digital image correlation, digital volume correlation

Abstract

Shear banding, the formation of narrow zones of intense shear strain (strain localisation), is a critical mechanism governing soil deformation and failure. Quantifying shear band thickness is essential for linking micro-scale particle processes with macro-scale mechanical behaviour. However, most reported values to date are derived from surface measurements using Digital Image Correlation (DIC) [1], while recent advances in X-ray Computed Tomography (CT) and Digital Volume Correlation (DVC) [2] have rarely been applied to this purpose. This study presents a systematic comparison of shear band thickness obtained from these two experimental approaches, highlighting their respective capabilities and limitations.

DIC, based on two-dimensional optical imaging, provides high-resolution surface displacement and strain fields that enable precise identification of shear localization on specimen boundaries (Fig 1). In contrast, DVC employs three-dimensional correlation of X-ray Computed Tomography (CT) images to capture full-field internal deformation, offering insights into strain localization within the specimen volume (Fig 2). Both methods were applied to triaxial compression tests on sand specimens but different dimensions, and shear band thickness was determined from the spatial distribution of incremental shear strain. The triaxial DIC/DVC setup and part of the results are shown in Fig 1 and Fig 2, respectively.

The comparison reveals minor differences between surface- and volume-based measurements. The measurements of shear band thickness using DIC and DVC were compared in this study. The results shows that the shear band thickness measured from both methods were very close, validating the effectiveness of approximating shear band thickness using surface displacement information captured from membrane's speckle pattern.

References

1. Rattez H, Shi Y, Sac-Morane A, et al (2022) Effect of grain size distribution on the shear band thickness evolution in sand. Géotechnique 72:350–363. https://doi.org/10.1680/jgeot.20.P.120

2. Stamati O, Andò E, Roubin E, et al (2020) Spam: software for practical analysis of materials. Int J Open Source Softw Process 5:2286. https://doi.org/10.21105/joss.02286

Figures

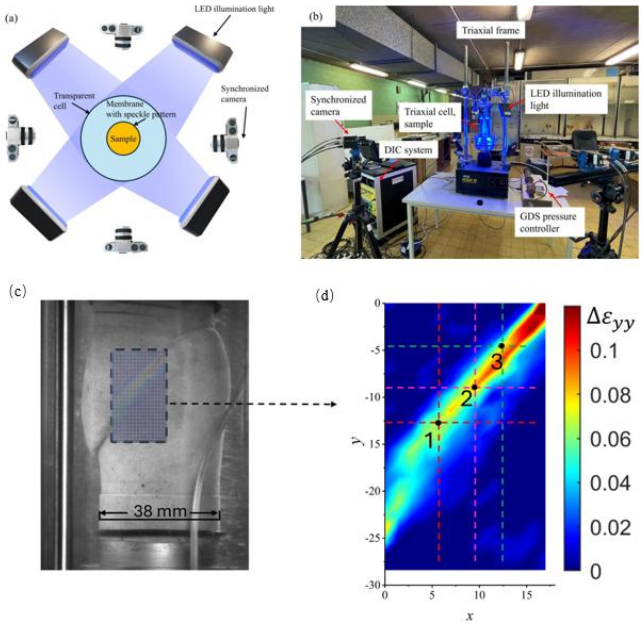

Figure 1: *Triaxial DIC setup (a) a sketch of the mini-triaxial cell; (b) The mini- triaxial cell mounted in the X-ray CT scanner; (c) Shear band captured by a camera; (d) the incremental deformation field* ($\Delta\boldsymbol{\varepsilon_{yy}}$)

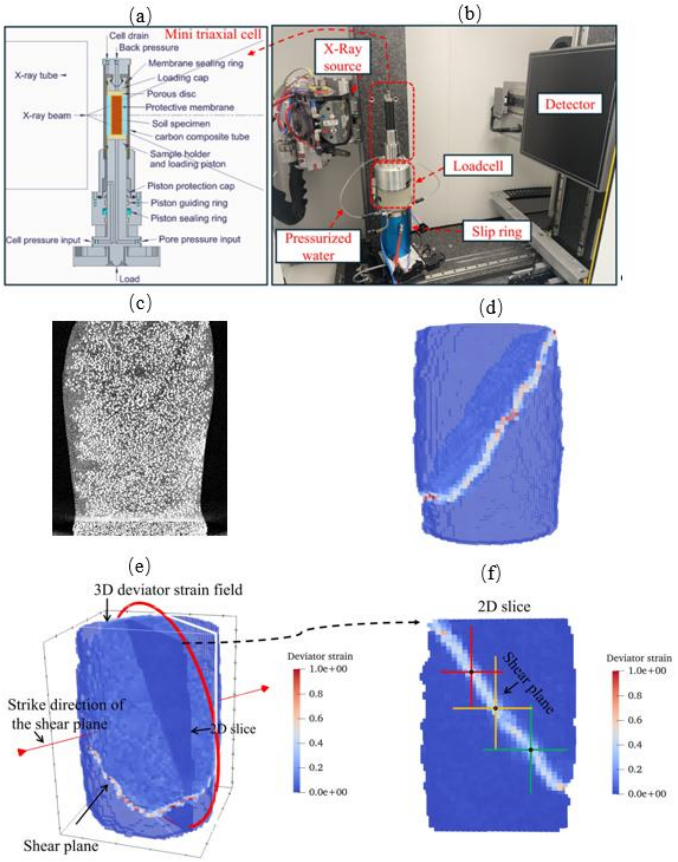

Figure 2: *(a) A sketch of the mini-triaxial cell; (b) The mini- triaxial cell mounted in the X-ray CT scanner; (c) a cross-section of reconstructed image from x-ray CT scan; (d) deviator strain field with shear band highlighted; (e) selection of a representative 2D slice from the 3D deviator strain field; (d) three measurement points on shear band in the extracted 2D slice*

Screened Poisson Averaging of µCT Data

P. Hofer,[a] M. Schreter-Fleischhacker,[c,a] M. Neuner,[d,a] G. Medicus[b]

[a]Department of Basic Sciences in Engineering Sciences, University of Innsbruck, Innsbruck, Austria
[b]Department of Infrastructure Engineering, University of Innsbruck, Innsbruck, Austria
[c]Institute for Computational Mechanics, Technical University of Munich, Munich, Germany
[d]Institute of Structural Engineering, BOKU University, Vienna, Austria

Paul.Hofer@uibk.ac.at

Keywords: Partial differential equations; Finite element method; Boundary effect; Porosity map; Spot the cow

Abstract

X-ray microtomography (µCT) scans reveal the inherent heterogeneity of granular materials at small scales. To account for this heterogeneity in geomechanical simulations rooted in continuum mechanics, the obtained µCT data must first be related to macroscopic quantities. In the literature, this is typically achieved by averaging over representative volume elements—either arranged in a fixed voxel grid [1] or centered at points of interest [2, 3]. However, such methods typically fail near the boundary and cannot be used if the size of this volume is large with respect to the specimen size. To alleviate these deficiencies, we introduce a novel method for relating µCT data to macroscopic quantities, which exploits the averaging property of the screened Poisson equation with homogeneous Neumann boundary conditions. In contrast to conventional methods, averaging is performed by solving a second order linear partial differential equation by means of an appropriate numerical technique. We introduce this method as screened Poisson averaging, which produces continuous distributions of the macroscopic quantity controlled by a single length parameter—the averaging length. By means of several benchmark examples in one, two and three dimensions, we demonstrate the feasibility of the method, compare it with conventional averaging methods, and evaluate its applicability to complex geometries (Fig. 1). Moreover, we obtain the void ratio distribution for a sample of dense Hostun sand (HNEA01) [4], which represents an important step toward accounting for the specimen's actual heterogeneity in numerical simulations in the future.

Acknowledgements

The authors are grateful to E. Andò for providing the HNEA01 µCT data set and permitting its use. Moreover, we acknowledge valuable discussions with members of the 3SR Laboratory, in particular G. Viggiani, A. Tengattini, C. Couture, and J. Desrues, during an invited stay in Grenoble last spring.
This research was funded in part by the Austrian Science Fund (FWF) 10.55776/V918. P. Hofer and G. Medicus are funded by the FWF.

References

[1] Alshibli, K. A. and A. Hasan (2008). “Spatial variation of void ratio and shear band thickness in sand using X-ray computed tomography”. In: Géotechnique 58.4, pp. 249–257. DOI: 10.1680/geot.2008.58.4.249.

[2] Shahin, G., G. Viggiani, and G. Buscarnera (2020). “Simulating spatial heterogeneity through a CT-FE mapping scheme discloses boundary effects on emerging compaction bands”. In: International Journal of Solids and Structures 206, pp. 247–261. DOI: 10.1016/j.ijsolstr.2020.08.016.

[3] Schmidt, S., M. Wiebicke, and I. Herle (2022). "On the determination and evolution of fabric in representative elementary volumes for a sand specimen in triaxial compression". In: Granular Matter 24.4, p. 97. DOI: 10.1007/s10035-022-01262-2.

[4] Andò, E., S. A. Hall, G. Viggiani, J. Desrues, and P. Bésuelle (2012). "Grain-scale experimental investigation of localised deformation in sand: a discrete particle tracking approach". In: Acta Geotechnica 7.1, pp. 1–13. DOI: 10.1007/s11440-011-0151-6.

[5] Crane, K., U. Pinkall, and P. Schröder (2013). "Robust fairing via conformal curvature flow". In: ACM Transactions on Graphics 32.4, pp. 1–10. DOI: 10.1145/2461912.2461986.

Figures

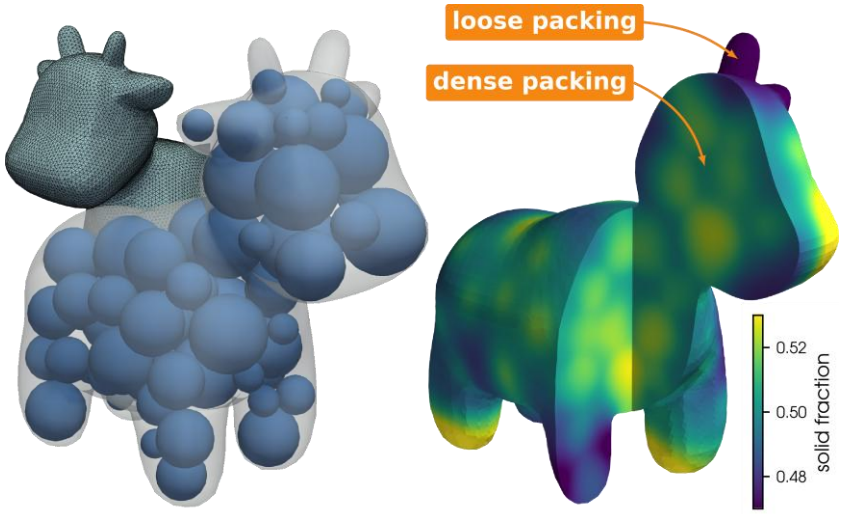

***Figure 1**: Screened Poisson averaging performed to obtain a continuum map of the solid fraction for Spot the cow [5] packed with spheres.*

An FFT-based method for computing the mechanical, hydraulic and thermal response of frozen soils

Maria Olarte-Garzon, Jean-Michel Pereira, Patrick Dangla

Navier, ENPC, Institut Polytechnique de Paris, Univ Gustave Eiffel, CNRS, Marne-la-Vallée, France

maria-camila.olarte-garzon@enpc.fr, jean-michel.pereira@enpc.fr, patrick.dangla@univ-eiffel.fr

Keywords: FFT-based homogenization, Thermoporomechanics, Frozen soils, Soil Freezing Characteristic Curve

Abstract

Fast Fourier Transform (FFT) methods have been extensively applied to numerical homogenization for over a decade, offering an efficient alternative to conventional numerical approaches. In this work, we develop a mathematical framework to homogenize composite media and analyze their thermo-hydro-mechanical (THM) behavior. The framework addresses: (i) thermoporomechanical response, through the evaluation of elastoplastic behavior, (ii) hydraulic behavior, via computation of the permeability tensor using the Darcy–Darcy problem, and (iii) thermal behavior, through derivation of the thermal conductivity tensor for Fourier-to-Fourier upscaling. The accuracy of these schemes is assessed by comparison with analytical solutions for simple microstructures and demonstrated through an application to frozen soils.

To validate our developments, we analyze a two-dimensional microstructure composed of a circular inclusion embedded in a continuous matrix, defined over the domain $\Omega = [0,1] \times [0,1]$. The representative volume element (RVE) is discretized using an NxN grid with N=256. The applied loading consists of a uniform pressure field of 1 MPa and a temperature field of 274.15 K. The inclusion radius is varied within the range 0.05 to 0.5. Based on the framework of Thermoporomechanics introduced by Coussy (2005), the isotropic homogenized operators B^{hom}, $1/N^{hom}$, κ^{hom}, A_ϕ^{hom}, and H^{hom} are obtained by summing the values of each corresponding local quantity over the domain Ω and normalizing by the total number of pixels. The analytical solutions for micro-poroelasticity and the homogenization of poroelastic properties follow the formulation proposed by Ghabezloo (2011).

The comparative results are presented in Fig. 1, where we obtained an accurate agreement between the results of our FFT-based homogenization solver and the analytical solutions. Note that both solutions move in a closed range from the value of the matrix to near the value of the inclusion when the radius is increased. In terms of time of computation, the solver requires less than 10 seconds, which is approximatively 0.8 seconds per iteration.

As an additional application, Fig. 2 shows the results of the FFT-based solver applied to a real segmented microstructure reported by Alavoine et al. (2020). In this case, the effective thermal conductivity tensor (Λ^{hom}) was evaluated as a function of temperature. The Soil Freezing Characteristic Curve was determined using the pore-morphology framework proposed by Suh et al. (2024). By applying Fourier's law at both micro- and macro-scales, Λ^{hom} can be obtained for a given temperature as a function of the relative saturation of water and ice. Consequently, the solver is not only capable of computing all operators required for a complete THM coupling, but also of extending these calculations to account for the presence of ice.

References

1. Alavoine, A., Dangla, P., & Pereira, J. M. (2020). Fast Fourier transform-based homogenisation of gas hydrate bearing sediments. Géotechnique Letters, 10(2), 367-376.

2. Coussy, O. (2005). Poromechanics of freezing materials. Journal of the Mechanics and Physics of Solids, 53(8), 1689-1718.

3. Ghabezloo, S. (2011). Micromechanics analysis of thermal expansion and thermal pressurization of a hardened cement paste. Cement and Concrete Research, 41(5), 520-532.

4. Suh, H. S., Na, S., & Choo, J. (2024). Pore-morphology-based estimation of the freezing characteristic curve of water-saturated porous media. Water Resources Research, 60(8), e2024WR037035.

Figures

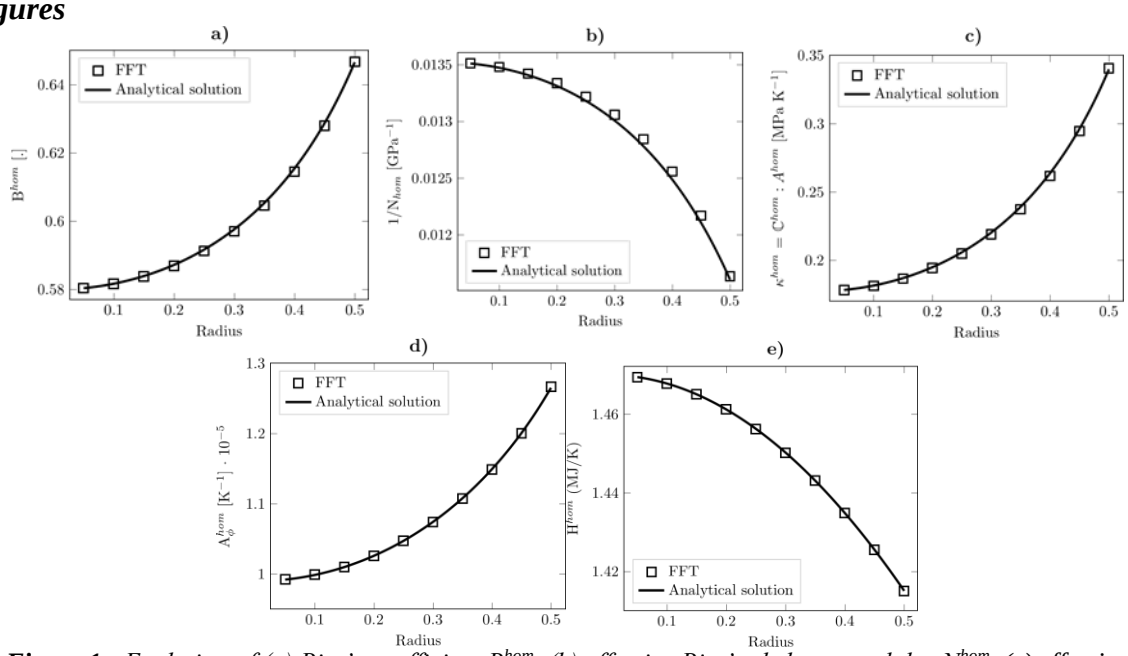

Figure 1: *Evolution of (a) Biot's coefficient B^{hom}, (b) effective Biot's skeleton modulus N^{hom}, (c) effective thermal eigenstrain κ^{hom}, (d) thermal dilatation coefficient A_ϕ^{hom}, and € heat capacity H^{hom} as a function of the radius in isotropic case.*

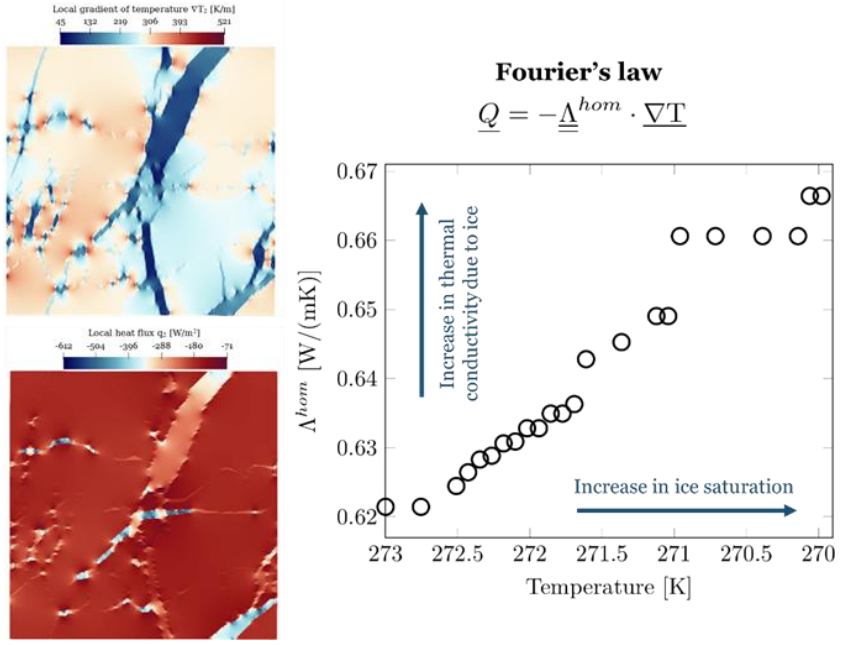

Figure 2: *Homogenized thermal conductivity Λhom determined from SFCC.*

Mechanical response of temporary supports of drifts excavated in the Callovo-Oxfordian claystone

Blaise-Pascal Allo[1, 2], Frederico Lara[1],
Jean Sulem[1], Lina-María Guayacan-Carrillo[1], Eric Boidy[2]

[1] Laboratoire Navier, Ecole Nationale Des Ponts Et Chaussées, Institut Polytechnique De Paris, Université Gustave Eiffel, Cnrs, 77455 Marne La Vallée, France

[2]Agence Nationale pour la gestion des déchets Radioactifs (ANDRA), Chatenay-Malabry, France

blaise-pascal.allo@enpc.fr

Keywords: Callovo-Oxfordian, convergence, support system, long-term behavior

Abstract

Built and operated by the French National Agency for Radioactive Waste Management (ANDRA) since the early 2000s, the Meuse/Haute-Marne underground research laboratory (M/HM URL) is designed for scientific experiments and demonstrations aimed at proving the feasibility and constructability of geological disposal of radioactive waste in Callovo-Oxfordian claystone (Cigéo project). It consists of a network of drifts excavated in the directions of the major and minor horizontal stresses (σ_h~12.4 MPa et σ_H~16.1 MPa).

Some drifts are designed to analyse rock-structure interaction and to test and to improve different support systems. This is the case, for example, of the GER drift, which was excavated in the direction of the minor horizontal stress and consists of five different sections (Figure 1a), two of which get a final concrete lining (Djizanne et al., 2019).

In recent years, direct analysis of in situ convergence measurements (Guayacán-Carrillo et al., 2016; Lara et al., 2025) has highlighted the anisotropy of convergences and the influence of different support systems tested in the M/HM URL. These studies have defined a set of parameters for a semi-empirical convergence law proposed by Sulem et al. (1987), which allows for reliable prediction of short- and medium-term convergence evolution and offers an extrapolation for the long-term.

Recently, Lara et al. (2025) introduced a numerical model addressing the delayed behavior observed in the GER drift (Figure 2). This model incorporates the fractured zone specifically, distinguishing its viscoelastic parameters from those of intact rock. They simulated concrete structures, whether sprayed or cast, using perfect elastoplastic behavior with Mohr-Coulomb failure criteria. These results successfully replicate the development and anisotropy of the convergences observed in situ (Figure 1b). The initial parameters for the fractured zone model were based on direct observational data. A retro-analysis methodology was consequently developed to determine the extent of the fractured zone through convergence measurements. Building on this, the present study examines the robustness and predictive capacity of the model regarding the load on drift shotcrete and concrete linings. The model's predicted stresses and deformations suggest that advanced behavior must be incorporated into the model to improve the accuracy of load predictions on the final lining.

References

Djizanne, H., Zghondi, J., Armand, G., Conil, N., & De La Vaissière, R. (2019). Some aspects of the hydro-mechanical behaviour of Callovo-Oxfordian (COx) claystone around a gallery parallel to the principal horizontal minor stress. Geomechanics for Energy and the Environment, 17, 3-15. https://doi.org/10.1016/j.gete.2018.11.003

Guayacán-Carrillo, L.-M., Sulem, J., Seyedi, D. M., Ghabezloo, S., Noiret, A., & Armand, G. (2016). Analysis of Long-Term Anisotropic Convergence in Drifts Excavated in Callovo-Oxfordian Claystone. Rock Mechanics and Rock Engineering, 49(1), 97-114., https://doi.org/10.1007/s00603-015-0737-7

Frederico Lara Diniz Oliveira. Comportement à long terme des galeries excavées dans l'argilite du Callovo-Oxfordien : développement d'une démarche d'analyse pour le dimensionnement des ouvrages. Géotechnique. École des Ponts ParisTech, 2024. Français. ⟨NNT: 2024ENPC0034⟩. ⟨tel-05045345⟩

Lara, Frederico, Lina-María Guayacán-Carrillo, Jean Sulem, Jana Jaber, and Gilles Armand. 2025. Time-Dependent Modeling of Supported Drifts Excavated in Callovo-Oxfordian Claystone Considering the Excavation-Induced Fractured Zone. Computers and Geotechnics 179: 107030. https://doi.org/10.1016/j.compgeo.2024.107030

Sulem, J., Panet, M., & Guenot, A. (1987). Closure analysis in deep tunnels. International Journal of Rock Mechanics and Mining Sciences & Geomechanics Abstracts, 24(3), 145-154. https://doi.org/10.1016/0148-9062(87)90522-5

Figures

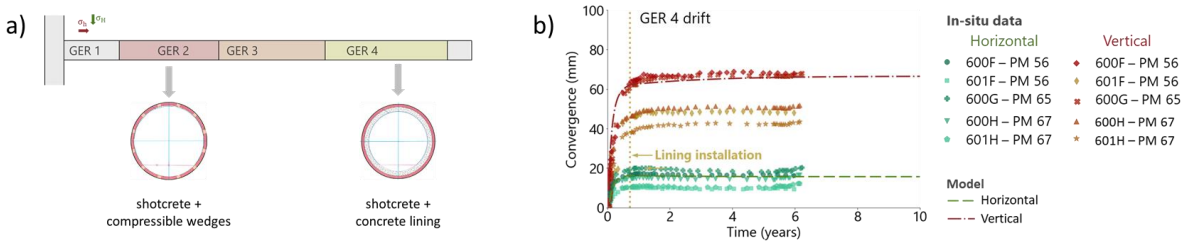

Figure 1: *a) The GER drift, b) In situ convergence measurements compared with the numerical results for GER 4 drift (Lara 2024)*

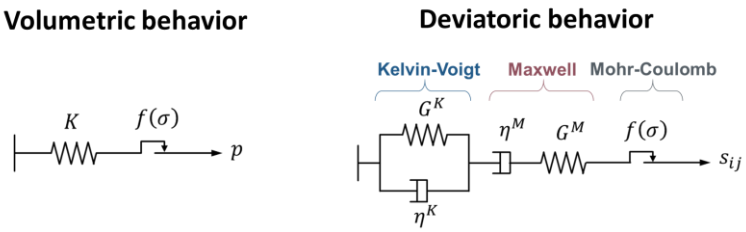

Figure 2: *Burgers-Mohr model, a visco-elasto-plastic model used in the numerical model for the rock mass behavior*

Assessing the stability of Arctic drilling wastes in a permafrost environment

Aaron Förderer[1], Tim Ensom[2], Moritz Langer[2,3], Raul Fuentes[1]

[1]Institute of Geomechanics and Underground Technology, RWTH Aachen

[2]Vrije Universiteit Amsterdam

[3]Alfred Wegener Institute, Helmholtz Center for Polar and Marine Research

foerderer@gut.rwth-aachen.de

Keywords: Permafrost, contamination, climate change, salt migration

Abstract

Past-century oil and gas exploration has resulted in extensive drilling operations in the Arctic. The resulting toxic waste fluids are often stored in drilling mud sumps (DMS), which are constructed within permafrost. Arctic warming and permafrost degradation has recently raised concerns over these sites' stability (Kanigan and Kokelj, 2010; Langer et al., 2023). Within the project ‚ThinIce', we investigate these sites' current and projected state.

Foundational for the project are three major field expeditions into the Canadian Mackenzie Delta. The delta and its uplands are host to over 200 DMS (Kanigan and Kokelj, 2010). Goal of the expedition is the characterization of DMS' geometry, composition, and potential degradation. Besides the fieldwork component, further measures include laboratory testing and modeling, as well as dissemination of the results to the local indigenous communities.

The challenges associated with remote Arctic fieldwork call for a set of lightweight investigation methods. Permafrost cores were obtained, and temperature & moisture loggers installed. Complementing this, active layer and upper permafrost were characterized with a handheld dynamic penetrometer. Subsurface sump geometry was measured using ground-penetrating radar (GPR). Electromagnetic mapping was employed in order to assess thawing and fluid migration.

While the DMS caps are found to be finegrained and cohesive, the surrounding tundra is mostly peaty. Peat lenses are at times found inside the cap material, and show significantly higher water contents than the surrounding clay. Thermokarst and slumping of the clay cap is often visible. The cap's thickness is inferred from GPR profiles to be around 2,5 m. In the case of Tuk L-09, located close to the seaside community of Tuktoyaktuk, the complete collapse of the sump cap and formation of a thermokarst lake was found (see figure 1). Some of the data furthermore suggests that subsurface fluid migration may occur. In sampling pits around the lower sump rim, increased groundwater electrical conductivities are found. Ground conductivities measured in the EM surveys can show significant anomalies around the rim, as is exemplified in figure 2, suggesting increased thawing and / or salt contents in these areas (Ge et al., 2025).

Further work includes freezing-curve and shear parameter determination in the frozen lab @ GUT. Subsequent modeling efforts will include different climate change scenarios, in order to assess thawing and thermokarst susceptibility in the coming decades. The resulting stability predicitions will inform stakeholders to make informed decisions about future DMS management in an increasingly warming Arctic.

References

Ge, J., Sun, H., Liu, R., Huang, Z., Tian, B., Liu, L., Zheng, Z., 2025. Permafrost thawing characterization in engineering scale by multi-geophysical methods: A case study from the Tibet Plateau. Eng. Geol. 350, 108012. https://doi.org/10.1016/j.enggeo.2025.108012

Kanigan, J.C.N., Kokelj, S.V., 2010. Review of current research on drilling-mud sumps in permafrost terrain, Mackenzie Delta region, NWT, Canada.

Langer, M., von Deimling, T.S., Westermann, S., Rolph, R., Rutte, R., Antonova, S., Rachold, V., Schultz, M., Oehme, A., Grosse, G., 2023. Thawing permafrost poses environmental threat to thousands of sites with legacy industrial contamination. Nat. Commun. 14, 1721. https://doi.org/10.1038/s41467-023-37276-4.

Figures

Figure 1: *Collapse of the DMS clay cap at Tuk L-09.*

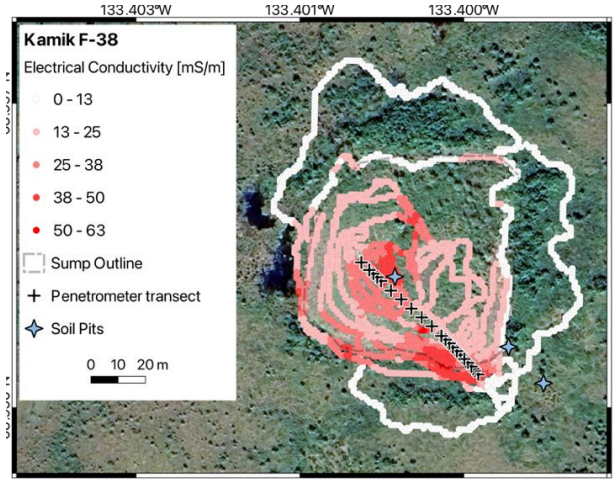

Figure 2: *Ground conductivity map measured at Kamik F-38.*

Insights into void ratio redistribution during undrained monotonic shearing of Malaysian kaolin

Elvis Covilla[1]*, David Mašín[1], Jose Duquel[1,2], Jan Najser[1]

[1]Faculty of Science, Charles University in Prague, Czech Republic

[2]Universidad de la Costa, Barranquilla, Colombia

**covillae@natur.cuni.cz*

Keywords: Void ratio redistribution, undrained shearing, inhomogeneities, triaxial, kaolin

Abstract

This poster combines experiments and fully coupled 3D simulations to evaluate void ratio redistribution in Malaysian kaolin during undrained monotonic shearing at different loading rates. Triaxial tests measured void ratio before and after shearing, while simulations used an anisotropic hypoplastic clay model [1]. Results showed constant global void ratio but internal redistribution at all rates, with densification at the ends and loosening in the middle, confirming significant internal variation at all rates, matching experimental trends [2]. Simulations revealed pore pressure inhomogeneity decreasing at lower rates, and rigid end platens caused total stress concentration. These findings highlight the importance of considering internal variability in undrained shear test interpretation and model calibration.

Acknowledgements

The authors appreciate the financial support given by the grant No. 21-35764J of the Czech Science Foundation. The first author appreciates the financial support given by the Charles University Grant Agency (GAUK) with project number 245223.

References

[1] D. Mašín. Clay hypoplasticity model including stiffness anisotropy. Géotechnique, 64(3):232–238, 2014

[2] E. Covilla, D. Mašín, J. Duque, J. Najser, and J. Roháč. On the influence of the shearing rate on the monotonic and cyclic response of Malaysian kaolin. Géotechnique, pages 1–30, 2024.

Figures

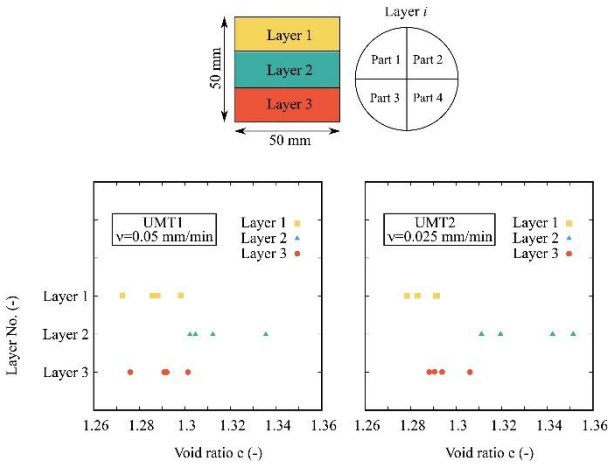

Figure 1: *Void ratio measurements after undrained monotonic shearing.*

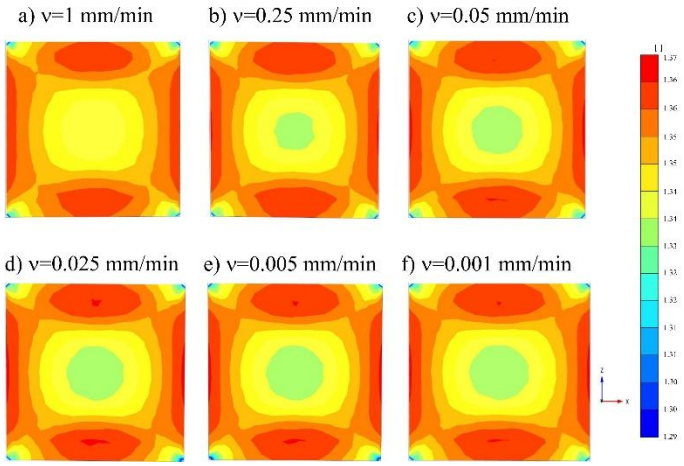

Figure 2: *Cross-section of predicted void ratios after undrained shearing, considering three-dimensional fully coupled simulations. Minimum and maximum values of void ratio: a) 1.365 – 1.239; b) 1.365 – 1.246; c) 1.366 – 1.244; d) 1.366 – 1.244; e) 1.366 – 1.245; f) 1.366 – 1.245*

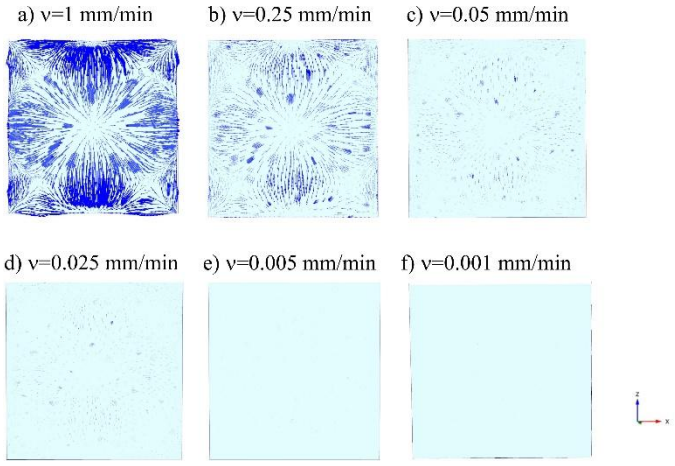

Figure 3: *Cross-section of predicted local ground water flow for three-dimensional fully coupled simulations at various shearing rates*

Implementation of an anisotropic thermo-poro-visco-plastic constitutive law in Plaxis

Borzouyeh Khanghahi-Bala, Siavash Ghabezloo

Laboratoire Navier, ENPC, CNRS, Univ. Gustave Eiffel, Marne-la-Vallée, France

borzouyeh.khanghahi-bala@enpc.fr

Keywords: PLAXIS, Anisotropy, creep, Visco-plasticity, Cam-Clay

Abstract

In geotechnical engineering and industry practice, simulation tools such as PLAXIS play a critical role in predicting the behavior of soil-structure systems under complex loading conditions. The choice of an appropriate constitutive model directly impacts the reliability of these predictions. Common models like Modified Cam Clay (MCC) or Hardening Soil Model, implemented in Plaxis, may inadequately capture essential response features such as anisotropy, time-dependent deformation, or asymmetric hardening, potentially leading to inaccurate forecasts in critical engineering applications [1-3].

This poster illustrates the development and implementation of an enhanced User Defined Soil Model (UDSM) in PLAXIS that incorporates an anisotropic elasto-visco plastic constitutive law with hydraulic and thermal couplings. The yield surface and plastic potential are based on Asymmetric Cam Clay (ACC) model [4], allowing differing hardening responses in compression and extension based on accumulated plastic strains. The model also incorporates thermal coupling and temperature-depending hardening functions, permitting to simulate thermal collapse phenomenon in claystones [5].

The model was embedded into PLAXIS via the UDSM interface and verified against routine problems exhibiting directional dependence, creep behavior, and asymmetric stress–strain response. It is applied to numerical simulations related to underground nuclear waste disposal projets. Several other practical engineering case studies demonstrate its utility: foundation settlement under long-term loading, embankment consolidation exhibiting creep effects, tunnel in anisotropic ground.

References

[1] Cudny, M., Truty, A. "Refinement of the Hardening Soil model within the small strain range. " Acta Geotech. 15, 2031–2051 (2020). https://doi.org/10.1007/s11440-020-00945-5

[2] Obradović, Nikola, Sanja Jocković, and Mirjana Vukićević. "Application of hardening state parameter constitutive model for prediction of overconsolidated soft clay behavior due to embankment loading." Applied Sciences 13.4 (2023): 2175. https://doi.org/10.3390/app13042175

[3] Bentley website GeoStudio | PLAXIS - User Defined Soil Models - Communities

[4] Pierre, M., Samudio, M., Ghabezloo, S., Dangla, P., 2025. “Modelling the poromechanical behaviour of class G cement paste: A multiphysics approach from early age to hardened state”. Cement and Concrete Research 193, 107852. https://doi.org/10.1016/j.cemconres.2025.107852

[5] Braun, P., Ghabezloo, S., Delage, P., Sulem, J., Conil, N., 2020. “Thermo Poro Elastic Behaviour of a Transversely Isotropic Shale : Thermal Expansion and Pressurization”. Rock Mechanics and Rock Engineering https://doi.org/10.1007/s00603-020-02269-y

Figures

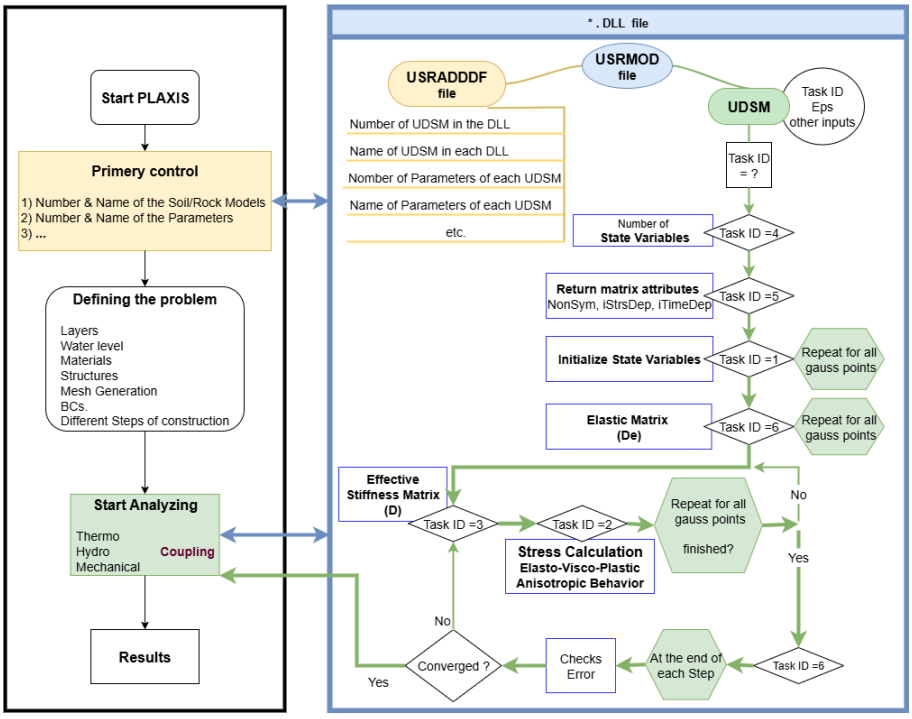

Figure 1: *Flow chart of the User Defined Soil Model (UDSM) in PLAXIS*

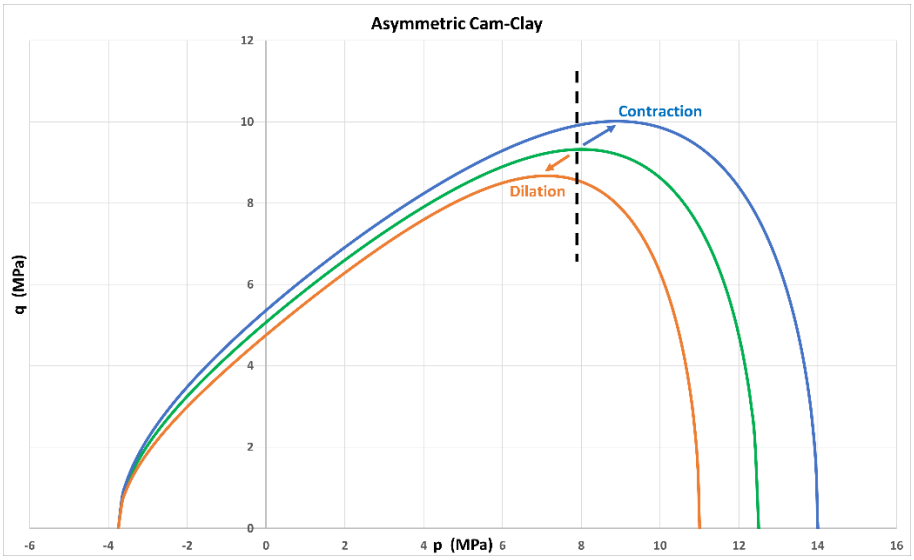

Figure 2: *Asymmetric Cam-Clay yield surfaces (ACC)*

Anisotropy analysis of clay microstructure under shear using SAXS

Viet Khuyen Bui[1,2], Kenichi Soga[2] , Itai Einav[1], François Guillard[1]

[1]School of Civil Engineering, the University of Sydney, Sydney, NSW 2006, Australia

[2]Department of Civil and Environmental Engineering, University of California, Berkeley, USA

Vbui0008@uni.sydney.edu.au

Keywords: SAXS, shear, Couette cell, clay, anisotropy measurement, fabric orientation

Abstract

Small-Angle X-ray Scattering (SAXS) is a powerful non-destructive technique that provides information on the size and shape of particles in suspension and colloids, as well as the ordering and structure of their internal arrangement [1]. This makes it particularly relevant for clay materials, whose mechanical response is highly dependent on the micro-structure. SAXS has been used to study the consistency characteristics of Na-montmorillonite, which demonstrates its effectiveness in capturing micro structural details [2]. Moreover, when combined with a rheometer, SAXS can track particle orientation under shear conditions [3]. Here, we develop a novel method for analysing SAXS images which extracts the degree of orientation and preferred angles from SAXS images (Figure 1). This objective characterisation of the internal material fabric is applied to clay slurries sheared in a Couette cell under various shear rates and similar relative liquidity for three different clay minerals: kaolinite, halloysite and Na-montmorillonite. Kaolinite exhibits significantly higher anisotropy compared to halloysite and Na-montmorillonite and reaches its maximum anisotropy under a lower shear rate (Figure 2). The results of particle orientation including anisotropy ratio and angle of rotation provide experimental evidence of how fabric arranges itself during shearing. These results can inform and validate clay models, such as the thixotropy-viscoelastic models [4]. Beyond clay science, the methodology developed in this study opens new possibilities in broader materials science and nanotechnology for studying the size, shape and orientation of other particles and internal fabrics.

References

[1] Guinier, A., Fournet, G., Walker, C. B., & Yudowitch, K. L. (1955). Small-angle scattering of x-rays. Wiley New York.

[2] Okawara, M., Saito, Y., & Soga, K. (2019). Study on the mechanism of consistency characteristics of na–montomorillonite using small-angle x-ray scattering method. Clay Science, 23 (2), 19–24.

[3] Philippe, A., Baravian, C., Imperor-Clerc, M., De Silva, J., Paineau, E., Bihannic, I., Davidson, P., Meneau, F., Levitz, P., & Michot, L. (2011). Rheo-saxs investigation of shear-thinning behaviour of very anisometric repulsive disc-like clay suspensions. Journal of Physics: Condensed Matter, 23 (19), 194112.

[4] Blackwell, B. C., & Ewoldt, R. H. (2014). A simple thixotropic–viscoelastic constitutive model produces unique signatures in large-amplitude oscillatory shear (LAOS). Journal of Non-Newtonian Fluid Mechanics, 208, 27–41.

Figures

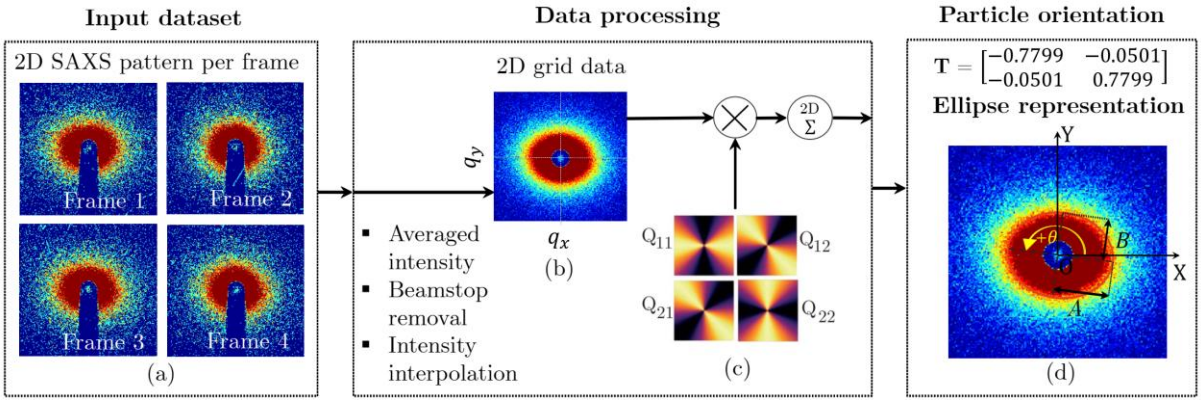

Figure 1: *Determination method of two-dimensional fabric orientation: (a) 2D scattered data from the SAXS experiments for each frame in logarithmic scale, (b) Data processing includes averaging intensity, rotating, and combining to remove the beam stop, followed by interpolation to create a regular 2D grid structure in logarithmic scale. (c) The 2D grid data is multiplied by the orientation matrix Q(q) and summed over all scattering vectors q to calculate the symmetric matrix T, (d) This matrix T can be visualised as an ellipse, characterised by its semi-major axis A and semi-minor axis B, indicating the particle alignment and fabric properties within the sample.*

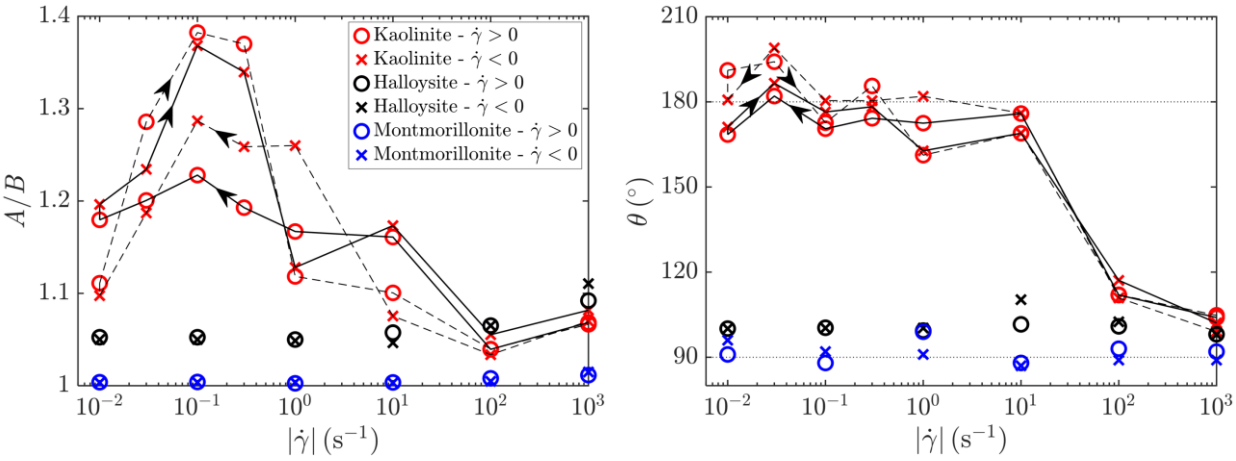

Figure 2: *SAXS fabric measurements of clay slurries with a Liquidity Index (LI) of 3: (a) A/B versus shear rate and (b) The angle of rotation (degrees) versus shear rate (s−1). The solid and dashed lines in both panels represent different tests on kaolinite with varying shear rate directions, where one test begins with positive shear rates (solid line) and the other with negative shear rates (dashed line). Arrows indicate the chronological order of the tests.*

Multivariate statistics link between displacement fluctuations and material morphology in coarse geomaterials

Michail Komodromos, Vincent Richefeu, Gioacchino Viggiani, Gaël Combe

Laboratoire 3SR, Grenoble, France

michail.komodromos@3sr-grenoble.fr

Keywords: granular media, displacement fluctuations, multivariate statistics

Abstract

Granular media are associated with non-affine displacements, which distances the actual grains motion from the predictions made by equivalent continuum. In order to study this phenomenon a polydisperse assembly of cylindrical rods is mounted on the 1Γ2E shearing device [1] and it is subjected to cyclic isochoric shearing, which is expressed by the following weak formulation.

$$\dot{\varepsilon}_{xx} = \dot{\varepsilon}_0 \, cos(\omega t) \qquad \dot{\gamma} = \gamma_0 \, sin(\omega t) \qquad \dot{\varepsilon}_{yy} = -\dot{\varepsilon}_0 \, sin(\omega t)$$

The experiment is recorded by means of high-resolution digital photography as an image sequence. This sequence is processed by Digital Image Correlation algorithms [2], which determine the position and radius of each constituent particles, along with the position of the boundaries. The vectorial difference between the actual and the predicted particles displacements, i.e. *displacement fluctuations*, is computed and it results into a vector field which presents striking similarities with the vortex patterns in turbulent flows [3]. Moreover, the contact network of this physical particle assembly is computed by applying a Delaunay triangulation-aided penalty method, which allows the identification of all the geometrical permitted body contacts. The total list of the contact segments can be individualized to each and every particle via the calculation of its fabric tensor. The derivation of its second invariant quantifies the anisotropy of the contact branches applied.

The identification of the causes that trigger the displacements fluctuations requires the correlation between the evolving displacement fluctuation vector fields and the variable morphology of the granular assembly. A multivariate statistical analysis is mobilized as following. All fluctuation vectors are projected as points on the fluctuations plane domain, carrying the attributes of the corresponding particles radii and the second invariant of the fabric tensor and neglecting the information over the particles position. The domain is discretized into quad finite elements; the number of points inside each element is counted, forming an initial function determined over this plane domain. This function is then normalized by its double integral over the plane, thus resulting into a Probability Density Function. By construction, this formulation places all the vectors that form the patterns at the edge slopes, characterized by large norms. Simultaneously, the morphological attributes form local distributions inside each cell, whose statistical descriptive equivalents, such as averages, minima or maxima offer the link between vortex patterns and material morphology.

The direct comparison of contour evidence suggests that the grains that produce pattern related fluctuations are of minimum dimensions, under anisotropic contact states. This is concluded by considering that all fluctuations at the tails of the PDF are associated to small maximum particle radii per cell (Figures 2 (a, b)). Moreover, there is trend of increasing magnitudes of the second invariant of the fabric tensor while radially moving away from the reference point (Figure 2

(c)). Eventually, this is basic statistical evidence that the divergence between granular media kinematics and continuum-based predictions originates from fabric anisotropy. The derived evidence has led to the hypothesis that the grains are driven by the tendency to fill the surrounding space [4], which is accessible by the available pore network, which is developed under anisotropic positioning of particles and serves only the particles that fit along its paths.

References

[1] Joer, H., Lanier, J., Desrues, J., Flavigny, E. "1γ2ε": A New Shear Apparatus to Study the Behavior of Granular Materials. Geotechnical Testing Journal 15(2), 129–137 (1992). doi: https://doi.org/10.1520/GTJ10235J

[2] Richefeu, V., Combe, G. The particle image tracking technique: An accurate optical method for measuring individual kinematics of rigid particles. Strain 56, 12362 (2020). doi: https://doi.org/10.1111/str.12362

[3] Radjai, F., Roux S. Turbulentlike Fluctuations in Quasistatic Flow of Granular Media. Physical Review Letters 89, 064302 (2002). doi: https://doi.org/10.1103/PhysRevLett.89.064302

[4] Voivret, C., Radjai, F., Delenne, J.-Y., El Youssoufi, M. S. Space-filling properties of polydisperse granular media. Physical Review E 76, 021301(2007). doi: https://doi.org/10.1103/PhysRevE.76.021301

Ruina, Andy. "Influence of coupled deformation-diffusion effects on the retardation of hydraulic fracture." *ARMA US Rock Mechanics/Geomechanics Symposium*. ARMA, 1978.

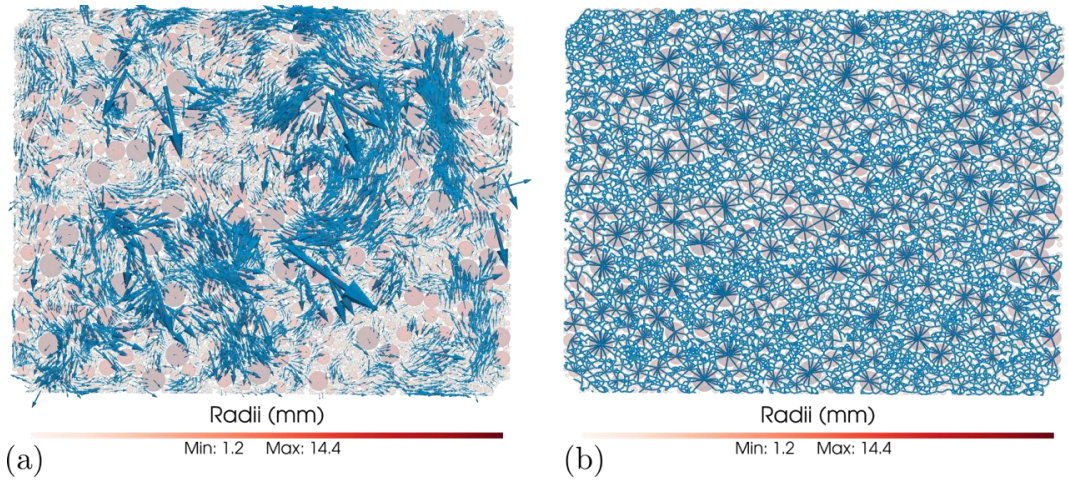

Figure 1: *(a) Typical displacement fluctuations vector field, (b) typical contact network*

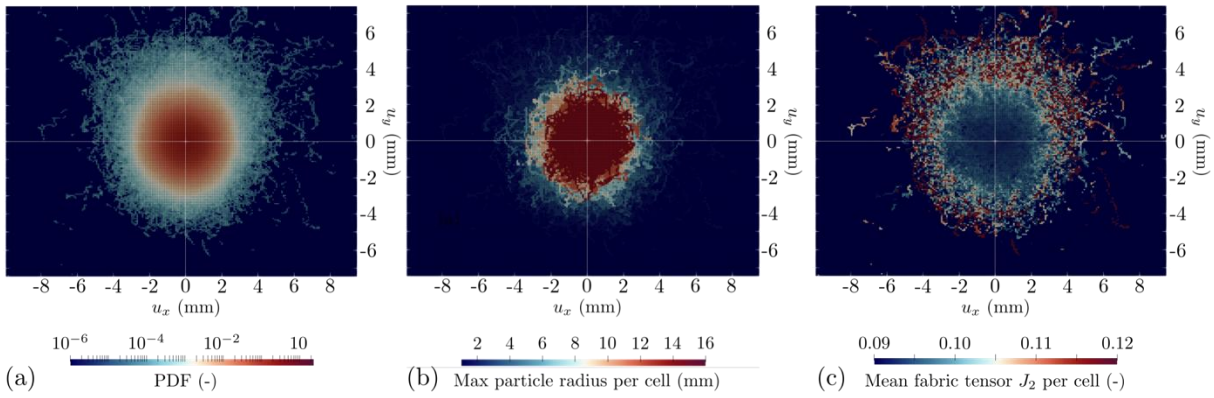

Figure 2: *(a) Vector PDF, (b) max radius per cell, (c) mean fabric tensor second invariant per cell*

Determination of the intergranular strain tensor from the contact fabric

Zekeriya Metehan Karslioglu, Sebastian Ullmann, Selma Schmidt, Ivo Herle

Institute of Geotechnical Engineering, TU Dresden, Germany

zekeriya_metehan.karslioglu@tu-dresden.de

Keywords: Contact fabric, Intergranular strain, DEM, Element tests

Abstract

The mechanical response of soil is influenced by the arrangement of its grains and their contacts, commonly described as the soil fabric. The importance of the initial fabric on the macroscopic soil response was studied over 50 years ago by Oda (1972). This study focuses on the contact fabric, the network of grain-to-grain contacts that develops through deposition, compaction, loading, and laboratory sample preparation. It encodes key aspects of the internal structure that directly influence soil behavior at larger scales. When contacts are preferentially oriented in one direction, the soil tends to resist deformation more effectively along that direction. This leads to a directional dependence of the soil behavior which reflects the influence of the initial contact fabric.

To capture this behavior within a continuum framework, the constitutive model must account for stiffness variations that depend on the loading direction. In this work, the extension of the hypoplastic model by von Wolffersdorff (1996) with the intergranular strains (Niemunis & Herle 1997) has been used to represent the effect of the initial contact fabric. The intergranular strain extension allows the model to reflect the dependence of incremental stiffness on the loading direction.

To incorporate the contact fabric into the intergranular strain framework, the link was established through the deviatoric fabric tensor F and the anisotropy factor a derived from it, which together reflect the deviation of contact normal orientations from the isotropic state (Gu et al. 2017). Since the stiffness in the intergranular strain concept is dependent on the angle between the loading direction and the intergranular strain tensor, defining its initial state on this basis seemed to be a meaningful representation of microscale anisotropy. The procedure for the proposed method is outlined in this study (Karslioglu et al., 2026).

The approach was evaluated using discrete element method (DEM) and element test simulations to show how the initial contact fabric can be represented by the intergranular strain tensor. DEM samples with different initial fabrics were generated, and their deviatoric fabric tensors F and anisotropy factors a were used to define the initial intergranular strain tensors for the element tests. For each simulation method, two strain-controlled loading tests were performed in different directions under plane stress conditions, using the two different initial fabrics (DEM) or the corresponding initial intergranular strain tensors (element test). Figures 1 and 2 present the stress–strain curves and volumetric responses for both simulation methods, from which the influence of the initial fabric (DEM) or the initial intergranular strain tensor (element test) on material behavior can be inferred. It should be noted, that the constitutive model parameters were not calibrated to match with the spherical material used in the DEM simulations beforehand, leading to quantitative differences between the simulation methods. It is therefore

also difficult to judge whether the higher relative stiffness of the isotropic fabric in the DEM simulations is due to the material parameters or to the fabric effects. Overall, the mechanical responses from both simulation methods showed a good qualitative agreement, indicating that the intergranular strain tensor derived from F and a can be used to reflect the influence of fabric anisotropy on incremental stiffness and volumetric behavior under different loading directions.

References

Gu, X., Hu, J. and Huang, M. 2017. Anisotropy of elasticity and fabric of granular soils. Granular Matter, 19, 33.

Karslioglu, Z. M., Ullmann, S., Schmidt, S., Herle, I. 2026. On the link between the contact fabric tensor and the intergranular strain tensor. Submitted to Proceedings of the 21st International Conference on Soil Mechanics and Geotechnical Engineering, Vienna.

Niemunis, A. and Herle, I. 1997. Hypoplastic model for cohesionless soils with elastic strain range. Mechanics of Cohesive-frictional Materials, 2(4), 279–299.

Oda, M. 1972. Initial Fabrics and their Relations to Mechanical Properties of Granular Material. Soils and Foundations, 12(1), 17–36.

von Wolffersdorff, PA. 1996. A hypoplastic relation for granular materials with a predefined limit state surface. Mechanics of Cohesive-frictional Materials, 1(3), 251–271.

Figures

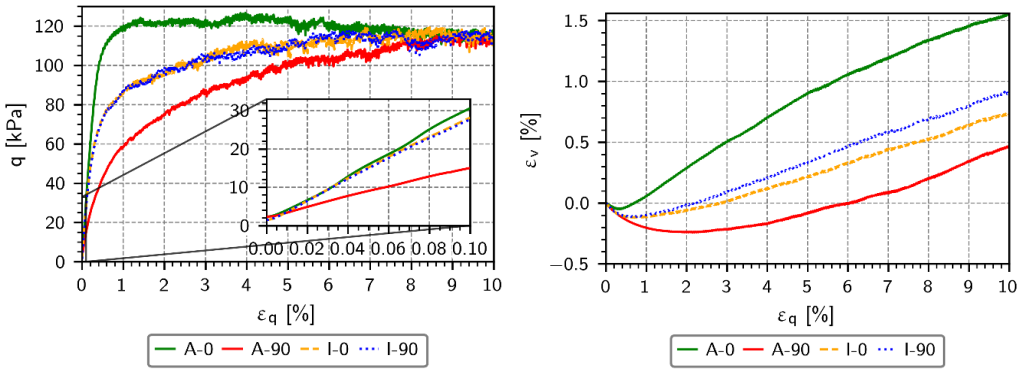

Figure 1: *DEM: Stress-strain (left) and volumetric strain (right) curves of the tests with different initial fabric configurations and loading conditions. Predominantly vertically oriented contact normals under vertical (A-0) and horizontal (A-90) loading. Isotropic contact fabric under vertical (I-0) and horizontal (I-90) loading (Karslioglu et al., 2026).*

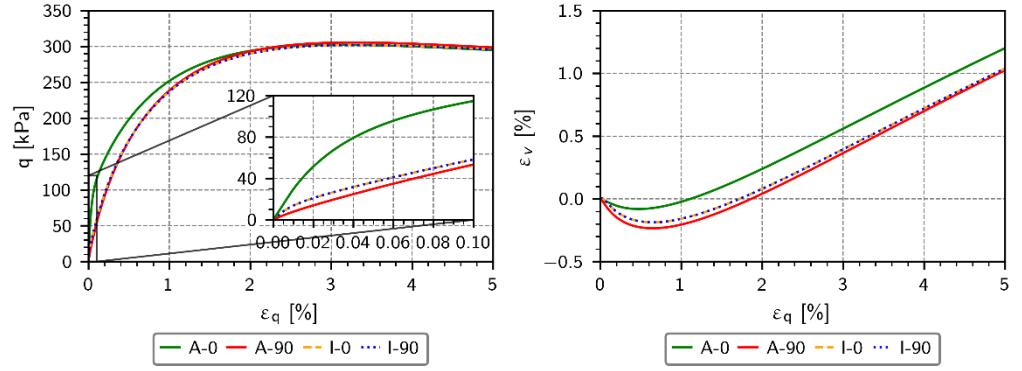

Figure 2: *Element test simulations: Stress-strain (left) and volumetric strain (right) curves of the tests with different initial intergranular strain tensors derived from the initial contact fabric of the DEM samples. Predominantly vertically oriented contact fabric under vertical (A-0) and horizontal (A-90) loading. Isotropic contact fabric under vertical (I-0) and horizontal (I-90) loading (Karslioglu et al., 2026).*

Benchmarking of TH2M simulators: the BenVaSim II project

Jan Philipp Kruse[1], Jörg Feierabend[2], Abdati Laatigue[2], Junqing Sun-Kurczinski[2], Ralf Wolters-Zhao[2], Larissa Friedenberg[3], Matthias Hinze[3], Jonny Rutqvist[4], Guanlong Guo[4], Manuel Sentis[5], Philipp Schädle[5], Tore Ingvald Bjørnarå[6], Ingo Kock[7], Carsten Rücker[7], Stephan Hotzel[7], Michael Pitz[1], Jobst Maßmann[1],Eleni Gerolymatou[2]

[1]Federal Institute for Geosciences and Natural Resources (BGR), Hannover, Germany

[2]Technical University Clausthal (TUC), Chair for Geomechanics and Multiphysics Systems, Germany

[3]Gesellschaft für Anlagen- und Reaktorsicherheit (GRS) gGmbH, Braunschweig, Germany

[4]Lawrence Berkeley National Laboratory (LBNL), Berkeley, USA

[5]Swiss Federal Nuclear Safety Inspectorate (ENSI), Brugg, Switzerland

[6]Norwegian Geotechnical Institute (NGI), Oslo, Norway

[7]Federal Office for the Safety of Nuclear Waste Management (BASE), Berlin, Germany

eleni.gerolymatou@tu-clausthal.de

Keywords: Benchmarking, Multiphysics, Simulation

Abstract

The safety analyses for a potential repository for high level radioactive waste (HLW) in Germany require long term predictions of at least one million years[1]. Hydraulic, thermal and mechanical processes which may be strongly coupled with each other need to be taken into account, resulting in a high level of complexity. Analytical solutions are not available for such complex scenarios and therefore can only provide limited verification for multiphysics simulators. However, comparative benchmarking of different simulators for the same problem statement can fill this gap and ensure the correct implementation of physical processes.

BenVaSim II is an international project aiming to verify the implementation of multiphysics processes (thermal, mechanical and hydraulic with two phase flow - TH^{2}M) in the simulators used by the participating institutions, namely TOUGH-FLAC[2] (LBNL), CODE_BRIGHT[3] (GRS), COMSOL Multiphysics[4] (ENSI/NGI), OpenGeoSys 6[5] (BGR), Oskar (BASE), FTK simulator, and FEniCSx[6] (TUC). Scenarios of increasing complexity are considered, both as far as the number of dimensions is concerned (one-, two- or three-dimensional), as well as with respect to the considered processes, ranging from TM to TH^{2}M. Anisotropic is also considered in a subset of the scenarios in the form of thermal, hydraulic and mechanical material properties.

In the present poster, results are presented for two selected scenarios, namely a TH^{2}M scenario involving gas generation due to canister corrosion in one dimension and an anisotropic TM scenario in two dimensions. The results of the different simulators show excellent agreement for the simpler scenarios, especially where linear processes are concerned. Non-negligible differences are also present, mainly in highly nonlinear multiphase flow scenarios. An example of the time evolution at a specific point is shown in Figure 1 for the one-dimensional TH^{2}M problem, showing excellent agreement for the temperature on the left and good agreement with deviations for the hydraulic processes in the form of the degree of saturation on the right. Potential reasons for the observed deviations between the different simulators are discussed. It is hoped that the results of the project will prove useful to researchers wishing to benchmark their numerical implementation.

References

[1]StandAG (2016) Gesetz zur Suche und Auswahl eines Standortes für ein Endlager für Wärme entwickelnde radioaktive Abfälle (Standortauswahlgesetz – StandAG) (in German)

[2]Rutqvist, J., Wu, Y.-S., Tsang, C.-F. and Bodvarsson, G. (2002) A modeling approach for analysis of coupled multiphase fluid flow, heat transfer, and deformation in fractured porous rock, International Journal of Rock Mechanics and Mining Sciences, vol. 39 (4), p. 429-442.

[3]Olivella, S., Vaunat, J., and Rodriguez-Dono, A. (2025). CODE_BRIGHT 2025: User's Guide. Universitat Politècnica de Catalunya (UPC); Department of Civil and Environmental Engineering, UPC-Barcelona Tech.

[4]COMSOL Multiphysics®, www.comsol.com. COMSOL AB, Stockholm, Sweden.

[5]Kolditz, O. and Bauer, S. and Bilke, L. and Böttcher, N. and Delfs, J. and Fischer, T. and Görke, U. and Kalbacher, T. and Kosakowski, G. and McDermott, C. and Park, C. and Radu, F. and Rink, K. and Shao, H. and Shao, H. and Sun, F. and Sun, Y. and Singh, A. and Taron, J. and Walther, M. and Wang, W. and Watanabe, N. and Wu, Y. and Xie, M. and Xu, W. and Zehner, B. (2012): OpenGeoSys: an open-source initiative for numerical simulation of thermo-hydro-mechanical/chemical (THM/C) processes in porous media. Environmental Earth Sciences, vol. 67, p. 589-599.

[6]Alnaes, M.S., Blechta, J., Hake, J., Johansson, A., Kehlet, B., Logg, A., Richardson, C., Ring, J., Rognes, M.E. and Wells, G.N. (2015) The FEniCS Project Version 1.5, Archive of Numerical Software, vol. 3 (100), p. 9 – 23.

Figures

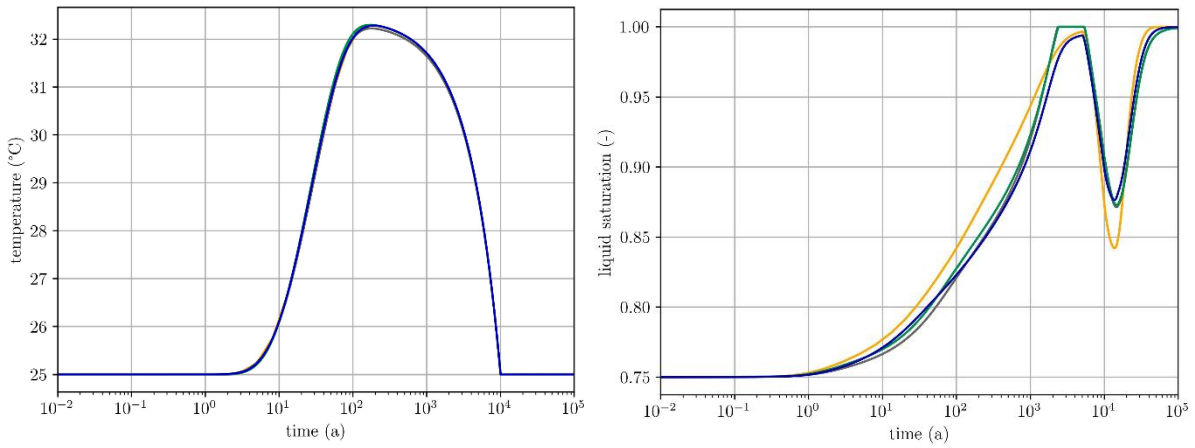

Figure 1: *Comparison of temperature (left) and degree of saturation (right) for four partners.*

The Role of Solid Bridges in the Mechanics of Cohesive Granular Materials: A Multiscale Simulation Framework

Athina Alexiou, Saeid Nezamabadi, Farhang Radjai, Katerina Ioannidou

LMGC, Univ. Montpellier, CNRS, 860 Rue de St-Priest, 34090, Montpellier, France

athina.alexiou@umontpellier.fr

Keywords: solid bridges, multiscale models, granular systems, MD, DEM

Abstract

Predicting the bulk mechanical behavior of cohesive granular materials remains a significant challenge. This is particularly true in industrial processes like granulation, where fine powders are deliberately agglomerated to improve their handling and mechanical properties [1]. The strength and stability of the resulting granules are not intrinsic material properties but instead emerge from a complex interplay of forces and structural arrangements at the particle scale.

It's now understood that a key mechanism determining this macroscopic strength is the formation of solid bridges—stable, hierarchical aggregates where fine particles, bound by nanoscale cohesive forces, adhere to and connect larger ones [2]. While these structures are known to govern the material's final tensile strength, a significant gap remains in systematically linking their microscopic architecture to the macroscopic parameters used in engineering models.

This work addresses this challenge by developing a hierarchical multiscale framework. We focus on the final, dry state of these aggregates, where cohesion is dominated by van der Waals forces. Using Molecular Dynamics (MD) [3], we simulate the compaction of highly bidisperse granular systems with Lennard-Jones interactions. Our preliminary results confirm the formation of solid bridges through the preferential coating of large particles by a layer of smaller, cohesive grains. This distinct structural characteristics is quantified through the system's radial distribution function, g(r) and structure factor S(q).

These microstructures will be used to derive the physically-grounded friction and cohesion parameters required for predictive, large-scale DEM simulations [4]. The next steps involve performing mechanical tests to derive effective friction and cohesion parameters directly from these structures. Implementing these physically-grounded parameters into large-scale Discrete Element Method (DEM) simulations will ultimately allow for more accurate, bottom-up predictions of the strength of cohesive granular media.

References

[1] A. Szulc, E. Skotnicka, M.K. Gupta, and J.B. Królczyk, Powder agglomeration processes of bulk materials – A state of the art review on different granulation methods and applications, Powder Technol. 423, 119092 (2023).

[2] A. Seiphoori, X. Ma, P.E. Arratia, and D.J. Jerolmack, Formation of stable aggregates by fluid-assembled solid bridges, Proc. Natl. Acad. Sci. U.S.A. 117 (7), 3375–3381 (2020).

[3] D. Frenkel and B. Smit, Chapter 4 – Molecular dynamics simulations, in Understanding Molecular Simulation: From Algorithms to Applications, 3rd ed., Elsevier, Amsterdam, pp. 97–152 (2023).

[4] P.A. Cundall and O.D.L. Strack, A discrete numerical model for granular assemblies, Géotechnique 29 (1), 47–65 (1979).

Figures

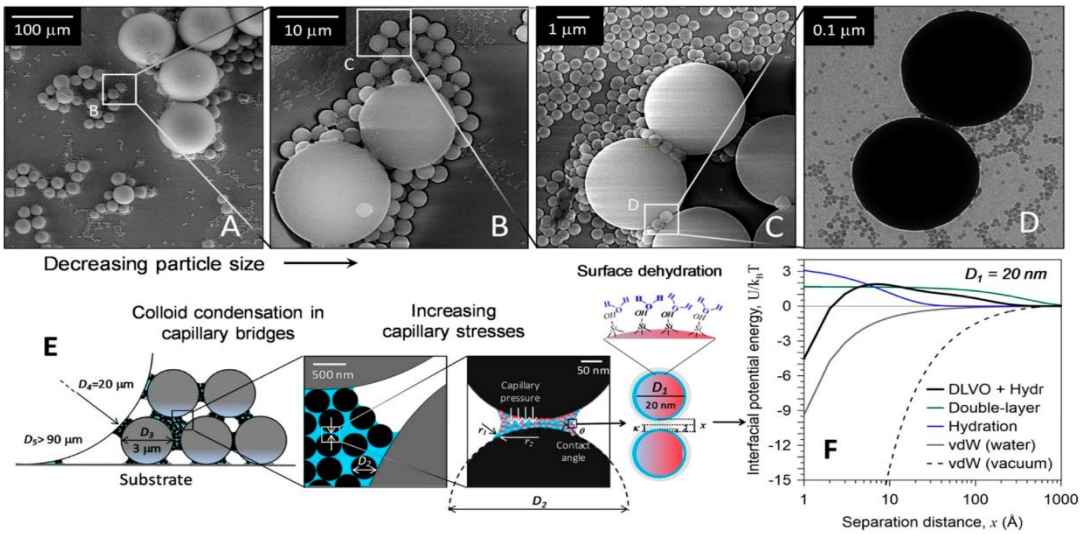

Figure 1: *Hierarchical structures of aggregates. Multiscale observation of a polydisperse colloidal system composed of silica spheres with particle sizes of 90, 20, 3, and 0.4 µm. Figure reproduced from reference [2].*

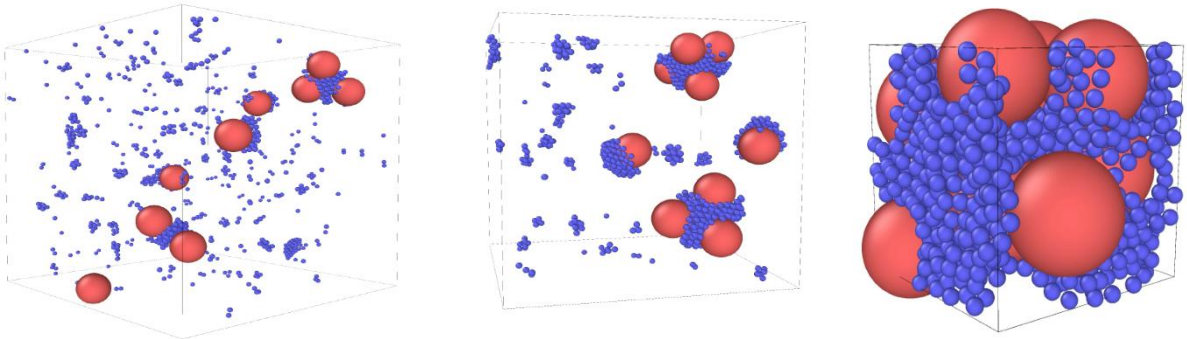

Figure 2: *Configurations from MD simulations performed using LAMMPS under NVT and NPT ensembles showing selective adhesion of small to large particles. The particle radius ratio is 6.6*

Laboratory investigation of one-dimensional creep in clayey soils

Manh Nguyen Duy, Jan Jerman, Jan Najser

Institute of Hydrogeology, Engineering Geology and Applied Geophysics, Faculty of Science, Charles University, Albertov 6, 128 00, Prague, Czech Republic

jan.jerman@natur.cuni.cz

Keywords: creep, plasticity, viscous behaviour, secondary compression, overconsolidation ratio, temperature

Abstract

Numerous geotechnical problems, particularly in clayey soils, involve creep deformations, where the viscous behaviour of soils governs their long-term mechanical response. These deformations are known to depend on factors such as overconsolidation ratio (OCR), soil plasticity, and temperature, yet systematic data on their combined influence remain scarce. This lack of understanding poses challenges for the design of long-lasting infrastructure including embankments, landfills, radioactive waste repositories, and energy-related underground structures. A better experimental basis is therefore needed to evaluate how stress history, mineralogical composition, and thermal conditions interact to control creep behaviour. To address this, we carried out an extensive experimental programme of one-dimensional creep tests on Malaysian kaolin, bentonite, and their mixtures. A modified oedometer was developed by incorporating a circulating water bath, enabling constant thermal conditions and stable operation across a wide temperature range (20°C – 80°C). Detailed calibration was carried out to ensure precise temperature control and to quantify thermal losses and variations within the sample. This low-cost device provides a reliable platform for investigating the influence of OCR, plasticity, and temperature on creep, while maintaining comparability with standard oedometer testing procedures. The results show clear trends regarding stress history and soil composition. Samples with higher OCR consistently exhibited reduced secondary compression coefficient, whereas normally consolidated specimens were significantly more susceptible to long-term deformation. Similarly, materials with higher plasticity indices showed larger secondary compression compared to low-plasticity soils, underlining the role of mineralogical composition in controlling viscous behaviour. Alongside OCR and plasticity, temperature was investigated as a governing factor for creep behaviour. Creep tests were carried out on kaolin and bentonite samples for durations of seven days at controlled temperatures of 20 °C and 60 °C. This study provides new experimental evidence on how stress history, plasticity, and thermal conditions jointly shape time-dependent deformation in clayey soils. The outcomes contribute to a more comprehensive framework for assessing long-term soil behaviour in geotechnical and energy-related applications.

Figures

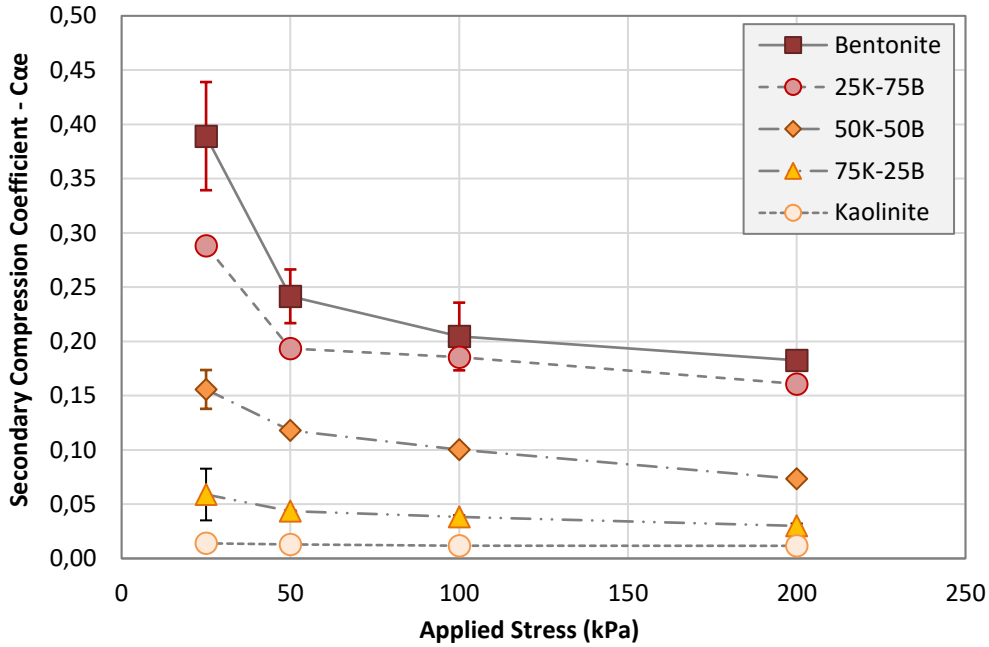

***Figure 1**: Influence of plasticity on compression characteristics.*

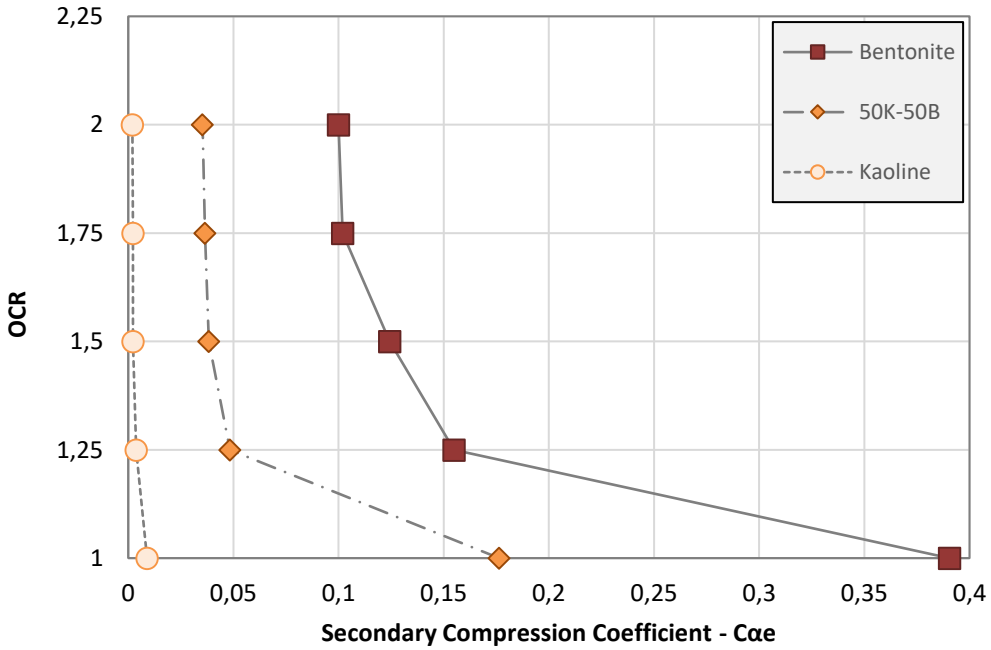

***Figure 2:** Influence of OCR on secondary coefficient (C_{ae}) for different mixtures and stress levels.*

Effect of Electrolyte Concentration on Clay Behavior under Loading-Unloading Cycles: A DEM Approach

Israt Jahan, Takashi Matsushima

University of Tsukuba, Japan

isratjahan5765@gmail.com, tmatsu@kz.tsukuba.ac.jp

Keywords: Clay Compression, Electrolyte Concentration, Discrete Element Method (DEM), Particle-Scale Modeling

Abstract

Particle-scale arrangements, electrochemical interactions, and highly reactive surface characteristics all contribute to the complex mechanical behavior of clayey soils [1]. An important determinant of clay behavior under mechanical loading is the electrolyte content in the pore fluid, which influences aggregation, interparticle forces, and fabric evolution. According to the Derjaguin–Landau–Verwey–Overbeek (DLVO) theory [2], low electrolyte concentrations in the medium cause dispersion and larger void ratios, whereas increasing concentrations thin the charged layer surrounding clay particles, encouraging floculation and aggregation. The primary objective of this study is to analyze how different ion concentrations affect the compressibility and resulting microstructure of clay under loading-unloading situations using numerical simulations by two-dimensional Discrete Element Method (DEM) [3].

DLVO Theory and Electrochemical Interactions

The stability and flocculation of clay suspensions are fundamentally explained by the DLVO hypothesis [2]. This theory explains how the repulsive electrostatic double-layer (EDL) forces and the attractive Van der Waals (VdW) forces, which control particle interactions, are balanced. The total interaction potential (U) between two clay particles is given in Eq. 1.

$$U = -\frac{AR}{12h} + \frac{2\pi R\sigma^2}{\kappa^2 \varepsilon} exp(-\kappa h) \qquad (1)$$

where A: Hamaker constant, R: Particle radius, h: Separation distance between particles, σ: Surface charge density, κ^{-1}: Debye length, which defines the thickness of the electrostatic double layer, ε = Dielectric constant of the medium. Table 1 lists the parameters used in this study.

Discrete element method (DEM)

The DEM-based numerical simulations were conducted with 2122 particles, representing a clay matrix with an initial void ratio of 5.0, friction angle of 27°, and including a double-periodic boundary condition with various isotropic stresses applied to represent the load conditions [3].

Results

Figure 1 shows the relationship between the applied external pressure and the resulting void ratio at equilibrium in the form of e-log(p) curve. The loading curve is not a straight line, which indicates the classical bi-linear e-log(p) model cannot be applied in this numerical simulation. There are three unloading paths from different loading state (a), (b), and (c), which shows

different inclinations, which also indicates the inapplicability of the classical model. The grain configuration will be shown in the main poster with explaination and the influence of such differences in microstructure on the stress-strain curve will be explored in the poster.

Table 1. DLVO parameters used in this study

Parameters	Value
Element radius R (=W/2)	2.5 (nm)
Hamaker constant A	2×10^{-20} (J)
Surface charge density σ	0.05 （C/m^2）
Inverse of Debye length κ (0.5M NaCl)	$2.326\times10^{-8}(m^{-1})$
Permittivity ε	$8.85\times10^{-12}\times$ 80 (S^4A^2/m^3kg)
Absolute Temperature T	293 (K)
Unit charge e	1.38×10^{-23}(C)

Conclusion

The present study uses DEM to demonstrate the important effects of electrolyte concentration on the compression behavior and microstructural change of clay particles. It was found that the loading/unloading process greatly affects the resulting microstructure of clay when the particle interaction model has an energy barrier due to low ion concentrations.

References

1) Mitchell JK, Soga K (2005) Fundamentals of soil behavior. 3rd edn. John Wiley & Sons, New York.

2) Israelachvili JN (2011) Intermolecular and surface forces. 3rd edn. Academic Press, London.

3) Suzuki A, Matsushima T (2014) Meso-scale structural characteristics of clay deposit studied by 2D Discrete Element Method. In: Soga K et al. (eds.) Geomechanics from Micro to Macro, pp. 33–40. Taylor & Francis, London.

Figures

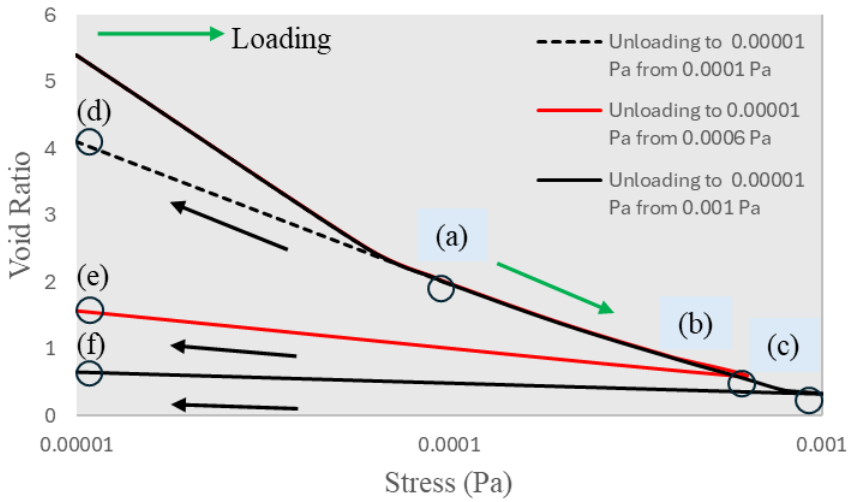

Figure 1: *Relationship between the external pressure and the resulting void ratio for loading/unloading process.*

Influence of material heterogeneity on strain localisation: a finite element study with second gradient model and random fields

Lou-Anne Marchadour, Pierre Bésuelle, Quentin Rousseau

Univ. Grenoble Alpes, CNRS, Grenoble INP, 3SR, F-38000 Grenoble, France

lou-anne.marchadour@3sr-grenoble.fr

Keywords: Strain localisation, FEM, second gradient, random field

Abstract

Understanding the mechanical behaviour of geomaterials at failure, characterised by the formation of kinematic heterogeneities in the form of shear bands, is crucial for assessing and predicting disorders in geotechnical structures. It has been observed that the spatial variability of the initial mechanical properties of geomaterials significantly influences the mode of strain localisation [1]. Our objective is to examine the effect of these initial material heterogeneities on the strain localisation process, from early diffuse to final localisation, seeking to extract quantitative information.

We use a second-gradient continuum model introducing a regularising internal length [2]. Using the FEniCS library [3], the finite element method is employed to model compressive tests in plane strain conditions. The material follows an elastoplastic von Mises model with softening. Material heterogeneity is modelled by Gaussian random fields applied to the initial elastic limit, characterised by a variance and a practical range (correlation distance). Several realisations of a random field lead to different spatial distributions of material heterogeneity, whose impact is investigated. The competition between the internal length of the second gradient model and the practical range is also studied.

Three stages of deformation mode are identified: the nucleation phase, characterised by small clusters of plastic deformation; the diffuse localisation phase, characterised by a network of numerous bands; and finally the mature localisation phase, characterised by one or a few persistent bands. The study highlights that the internal length of the model controls the width of the bands in the diffuse and mature localisation phases, whilst the practical range influences the number and distance between bands in the diffuse localisation phase. Finally, a sequential analysis of the strain fields reveals that the mature band location can be detected in the diffuse localisation phase in most cases.

These results highlight the influence of material heterogeneity and competition between characteristic lengths of the medium on the development of strain localisation.

References

[1] Mourlas, C., Pardoen, B., & Bésuelle, P. (2023). Large-scale failure prediction of clay rock from small-scale damage mechanisms of the rock medium using multiscale modelling. *International Journal for Numerical and Analytical Methods in Geomechanics*, *47*(7), 1254-1288.

[2] R. Chambon, D. Caillerie, and N. El Hassan, "One-dimensional localisation studied with a second grade model," *Eur. J. Mech. A/Solids*, vol. 17, no. 4, pp. 637–656, 1998.

[3] Logg, A., Mardal, K. A., & Wells, G. (Eds.). (2012). *Automated solution of differential equations by the finite element method: The FEniCS book* (Vol. 84). Springer Science & Business Media.

Figures

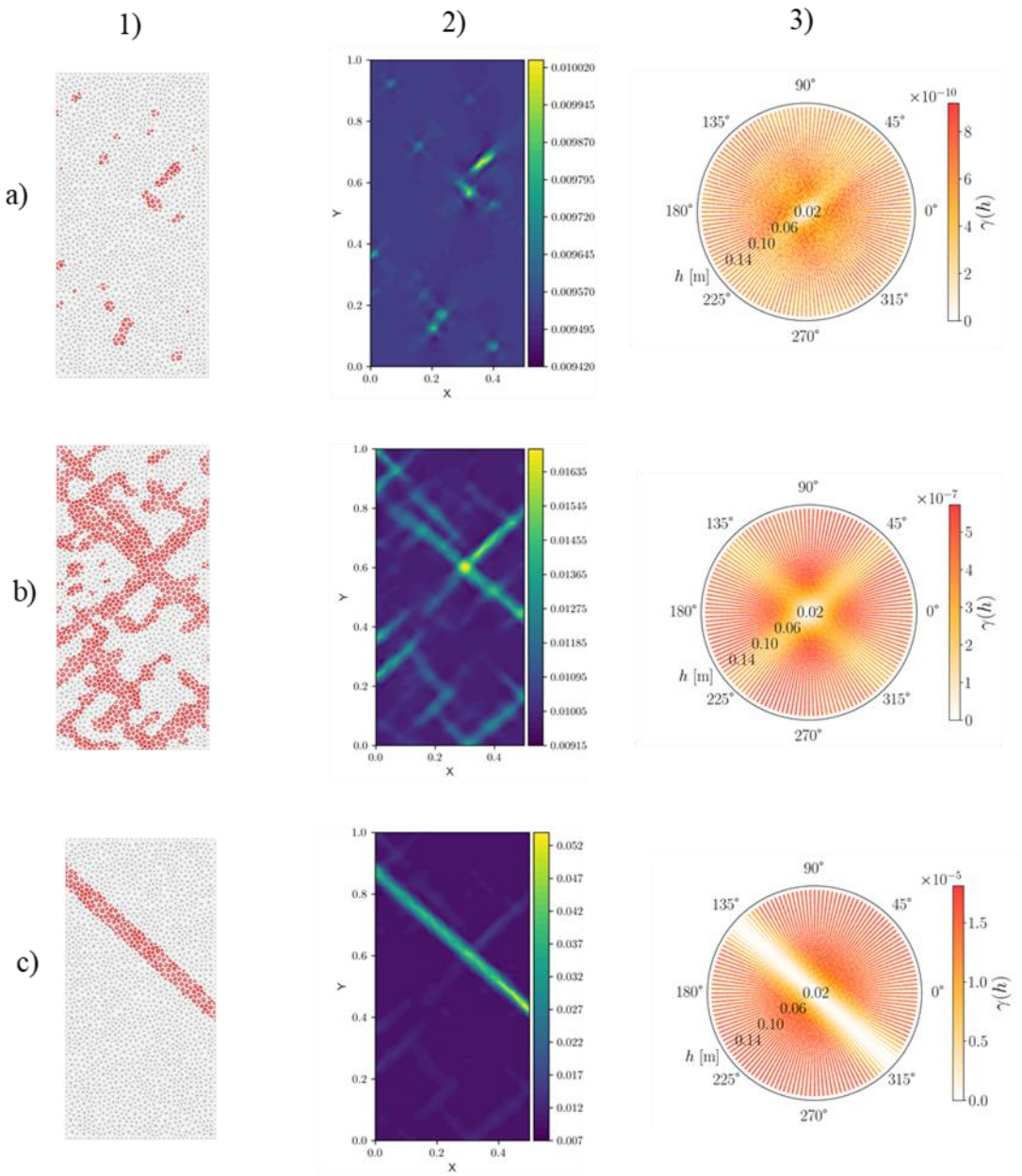

Figure 1: *1) Spatial distribution maps of yielding Gauss points for three loading steps. In red, the Gauss points in the plastic regime. The other Gauss points are in the elastic regime. 2) Maps of the cumulated deviatoric strain norm for the same loading steps. 3) Polar variograms of the deviatoric strain norm for the corresponding loading steps. a) Nucleation phase. b) Diffuse localisation phase. c) Mature localisation phase.*

Fibre Reinforced Sand: A Multiscale Study with X-ray Tomography

Michela Arciero[1,2], Erminio Salvatore[1], Alessandro Tengattini[2], Giuseppe Modoni[1], Gioacchino Viggiani[2]

[1]University of Cassino, Italy

[2]Université Grenoble Alpes, France

michela.arciero@unicas.it

Keywords: Multiscale Study, Fibre-Reinforced Sand, X-Ray Tomography, Triaxial Test, Direct Shear Test, Fibre-Grain Interaction, Deformation field, Porosity

Abstract

Although fibre reinforcement of sand has long been recognized as an effective strategy to improve strength and ductility, its practical application remains limited. This is largely due to an incomplete understanding of soil–fibre interaction mechanisms and the role of fibres in controlling soil deformation and failure. Among the others, length and orientation of fibres play a paramount role in ruling the stress-strain response, guiding strain distribution and controlling the failure process. A multi-scale experimental program was developed, combining macro-scale mechanical testing (triaxial compression, triaxial extension and direct shear test) with micro-scale investigation (X-ray Computed Tomography, XRCT) measuring porosity, strain fields and grain kinematics during test. This integrated approach provides a direct link between global mechanical responses and fibre–grain interaction mechanisms. To be effective, fibres must be long enough to intercept shear bands and involve in the deformation process larger portions of the sample. Moreover, fibres provide their best contribution when aligned with the minor principal stress direction.

Macro-scale mechanical response

The study employed Hostun sand (d_{50} = 0.338 mm) reinforced with fluorocarbon fibres (d_f = 0.1 mm). The geometric ratios governing the selection of fibre length were carefully selected: l_f/d_{50}, the ratio between fibre length and the characteristic grain diameter, chosen to maximize fibre–grain interactions; and D_{sample}/l_f, the ratio between sample diameter and fibre length, set to avoid undesired boundary effects. Large-scale tests explored the influence of experimental parameters, with particular focus on fibre length (1, 2, 3, and 6.5 cm) and orientation (random and aligned with the minor principal stress direction). The main findings from these tests are summarized as follows:

- Reinforcement is more effective in dense sand (≈70%) and at low confining pressures (≈100kPa).
- The optimal fibre content is equal to 0.5% by sand dry weight.
- Fibre length and orientation govern stress-strain response and deformation patterns (Figure 1):
  - **Short fibres (1–2 cm)** → promote brittle behaviour and localized shear bands.
  - **Long fibres (3–6.5 cm)** → induce a more diffuse, pseudo-continuous deformation pattern.
  - **Horizontally oriented long fibres (6.5 cm)** → introduce a pronounced confinement effect.

These results show that fibre inclusion fundamentally alters the soil failure mechanisms, as shown in Figure 1.

Micro-scale insights from X-ray Computed Tomography

High-resolution X-ray Computed Tomography analyses, performed on miniature triaxial and direct shear specimens, revealed that:

- Fibres promote diffuse deformation zones, engaging a larger portion of the sample in the overall strain process.
- Fibres aligned with the minor principal stress direction increase shear band thickness by ~25% under compression and stabilize the central specimen regions under extension.
- Fibres modify grain rotations. Grain–fibre interactions exhibit a localized "influence radius" (≈ 2 grain diameters) where fibres modify grain rotation.

X-ray computed tomography analyses showed that fibres undergo elongation and bending, confirming their role as active reinforcement elements rather than passive inclusions, and that their length should be at least six times the shear band thickness.

Research Highlights

By combining macro-scale mechanical tests with micro-scale imaging, this research shows why specific fibre configurations are more effective. The reinforcement arises from the active tensile mobilization of fibres, which bridge shear planes, redistribute strains, and maintain structural integrity under various loading conditions. The findings improve understanding of fibre-reinforced sand and support optimized geotechnical use. Multiscale investigations are essential to capture the complex nature of granular materials and to understand the processes governing their behavior.

References

Arciero, M., Salvatore, E., Tengattini, A., Modoni, G., & Viggiani, G. (2024). Effect of fibre orientation on the mechanical response of reinforced sand, detected with x-ray tomography. In E3S Web of Conferences (Vol. 544, p. 11017). EDP Sciences.

Desrues, J. (2004, October). Tracking strain localization in geomaterials using. In Xray CT for Geomaterials: Soils, Concrete, Rocks International Workshop on Xray CT for Geomaterials, Kumamoto, Japan (p. 15). CRC Press.

Shukla, S. K. (2017). Fundamentals of fibre-reinforced soil engineering (Vol. 440). Singapore: Springer.

Figures

Figure 1: *Different soil failure mechanisms: end-of-test configurations of triaxial compression samples under 100 kPa confining pressure — Natural Sand, Fibre-Reinforced Sand with short horizontal fibres (1 cm), and Fibre-Reinforced Sand with long horizontal fibres (6.5 cm).*

Coupled THM finite element modeling of energy piles subjected to cyclic thermal loading using hypoplasticity

María Pico, David Mašín

Faculty of Science, Charles University, Czech Republic

picoduam@natur.cuni.cz

Keywords: energy piles, hypoplasticity, temperature, suction, cyclic loading

Abstract

Energy piles are becoming increasingly popular due to the benefits they offer. They serve as foundations for buildings but also as Ground Source Heat Pump (GSHP) systems, taking advantage of the relatively constant temperature of the soil ground throughout the year. They operate with a dual system. During summer, cooling of the building is achieved by injecting heat to the ground, while during winter, the process is reversed and heat is extracted from the ground to heat the building. Consequently, coupled Thermo-Hydro-Mechanical (THM) loading is induced in the surrounding soil. To reproduce this behavior numerically, proper validation and analysis of new developed constitutive models are necessary.

In this research, the coupled THM hypoplastic constitutive model (THM-hypo-ISI) for monotonic and cyclic loading proposed by Pico & Mašín (2024) was incorporated into the finite element software for coupled thermo-hydro-mechanical-chemical analysis, *OpenGeoSys* (Kolditz et al., 2012), using the interface MFront. The interface was previously linked with the single-element software *Triax* (Mašín, 2023) for user defined materials implemented in the "generalmod" subroutine. The centrifuge experiments of energy piles subjected to cyclic loading performed by Ng et al. (2014) were simulated in *OpenGeoSys* to evaluate the capabilities of the constitutive model. The numerical simulations considered an aluminum pile with a diameter of 0.88 m and a length of 9.45 m. The pile material was simulated as thermo-poro-elastic, while the surrounding clayey soil was modeled using the THM-hypo-ISI constitutive model. Additionally, the interface between the soil and the pile was modeled using the THM-hypo-ISI constitutive model with a lower critical state friction angle to reproduce a coefficient of resistance of $R = 0.5$, where $R = tan\,\varphi_{int} / tan\,\varphi_s$, where φ_{int} and φ_s denote the critical state friction angles of the interface and the soil, respectively.

A total of 4 simulations were performed with two different loading types. The first type of loading corresponded to the mechanical loading of the pile until failure, in order to calculate the maximum pile capacity. For the second type, the working load was applied to the pile and consolidation was allowed. Afterwards, the mechanical load was maintained and five heating-cooling cycles were applied to the pile, with temperatures ranging from 38 C to 9 C. Two different over-consolidation ratios were used for each loading type (OCR=1.7 and 4.7).

The results of the finite element simulations showed that the numerical model accurately reproduces the effects of coupled thermo-hydro-mechanical cyclic loading of energy piles. The constitutive model effectively reproduces the non-linear soil response and its dependency on over-consolidation ratio when the pile is subjected to mechanical loading. Additionally, good agreement was observed between the numerical model and the experimental results in capturing the response to cyclic thermo-mechanical loading. See Figure 1. In particular, at low-over

consolidation ratio, heating induced compaction was reproduced, while, at high over-consolidation ratio, a more reversible behavior was observed, governed by the thermal expansion coefficient of the particles. Some limitations were also encountered are further discussed.

References

Kolditz, O., Bauer, S., Bilke, L., Böttcher, N., Delfs, J. O., Fischer, T., Görke, U. J., Kalbacher, T., Kosakowski, G., McDermott, C. I., Park, C. H., Radu, F., Rink, K., Shao, H., Shao, H. B., Sun, F., Sun, Y. Y., Singh, A. K., Taron, J., … Zehner, B. (2012). OpenGeoSys: An open-source initiative for numerical simulation of thermo-hydro-mechanical/chemical (THM/C) processes in porous media. Environmental Earth Sciences, 67(2), 589–599. https://doi.org/10.1007/s12665-012-1546-x

Mašín, D. (2023). Triax. In TRIAX user's manual. https://soilmodels.com/triax/

Ng, C. W. W., Shi, C., Gunawan, A., & Laloui, L. (2014). Centrifuge modelling of energy piles subjected to heating and cooling cycles in clay. Proceedings of the Institution of Civil Engineers: Structures and Buildings, 4, 310–316. https://doi.org/10.1680/geolett.14.00063

Pico, M., & Mašín, D. (2024). Coupled thermo-hydro-mechanical hypoplastic model for partially saturated fine-grained soils under monotonic and cyclic loading. Computers and Geotechnics, 172. https://doi.org/10.1016/j.compgeo.2024.106447

Figures

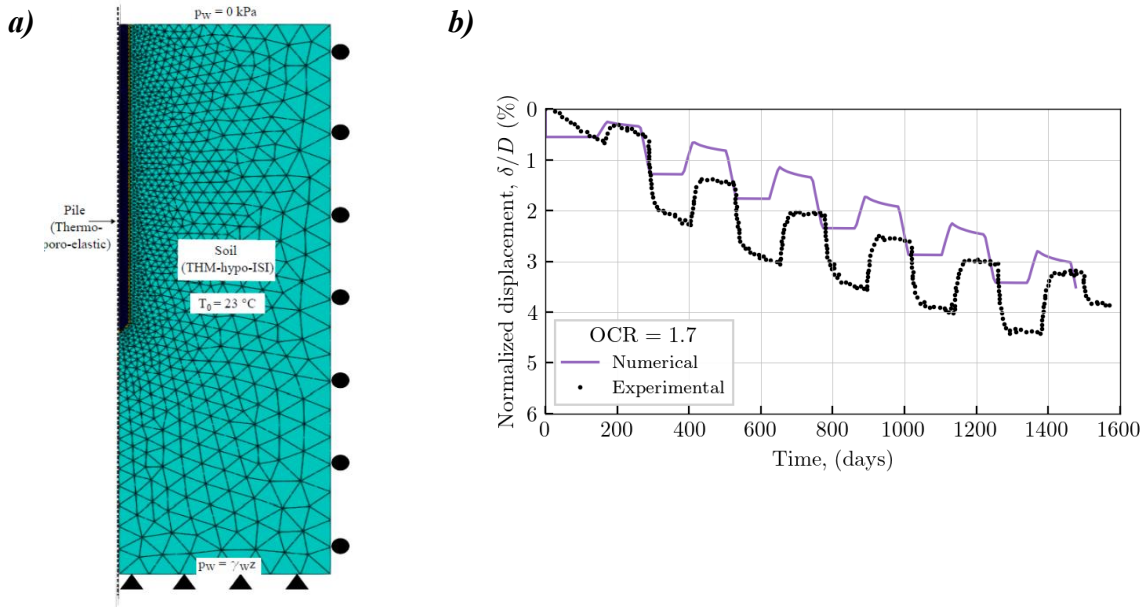

Figure 1: *a) Finite element model and boundary conditions b) Comparison between numerical simulations and experimental results in terms of normalized displacement vs. time for OCR=1.7.*

Hydro-mechanical behaviour of host formation during deep tunnel excavation for geological disposal

Vidushi Toshniwal[1*], Wout Broere[1], Michael A. Hicks[1], Anne-Catherine Dieudonné[1]

[1]Delft University of Technology, Delft, The Netherlands

V.T.Toshniwal@tudelft.nl

Keywords: Deep tunnel excavation, Finite element model, TBM tunnel, Clay formations, Geological disposal

Abstract

The most regarded solution for safe and long-term management of radioactive waste is deep geological disposal. Clay formations are viewed as potential formations to host such a facility in the Netherlands, Belgium, France, and Switzerland. In the Netherlands, the disposal concept is at an early stage and considers depths between 200 and 1000 m as suitable for the emplacement of radioactive waste in the Paleogene clay formations. The disposal concept involves the excavation of a tunnel structure with shafts, transport tunnels, and disposal tunnels in the host rock [1]. Due to this excavation the local stress field is inevitably altered as the host rock experiences stress redistribution and pore water pressure decreases locally due to drainage. This leads to local deformation and creates an Excavation Damaged Zone (EDZ) with modified hydro-mechanical properties. In poorly indurated clays, the tunnel needs to be supported by a liner due to the fast convergence of clay when subjected to stress release upon excavation. In the vicinity of the excavation, the host formation may experience different stress paths depending on the initial stress conditions and soil behaviour. There is limited research that looks at these stress paths during deep tunnel excavation in clays. In this study, Finite Element (FE) modelling is used to analyse stress redistribution and stress paths in the vicinity of a disposal tunnel excavated using a tunnel boring machine (TBM).

A 2D coupled hydro-mechanical analysis in plane strain conditions is performed using the Finite Element code, LAGAMINE, to model a quarter of the gallery at the depth of 400 m (Figure 1), by assuming symmetry along x- and y-axes. It has an inner radius of 2 m, the thickness of concrete segment is 0.4 m similar to the Connecting Gallery of the HADES Underground Research Laboratory (URL) in Mol, Belgium. Clay will converge upon loss of stress during excavation; therefore, a gap of 0.09 m is introduced in the model between gallery wall and lining. Contact elements are used to model the interaction between clay and concrete lining. There is a lack of high-quality test data on intact samples from the proposed disposal depths in the Netherlands [1]. Therefore, in this study the soil parameters are informed from literature on Boom Clay, since this is a well-characterised formation at the depth of HADES URL. Parametric study is done to check the sensitivity of results on estimated soil parameters. An elasto-plastic constitutive model based on the Drucker–Prager yield criterion with strain hardening/softening is used to model the soil behaviour [2].

As the excavation progresses there is an increase in hoop stress and reduction in radial stress which leads to generation of important deviatoric stress (q) near the gallery wall. The elements at the spring line come in contact with liner first which activates the liner and provides support to the soil near the gallery wall. Maximum shear strains developed near the gallery wall are in order of 5-6%. Due to stress anisotropy stress relief is non uniform which causes directional

pore pressure distribution in short-term, but it becomes concentric during the drainage phase in the long-term due to isotropic intrinsic permeability used in the model. The maximum normal contact pressure on the interface between clay and lining at the end of excavation phase is 4.2 MPa and increases up to 4.9 MPa in 100 years with progressive dissipation of pore pressures. The effect of creep is not considered in the model. Due to *in situ* stress anisotropy (K_0 = 0.8) the stress paths followed by soil elements at the spring line and the crown are different (Figure 2). Progressive dissipation of pore pressures and activated supporting stress leads to an increase in mean effective stress (p') and reduction in deviatoric stress (q) with time. This study provides information on the possible stress paths during tunnel excavation which should be considered in experimental investigations while analysing the mechanical behaviour of intact soil samples in context of deep geological disposal.

Acknowledgement

This work is part of the Safe Environment for Clay Underground Repository (SECUUR) project (no. 19986), which is financed by the Dutch Research Council (NWO) and co-financed by COVRA.

References

[1] P. Arnold, P. Vardon, M. A. Hicks, J. Fokkens, and P.A. Fokker. A numerical and reliability-based investigation into the technical feasibility of a Dutch radioactive waste repository in Boom Clay. OPERA-PU-TUD311, 2015.

[2] B. François, V. Labiouse, A. Dizier, F. Marinelli, R. Charlier, and F. Collin. Hollow cylinder tests on boom clay: modelling of strain localization in the anisotropic excavation damaged zone. Rock mechanics and rock engineering, 47, 71-86, 2014.

Figures

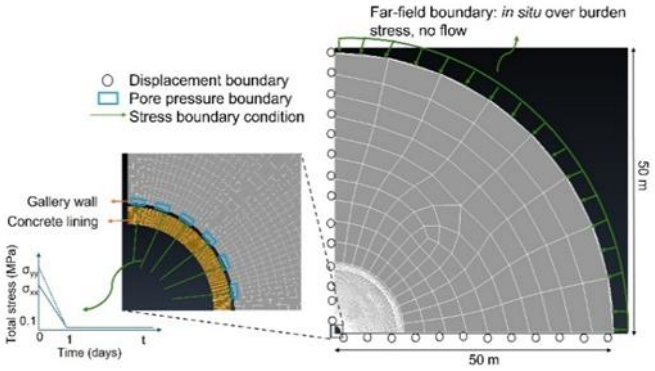

Figure 1: *Model geometry and boundary conditions for tunnel excavation simulation*

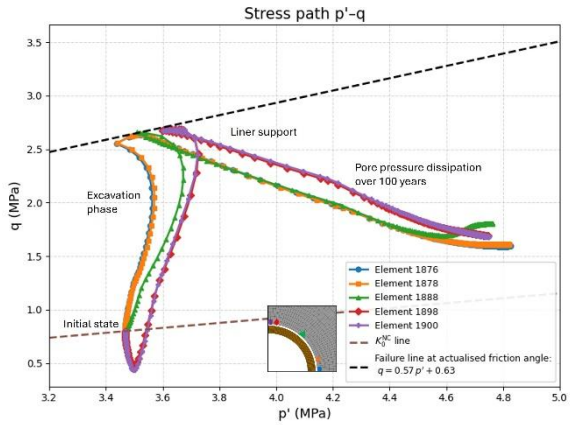

Figure 2: *Stress path followed by soil near gallery wall during different phases of simulation*

Simulation of the Behavior of Cohesive Powders: Linking the Atomic and Granular Scales

Aurélien Pujol[1,2], Jean-Mathieu Vanson[2], Farhang Radjai[1], Katerina Ioannidou[1]

[1]LMGC, Univ. Montpellier, CNRS, 860 Rue de St-Priest, 34090, Montpellier, France

[2]CEA, DES, IRESNE, DEC Cadarache F-13108 Saint-Paul-lez-Durance France

aurelien.pujol@cea.fr, jean-mathieu.vanson@cea.fr, franck.radjai@umontpellier.fr, aikaterini.ioannidou@umontpellier.fr

Keywords: Powder, multiscale Discrete Element Method, Molecular Dynamics, Coarse-Grained Method, van der Waals, capillary, uranium dioxide

Abstract

Predicting the cohesive behavior of uranium dioxide powders is a critical challenge in nuclear fuel manufacturing. Current simulations using the Discrete Element Method often fail because the underlying contact laws neglect key physical phenomena, such as van der Waals and electrostatic forces [1], surface roughness, and water-mediated interactions. To address this issue, we are developing a hierarchical, bottom-up framework to create a more predictive, physically grounded contact law (Figure 1).

Our approach begins at the atomistic scale, where we use molecular dynamics to compute the fundamental van der Waals and electrostatic attraction between two uranium dioxide crystallites in vacuum. This foundational force-distance curve will serve as input for a coarse-grained model that accounts for the effects of realistic surface roughness. Finally, we will incorporate water-mediated forces informed by recent first-principles studies [2] to capture crucial capillary and electrostatic effects arising in humid conditions. By systematically combining these phenomena, our work will provide a cohesive law for discrete element method (DEM), enabling more accurate simulations of uranium dioxide (UO_2) and plutonium dioxide (PuO_2) powders behavior under realistic industrial conditions.

References

[1] Giraud, M. (2020). *Analyse du comportement rhéologique des poudres à partir des propriétés des grains, application à l'étude d'un procédé de broyage/mélange pour la préparation du combustible nucléaire MOX* (Doctoral dissertation, Ecole des Mines d'Albi-Carmaux)

[2] Rodrik, G., Foucaud, Y., Siboulet, B., Duvail, M., Szenknect, S., & Dufrêche, J. F. (2025). Structure and chemistry of uranium dioxide (UO2) in water from first-principles molecular dynamics simulations. *Colloids and Surfaces A: Physicochemical and Engineering Aspects*, 136827

Figures

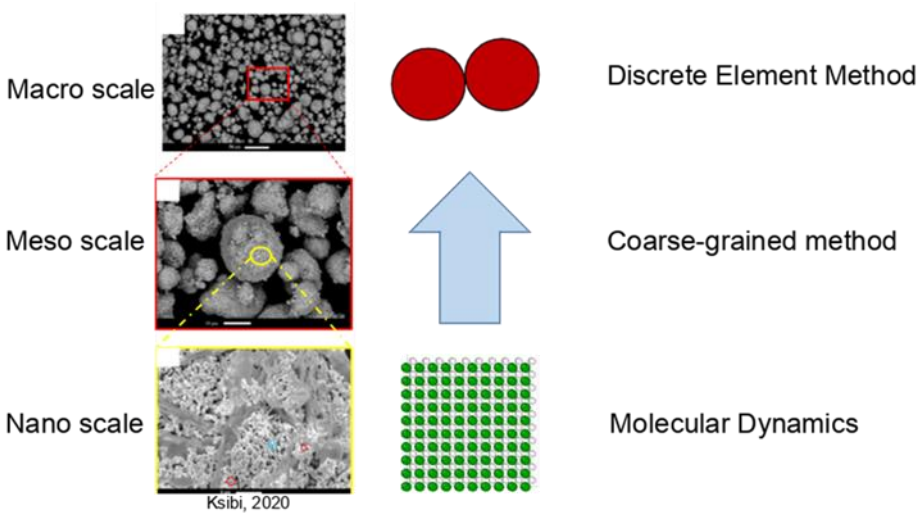

Figure 1: *Bottom-up framework of the simulation*

Cooling rate of clays: obtaining thermal parameters with an oven and thermal camera

Tomáš Mladý[1,*], Marco Loche[1,2], Gianvito Scaringi[1], Bhargavi Chowdepalli[1]

[1]Institute of Hydrogeology, Engineering Geology and Applied Geophysics, Faculty of Science, Charles University, Prague, Czech Republic

[2]Institute of Rock Structure and Mechanics, Academy of Sciences of the Czech Republic, Prague, Czech Republic

[*]mladyt@natur.cuni.cz

Keywords: Clay, Cooling rate, InfraRed Thermography, Heat capacity

Abstract

During this research we investigated compacted samples of Ca-bentonite and kaolin. To understand the impact of material and porosity on the cooling rate the samples were heated in an oven and subsequently air cooled to laboratory temperature. During cooling InfraRed Thermograms were taken to assess the cooling rate of the samples. We used the InfraRed thermograms to extract data for simple numerical model. This way we found the sought-after parameters. Our results show, that between values of thermal conductivity and heat capacity the latter is more sensitive to porosity and thus can be better constrained. This approach could prove useful for empirically calibrating thermal parameters for advanced constitutive models. However, more testing is necessary to establish a standard procedure and to sample and test more materials.

Methodology

In this experimental campaign we used bentonite from Czech Republic and kaolin from Malaysia. To prepare the cylindrical samples, 14 g of dry soil powder was compacted under various loads using a hydraulic press. When compacted the samples were ready, they were transferred on a tray and into a 105 °C oven for 24 hours to fully heat up. After the heating step thse samples are placed in the laboratory under FLIR C2 thermal camera that is set up perpendicularly to the tray. Thermograms were taken over 80 minutes every 5 minutes. After the experiment the data was analyzed and the cooling rate was extracted from the thermograms. This cooling behavior was used as input for GeoStudio's Temp/W and Air/W to simulate a uniaxial heat conduction test.

Results and conclusion

The prediction curves are quite close to each other (Figure 1) which may show, that this method is not very sensitive to changing properties in one material. However, there is substantial difference between the samples with different porosities in the first minutes of cooling. This could be investigated further with faster thermogram acquisition rate during the first few minutes.

The results of this method may change drastically with changes in water content, however in this simple experiment no sophisticated laboratory equipment is not required. And produces usable thermal parameters for numerical models.

.

References

Baryla P, Bernachy-Barbe F, Bosch JA, et al (2019) Bentonite mechanical evolution experimental work for the support of model development and validation. Deliverable 4.1 of EU EURATOM project BEACON—Bentonite Mechanical Evolution, https://www.beacon-h2020.eu/wp-content/uploads/2019/11/Beacon_WP4_Deliverable41_final.pdf.

Loche M, Scaringi G, Blahůt J, et al (2021) An Infrared Thermography Approach to Evaluate the Strength of a Rock Cliff. Remote Sens (Basel) 13:1265.

Loche M, Scaringi G, Blahůt J, Hartvich F (2022) Investigating the Potential of Infrared Thermography to Inform on Physical and Mechanical Properties of Soils for Geotechnical Engineering. Remote Sens (Basel) 14:4067.

Ren G-L, Chung C-C, Tsai C-E, et al (2022) Experimental Study on the Thermal Conductivity of Compacted SPV200 Bentonite. Minerals 12:932.

Svoboda J, Mašín D, Najser J, et al (2023) BCV bentonite hydromechanical behaviour and modelling. Acta Geotech 18:3193–3211.

Zheng L, Samper J, Montenegro L (2011) A coupled THC model of the FEBEX in situ test with bentonite swelling and chemical and thermal osmosis. J Contam Hydrol 126:45–60.

Figures

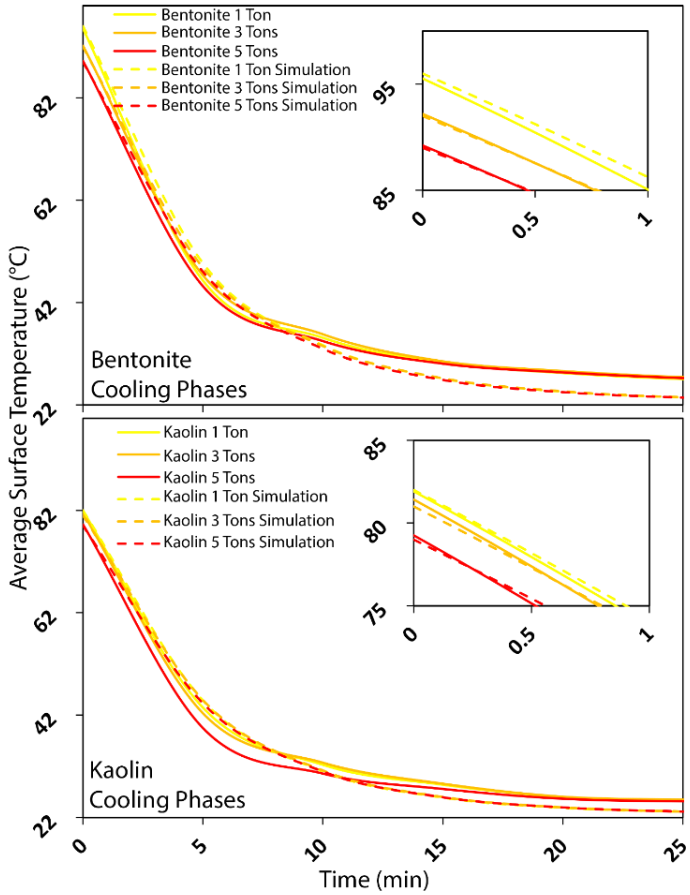

Figure 1: *Predictions of the cooling tests for compacted Bentonite and Kaolin under constant volume conditions at three differing initial compaction levels of 1, 3, and 5 tons.*

Sample preparation and constant-rate-of-strain (CRS) testing protocol for poorly indurated clays

Ties de Jong, Vidushi Toshniwal, Philip J. Vardon, Anne-Catherine Dieudonné

Delft University of Technology, Delft, The Netherlands

t.dejong@tudelft.nl

Keywords: sample preparation, CRS, poorly indurated clays, FE simulations

Abstract

Using undisturbed material to characterise the behaviour of stiff clays is essential to reduce uncertainty in engineering design, for example for geological disposal facilities [1]. However, standard sampling procedures and mechanical testing protocols [2] are not always suitable for these stiff clays, as relatively large forces are required for sampling and testing, which could damage the material. To ensure the reliability of laboratory results of mechanical tests, we propose a sample preparation method and an approach for determining optimum strain rates in constant-rate-of-strain (CRS) tests on stiff, poorly indurated clays. The tested material is surface Boom Clay collected from a quarry in Rumst, consolidated to 4 MPa in a Shelby tube to mimic conditions of material cored at 400 m depth.

First, full-length clay cores in steel Shelby tubes must be subsampled into workable pieces. Due to the material's relatively high strength, manual cutting is unsuitable. Instead, a band saw provided satisfactory subsampling. Unused portions of the core remain in the steel liner and flat edges are created. CT scans (Figure 1) confirmed that metal fragments from the liner do not penetrate the clay and that cutting does not cause fractures or significant drying. Only the outer few millimetres are affected, which should be trimmed before testing.

For consolidation tests, the next step is inserting a clay specimen into the testing ring. A cutting ring is used for this. In stiff clays manual insertion is not possible and instead a hydraulic press must be used. However, hydraulic pressing often induces shear and tensile stresses that exceed the soil's strength, causing fractures and making the samples unusable (Figure 2). We suggest adding confinement during ring insertion, which sufficiently reduces tensile stresses and prevents breakage.

The CRS test is a one-dimensional consolidation test where a constant axial strain rate is applied while pore pressure evolution is monitored. Selecting an appropriate strain rate is critical: if the strain rate is too high, the material behaviour will tend to undrained conditions; if it is too low, excess pore pressures do not develop sufficiently to be measurable, and tests take unnecessary long. Reported strain rates for stiff, poorly indurated clays range widely in the literature, from 0.05%/h [3] to 8%/h [4]. ASTM D4186 recommends applying a strain rate where the ratio of excess pore pressure to applied stress lies between 3–15%. Finite element simulations of the CRS test are compared with laboratory CRS results on the tested material (Figure 3). These suggest that a strain rate of about 0.05%/h is most suitable for clays with similar properties as tested here ($\lambda \approx 0.1$, $k \approx 10^{-19}$ m^2).

The sample cutting and preparation method of using a band saw to cut clay cores with steel Shelby liner and maintaining confinement while inserting in the cutting ring, will be applied to undisturbed clay cores obtained from the DAPGEO-02 borehole in Delft (+/- 400 m depth). Based on the results presented here, CRS tests on this material are conducted at strain rates in the order of 0.05%/h.

Acknowledgements

This work is part of the SECUUR (Safe Environment for Clay Underground Repository) project no. 19986, which is financed by the Dutch Research Council (NWO) and co-financed by COVRA.

References

[1] Arnold, P., Vardon, P., Hicks, M., Fokkens, J., & Fokker, P. (2015). A numerical and reliability-based investigation into the technical feasibility of a Dutch radioactive waste repository in Boom Clay (technical report OPERA-PU-TUD311.).

[2] ASTM. (2024). Standard Test Method for One-Dimensional Consolidation Properties of Saturated Cohesive Soils Using Controlled-Strain Loading (ASTM Standard D4186/D4186M-20e1).

[3] Kinslev, E. M., Hededal, O., Rocchi, I., & Zania, V. (2022). Mode-based characterisation of swell deformations in a high-plasticity Paleogene clay. Canadian Geotechnical Journal, 59(6), 796-807.

[4] Awarkeh, M. (2023). Investigation of the long-term behaviour of boom clay (Doctoral dissertation, Ecole des Ponts ParisTech)

Figures

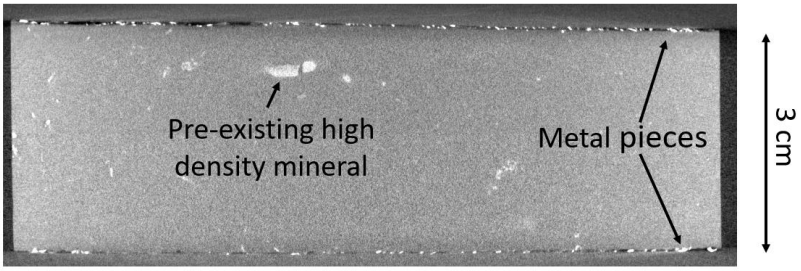

Figure 1: *µ-CT scan of clay core section cut with a band saw. Liner is removed prior to scanning. Pieces of metal are present only at the surface. No fractures or drying beyond the surface is observed.*

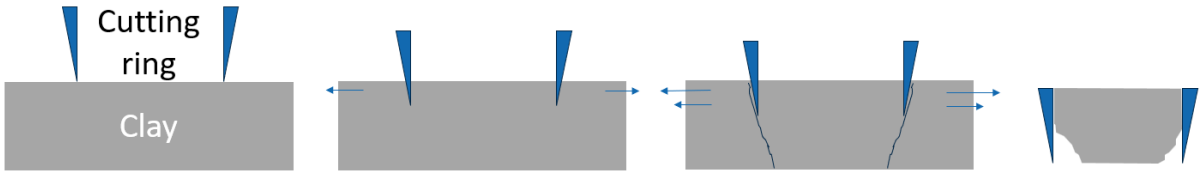

Figure 2: *Schematic of fractures forming while inserting a cutting ring in stiff clay.*

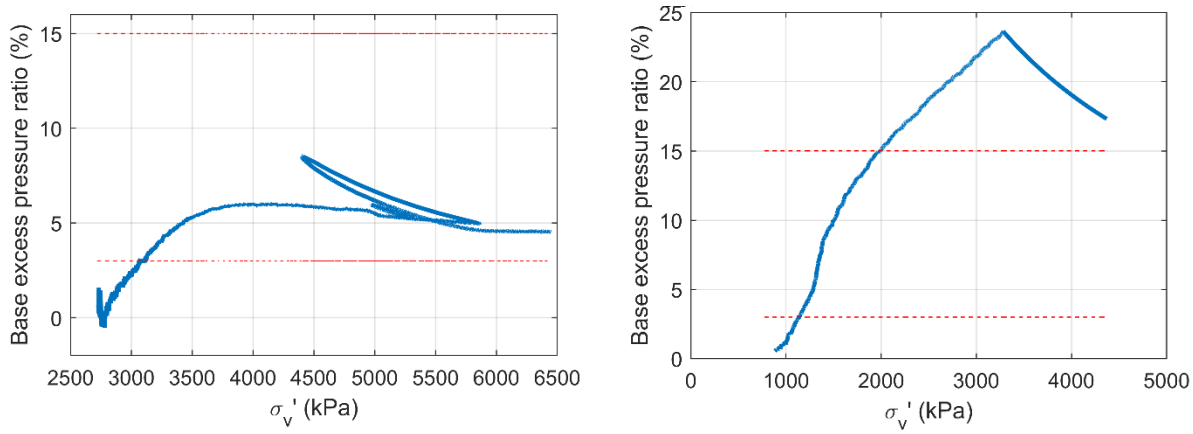

Figure 3: *Excess pore pressure ratio for a CRS test on surface Boom Clay conducted at 0.05%/h (left) and 1%/h (right). In the latter the maximum capacity of the pore pressure transducer was reached, causing the drop in pressure ratio after 3.2 MPa of vertical effective stress.*

Numerical model of magmatically driven hydrothermal system THM(C) in volcanic settings

Jens Niclaes[1], Thomas Poulet[2], Pierre Delmelle[3], Hadrien Rattez[1]

[1]Institute of Mechanics, Materials and Civil Engineering, Civil and environmental engineering, Université Catholique de Louvain, Louvain-la-Neuve, Belgium

[2]Commonwealth Scientific and Industrial Research Organisation (CSIRO), Mineral Resources, Discovery, Kensington (Perth, W.A.), Australia

[3]Earth and Life Institute , Environmental Sciences, Université catholique de Louvain, Louvain-la-Neuve, Belgium

jens.niclaes@uclouvain.be

Keywords: Volcano, FEM; Numerical model; Hydrothermal systems; Mineral deposits; Alteration

Abstract

Volcanic flank collapse is a recurrent natural disaster documented at volcanoes worldwide, including Mount St. Helens (1980), Bezymianny (1956), Bandai (1888), and Unzen (1792) ([1], [2]). These large-scale instabilities are often linked to hydrothermal alteration, in which circulating fluids and heat interact with volcanic rocks, altering their mineral composition and weakening their mechanical properties [3]. However, numerical investigation of mineral alteration and deposit formation in volcanic hydrothermal systems remains largely undeveloped. Current models of magmatically driven hydrothermal systems primarily address fluid and heat transport, often neglecting the mechanical response of host rocks. This limits their usefulness in assessing volcanic stability. In this context, modeling the coupled thermal, hydraulic, mechanical, and chemical processes offers a new way to identify zones prone to alteration and potential flank instability.

We constructed a two-dimensional numerical model of a magmatically driven hydrothermal system using the finite element method (FEM) within the open-source MOOSE framework, which is a multiphysics environment for solving coupled nonlinear problems. The PorousFlow module was used to simulate fluid flow, heat transfer, mechanical behavior, and chemical processes. The model couples heat from a magmatic source with fluid circulation in the surrounding porous medium, as well as the resulting stress changes in the host rock. Chemical processes are represented through indicators of conditions favorable to species transport rather than through explicit solute tracking. Currently, the mechanical response is limited to linear elasticity. This new model, still under development, offers insights into the dynamics of magmatically driven hydrothermal systems. Permeability is the main factor determining the driving heat transfer mechanism between conduction and advection ([4], [5]). Heat conduction coefficient affects the driving heat transfer mechanism less because its range of values in rock is smaller than that of permeability. Consequently, a variation in the order of magnitude of permeability between rock layers might cause heat accumulation and vaporization, or ,conversely, provide an easy escape route. Similarly, faults or other vertical heterogeneities, change the entire dynamic by creating a water freeway from deep within the earth to the surface.

Classifying hydrothermal systems as advective or conductive, also provides insight into how volcanic settings respond to regional stresses and strains. A low-permeability, conductive system, will experience a high stress peak when subjected to a high strain rate, such as during

an earthquake. On the other hand, a high permeability, advective system, will easily dissipate an increase in stress when subjected to a high regional strain rate.

In volcanic edifices, cold meteoric water flows from the head at the center to the toes on the sides ([4], [5]). This flow shields the volcanic edifice from the hot mineralized (magmatic) water from deep below. This creates relatively sharp temperature variations underneath and near the sides of the volcanic edifice. This process also facilitates the accumulation of high-temperature areas near the bottom of the volcanic slopes and mineral transport. Thermal stresses around the volcanic edifice can reach 20 MPa of tension when assessed elastically. Volcanic rocks do not have a tension strength of 20 MPa, so such elastic assessment is physically incorrect. Nevertheless, the thermal stresses are sufficient to explain the nucleation of faults and the opening of existing ones. Since this swelling behavior creates tension near the surface due to temperature variation alone, it could certainly explain magma rising. Indeed, heat travels faster than the magmatic and clearly creates faults. These faults cause depressions that suck magma to the top. As the magma come closer to the surface, it heats on its turn the area, creating even more faulting and depression.

The presence of the necessary conditions for the dissolution or precipitation of minerals in the hydrothermal system is used to track the transport of chemical species. Due to the shielding effect of the cold downward flow, the chemical species are not transported to or from the body of the volcanic edifice. Instead, they are transported on the sides at the base of the volcanic edifice's slopes. Since hydrothermal alteration decreases rock mechanical strength, it could explain volcanic flank instabilities, especially since it occurs at the critical slope toe.

The numerical model is still being developed mechanically to couple the opening of existing faults, the nucleation of faults, and plastic computations with the other physics.

References

[1] L. Siebert, "Large volcanic debris avalanches: Characteristics of source areas, deposits, and associated eruptions," *Journal of Volcanology and Geothermal Research*, vol. 22, no. 3–4, pp. 163–197, Oct. 1984, doi: 10.1016/0377-0273(84)90002-7.

[2] L. Siebert, H. Glicken, and T. Ui, "Volcanic hazards from Bezymianny- and Bandai-type eruptions," *Bull Volcanol*, vol. 49, no. 1, pp. 435–459, Feb. 1987, doi: 10.1007/BF01046635.

[3]M. Detienne, "Unravelling the role of hydrothermal alteration in volcanic flank and sector collapses using combined mineralogical, experimental, and numerical modelling studies," Université catholique de Louvain, Louvain-la-Neuve, 2016.

[4] S. Scott, T. Driesner, and P. Weis, "Geologic controls on supercritical geothermal resources above magmatic intrusions," *Nat Commun*, vol. 6, no. 1, p. 7837, July 2015, doi: 10.1038/ncomms8837.

[5] S. Scott, T. Driesner, and P. Weis, "Boiling and condensation of saline geothermal fluids above magmatic intrusions," *Geophysical Research Letters*, vol. 44, no. 4, pp. 1696–1705, Feb. 2017, doi: 10.1002/2016GL071891.

Figures

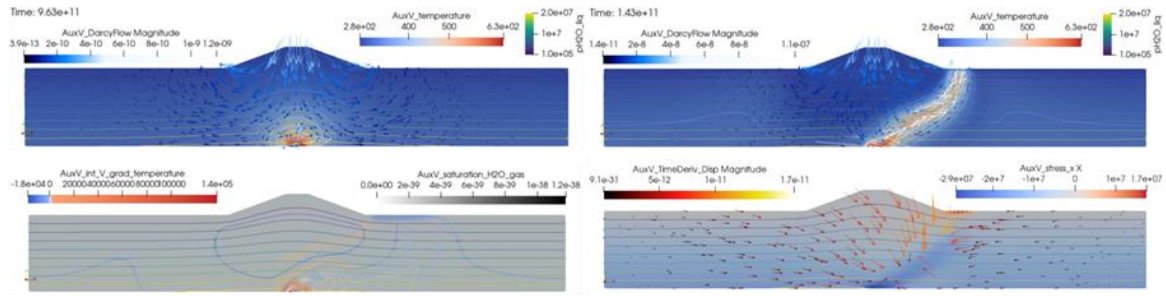

Figure 3: *Results out of a model for a homogeneous hydrothermal system. (A) K = 1e-16 (B-C-D) K = 1e-14. (A-B) Darcy flow, temperature and pressure distributions. (C) Chemical proxy (time integral of v.gradT). (D) Horizontal stresses.*

4D Imaging of Time-Dependent Behavior: Improving Space–Time Resolution for Flooding Tests in Geomaterials

H. Greggi [a], O. Stamati [b], A. Tengattini [c], S. Roux [d]

[a]Laboratoire 3SR, Grenoble, LMPS, Gif-sur-Yvette

[b]CNRS, Laboratoire 3SR, Paris

[c]Laboratoire 3SR, Institut Laue Langevin, Chaire IUF

[d]University Paris-Saclay / Centrale Supélec / ENS Paris-Saclay / CNRS, LMPS

hilario.greggi@3sr-grenoble.fr, olga.stamati@3sr-grenoble.fr, alessandro.tengattini@3sr-grenoble.fr, stephane.roux@ens-paris-saclay.fr

Keywords: Neutron imaging, 4D reconstruction, Transfer in porous media

Abstract

Computed Micro-Tomography is an ideal probe for studying micro-scale processes in geomaterials. Due to the high sensitivity of neutrons to hydrogen, neutron tomography has proven advantageous for tracking specifically water within geomaterials [1]. However, it suffers from low space and time resolution, which is an issue for high flow rates in porous media. The present study introduces a tomographic reconstruction formulation that enables temporal resolutions of up to 100 Hz.

In hydromechanical testing, 4D monitoring (a sequence of 3D tomographies at successive times) is typically performed through the sequential acquisition of tomographies at evolving hydric states. However, interrupting the flow for acquisition may alter the process through capillary-driven reorganization, whereas maintaining a steady flow causes a continuous evolution of the invaded pore volume during the scan, producing "motion-blur" effects in the reconstruction when tomographies are acquired over the typical neutron imaging time spans.

The proposed method is an alternative reconstruction strategy, adapted from the Projection-based Digital Volume Correlation (P-DVC) framework used for fluid tracking in [2]. The main idea is to construct a 4D spatio-temporal reduced representation of the gray-level scalar field, used as a proxy for the neutron attenuation field, and to optimize its parameters by minimizing the squared norm of the difference between measured and simulated projections.

The approach was applied to images from a flooding test on Ottawa sand, acquired at the ILL facility using the NeXT instrument [3]. Projections were recorded at 100 Hz while the sample was progressively invaded by descending droplets. Figure 1 compares projection sets over a full 0–360° angular range, captured around a specific and sudden event : the fall of a water drop. The measured projections (top row, ground truth) $\mu_0(r,t)$, the forward projections of a 3D volume reconstructed from the same set (middle row, conventional approach) $\mu_1(r,t)$, and the projections simulated from the 4D representation (bottom row, proposed method) $\delta_2(r,t)$. This last set of projections results from the projection of the 4D spatio-temporal model, optimized to better represent the time-dependent part of the signal.

The first row of projections corresponds to angles ranging from 0° to 180°. The droplet falls a few hundredths of a second before the 180° angle. The discrepancy within a full angular range is clearly illustrated. The second row shows motion blur resulting from the assumption of

temporal stability typically taken during reconstruction. The forward projections of the conventional reconstruction differ from the measured ones. In contrast, projections simulated with the proposed method are not affected by this assumption and exhibit greater temporal flexibility, allowing them to capture the temporal evolution of the hydric state within the scan.

The novelty of this work lies in the global approach to tracking the hydric state, giving up the classical assumption of time independence and accounting for the temporal evolution in the chosen parametric description, computed from the entire set of projections. The optimization is carried out using the squared norm between simulated and measured projections.

References

[1] A. Tengattini, N. Lenoir, E. Andò, et G. Viggiani, « Neutron imaging for geomechanics: A review », *Geomechanics for Energy and the Environment*, vol. 27, p. 100206, sept. 2021, doi: 10.1016/j.gete.2020.100206.

[2] C. Jailin, M. Etxegarai, E. Tudisco, S. A. Hall, et S. Roux, « Fast Tracking of Fluid Invasion Using Time-Resolved Neutron Tomography », *Transport in Porous Media*, 2018, doi: 10.1007/s11242-018-1055-9.

[3] A. Tengattini et al., « NeXT-Grenoble, the Neutron and X-ray tomograph in Grenoble », Nuclear Instruments and Methods in Physics Research Section A: Accelerators, Spectrometers, Detectors and Associated Equipment, vol. 968, p. 163939, juill. 2020, doi: 10.1016/j.nima.2020.163939.

Figures

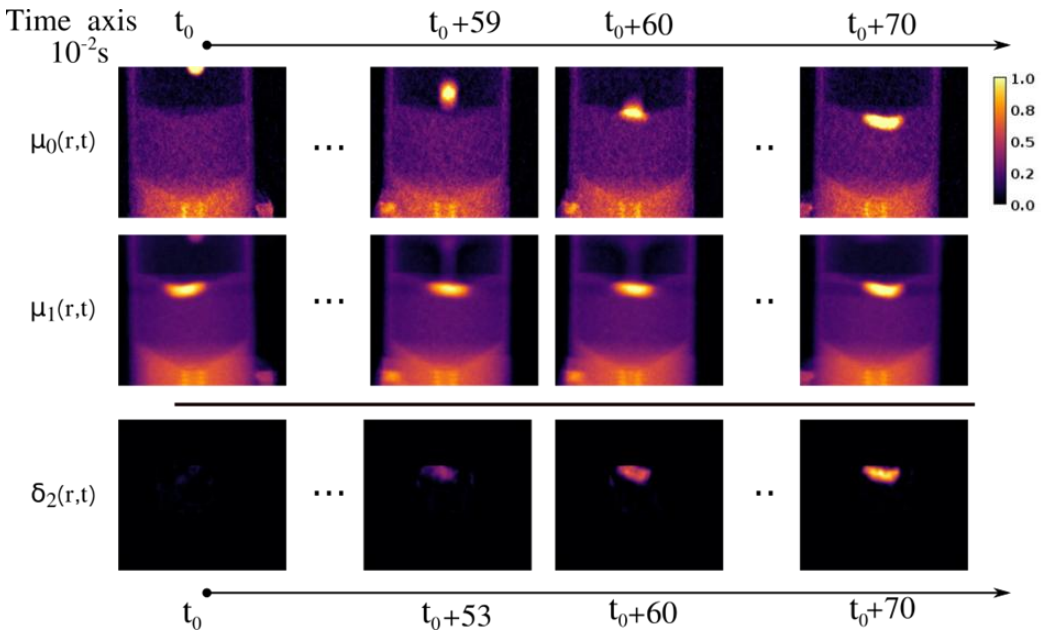

Figure 1: *Comparison of classical and proposed approaches for fluid tracking*

Vibration-Driven Densification of Ballast: 3D DEM Excitation Box and Regime Mapping

Diallo Abdourahmane, Takashi Matsushima, Akiko Kono, Nakamura Takahisa

University of Tsukuba, University of Tsukuba, Railway Research Technical Institute

s2420912@u.tsukuba.ac.jp, tmatsu@kz.tsukuba.ac.jp, kono.akiko.43@rtri.or.jp, nakamura.takahisa.19@rtri.or.jp

Keywords: granular material, bulk density, Vibration simulation

Abstract

This study investigates the dynamic behavior of irregularly shaped granular materials subjected to one-dimensional wall vibration using 3D clumped-sphere DEM. Granular assemblies were subjected to sinusoidal horizontal vibrations within a box container (fig. 1) across various amplitudes (0.5 to 10mm) and frequencies (10-100Hz). A comprehensive power law mathematical model was developed to quantify the settling behavior. The study reveals three regimes based on the dimensionless acceleration $\Gamma = (4\pi^2 f^2 A)/g$: quasi-consolidation, steady consolidation and Dynamic agitated regime.

Bulk density evolution of the granular system was clearly captured by the mathematical model, mapping the regimes. After analysis, an optimal Γ range was identified within the steady consolidation regime where densification is monotonic and stable. From the energy profiles analysis, the compaction work follows the same trend as the density gain of all Γ values (fig.2). Energy partitioning (fig.3) shows that most of the vibration wall input energy is dissipated. As a result, compaction efficiency is highest at low Γ and decreases with intensity. Overall, Γ provides superior predictive capability over amplitude or frequency alone and defines a practical operating window for efficient densification.

These findings provide insights into the optimal adjustment of vibration parameters to improve compaction efficiency in tamping operations, contributing to maintenance and track stability. Additional analysis will clarify the observed trends and support best practices for achieving maximum ballast layer compaction through controlled vibration.

References

Kim, D. S., Hwang, S. H., Kono, A., & Matsushima, T. (2018). Evaluation of ballast compactness during the tamping process by using an image-based 3D discrete element method, Journal of Rail and Rapid Transit, 0(0), 1–14. DOI 0.1177/0954409718754927.

Chi, Y., Xiao, H., Zhang, Z., Nadakatti, M. M., & Qian, Z. (2024). Analysis of the influence of vibration frequency and amplitude on ballast bed tamping operation in railway turnout areas. Computational Particle Mechanics 11(2). DOI:10.1007/s40571-023-00652-4.

Qian, Yu, Erol Tutumluer and Hai Huang. (2011). A Validated Discrete Element Modeling Approach for Studying Geogrid-Aggregate Reinforcement Mechanisms. Geo-Frontiers 2011: Advances in Geotechnical Engineering. https://doi.org/10.1061/41165(397)476.

Sonar, P., H Katsuragi, H. (2022). Decompaction wave propagation in a vibrated fine-powder bed. Physical Review E 106 (1), 014905.

Figures

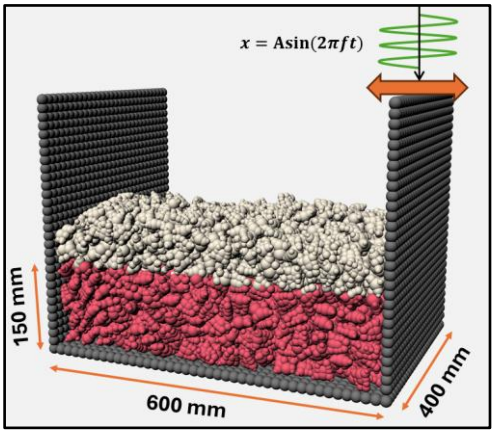

Figure 1: *3D model of the simulation Box*

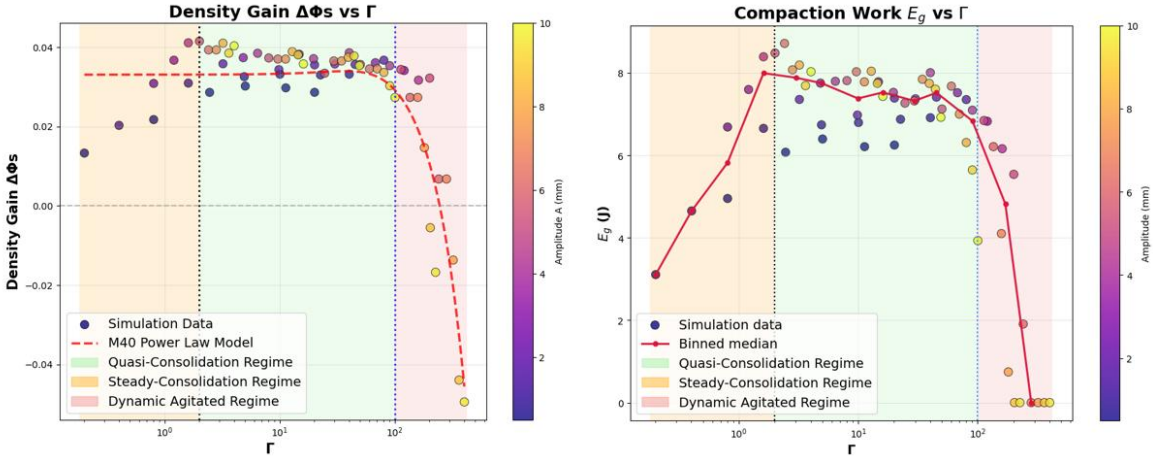

Figure 2: *Density Gain vs Vibrational Intensity (Power Law Model)*

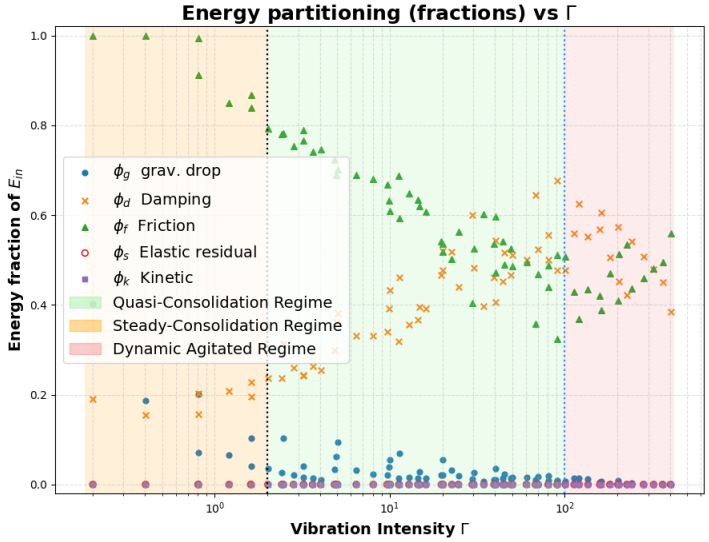

Figure 3: *Density Gain vs Vibrational Intensity (Power Law Model)*

Accelerated implicit cyclic loading with an interface implementation

Tomáš Kadlíček, Stanislav Pařez, David Mašín

Faculty of Science, Charles University, Czech Republic

tomas.kadlicek@natur.cuni.cz

Keywords: Cyclic loading, acceleration, numerical modelling

Abstract

In this contribution, we aim to improve the main drawback of the implicit cyclic loading against the explicit cyclic loading [1], i.e., its calculation speed. We pursue numerical acceleration based on an extrapolation of all state variables and nodal displacements, resulting in instantaneous jumps during the implicit cyclic loading. Aside from the mass elements acceleration studied earlier [2], in this work, we show the acceleration on a laterally loaded pile with the interface between the soil and the pile, see Fig. 1. The pile is represented by the linear elastic model, soil by the hypoplastic sand model [3], and the interface by the Mohr-Coulomb model. All three models are thus accelerated simultaneously at the designated times

Acceleration of the stress components used in the case of the hypoplastic sand model is shown in Fig. 2a where the linear extrapolation (red) is based on the recorded rate (blue) of the previous stress components. As shown in [2], the asymptotic behaviour of the hypoplastic sand model is sufficient to correct a local overestimation of the accelerated characteristics. Furthermore, the hypoplastic model does not explicitly define any limit yield surface. However, this approach cannot be used in the case of the Mohr-Coulomb model, which explicitly defines the yield surface F which cannot be violated during the integration and, consequently, cannot be violated even during the acceleration. The stress return to the yield surface is, therefore, based on the elastic prediction of N cycles. A proper intersection of the elastic stress path and yield surface is performed first see, Fig 2b.

Results of the numerical simulations with the span of 1000 cycles in shown in Fig 3. First, the implicit cyclic loading is performed first as the benchmark. Two accelerated simulations are performed designated as ACL1 and ACL2, where ACL1 is performed without the interface acceleration while ACL2 includes the interface acceleration in order to compare its importance. Local results measured at the distance 8 m, see Fig. 3a and Fig. 3b, show that the accelerated calculation follows closely the implicit simulation, however, ACL1 manifests locally distinct jumps is stress components during in the simulation. Global results are shown in Fig. 3c and Fig. 3d by the means of shear strains ε_{xz} isolines which indicates that the differences between the implicit and ACL1 simulations are almost indistinguishable.

References

[1] Kadlíček, T., and D. Mašín. 2014. Accelerated implicit cyclic loading with the hypoplastic sand. Geotechnical Engineering Challenges to Meet Current and Emerging Needs of Society. 3011-3014.

[2] Niemunis, A., Wichtmann, T., & Triantafyllidis, T. 2005. A high-cycle accumulation model for sand. Computers and geotechnics, 32(4), 245-263.

[3] Von Wolffersdorff, P. A. 1996. A hypoplastic relation for granular materials with a predefined limit state surface. Mechanics of Cohesive-frictional Materials: An International Journal on Experiments, Modelling and Computation of Materials and Structures, 1(3), 251-271.Lora, M., Camporese, M., Troch, P.A. and Salandin, P.

2016. "Rainfall-triggered shallow landslides: infiltration dynamics in a physical hillslope model." Hydrological Processes 30, 3239–3251.

Figures

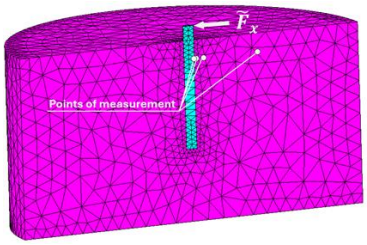

Figure 1: *Geometry of the numerical model.*

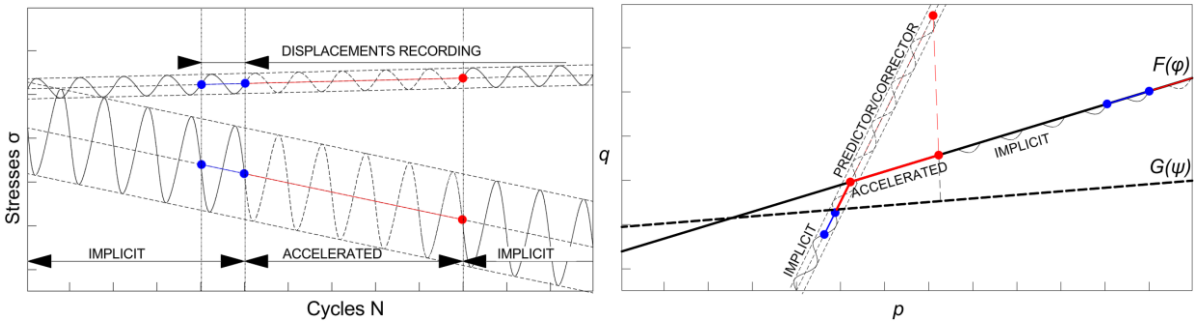

a) Illustration of stress acceleration

b) Interface extrapolation with the yield surface F and the plastic potential G

Figure 2: *Stress acceleration.*

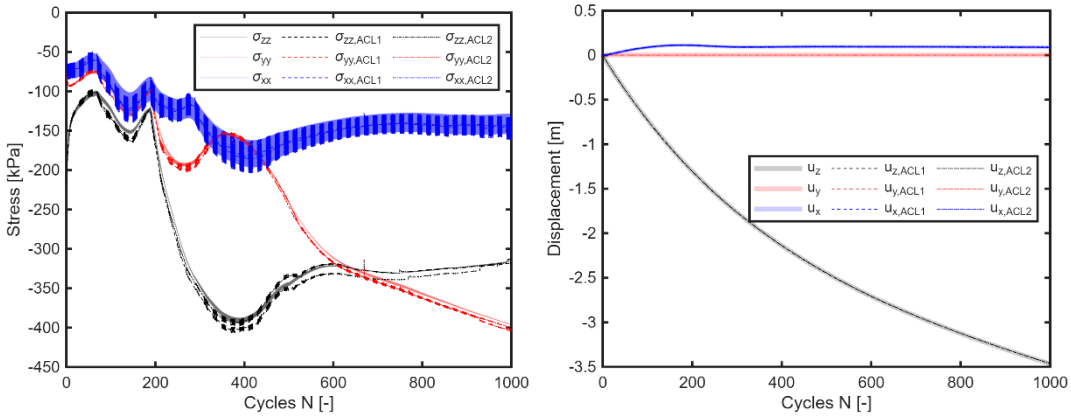

a) Stress at 8.0 m

b) Displacements at 8.0 m

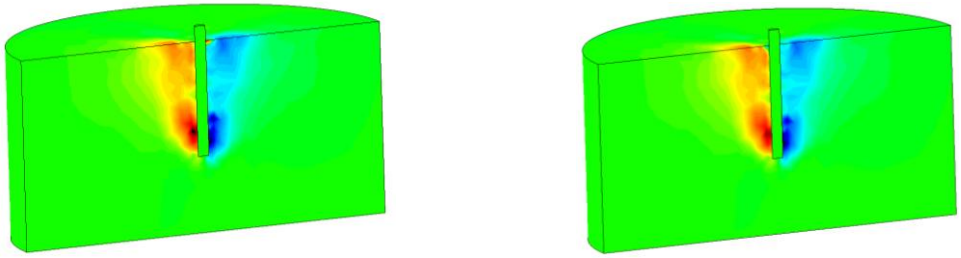

c) ε_{xz} – Implicit

d) ε_{xz} – Accelerated

Figure 3: *Comparison of the implicit and accelerated numerical simulation.*

Effect of clay content on frost heave and thaw settlement using MRI

Christelle Tabbiche, Jaime Elias Gil Roca, Rahima Sidi-Boulenouar, Benjamin Maillet, Baptiste Chabot, Jean-Michel Pereira, Michel Bornert, Patrick Aimedieu, Anh Minh Tang

Navier, ENPC, Institut Polytechnique de Paris, Univ Gustave Eiffel, CNRS, Marne-la-Vallée, France

Christelle.tabbiche@enpc.fr

Keywords: Sandy soils, clay content, frost heave, thaw settlements, heat and moisture transfer, Magnetic Resonance Imaging (MRI)

Abstract

Freeze - thaw processes in seasonally frozen soils involve complex interactions between heat transfer, moisture migration, phase changes and mechanical deformation (Hu et al. 2023; Wu et al. 2021). While the role of clay content in influencing frost heave susceptibility is well recognised, its effect on coupled heat and moisture transfer and thaw settlement in sandy soils remains insufficiently understood. This study investigates the impact of varying clay content on frost heave and thaw settlement in sandy soils, using Magnetic Resonance Imaging (MRI) to monitor water content profiles throughout the freeze - thaw process.

Materials

Quartz Fontainebleau sand (NE34), sourced from northern France, was mixed with Speswhite Kaolin clay. The resulting sandy soils had clay contents (defined as the ratio of the dry mass of clay to the dry mass of soil) of 0%, 5%, 10%, 15%, and 20%, labelled as K0, K5, K10, K15, and K20, respectively. The mixtures were prepared at an initial water content corresponding to the optimal value, as determined in Vu et al. 2023

Experimental setup

The experimental setup used to conduct freezing and thawing tests is illustrated in Figure 1. The system consists of the following components: A vertical MRI spectrometer (DBX 24/80 Bruker), an MRI-compatible testing cell, soil specimen measuring 100 mm in height and 94 mm in diameter, a saturation system, a temperature control system, a temperature monitoring system including sensors embedded in the soils. Further details of the experimental setup and calibration (for estimating the volumetric water content from the MRI signal) are provided in Tabbiche et al. 2025.

Results

A one-side freezing test was applied to the different soils, followed by a two-side thawing test. The results for the mixture with 10% clay are presented below (Figures 2 and 3), and a comparison of frost heave occurrence for all mixtures is shown in Figure 4.

References

Y. Hu, Z. Fu, X. Hou, Y. Zhang, Z. Wang, B. Li, Heat and water transfers for the frost heave behavior of freezing graded soil, International Communications in Heat and Mass Transfer 143 (2023).

Y. Wu, E. Zhai, X. Zhang, G. Wang, Y. Lu, A study on frost heave and thaw settlement of soil subjected to cyclic freeze-thaw conditions based on hydro-thermal-mechanical coupling analysis, Cold Regions Science and Technology (2021).

Q.H. Vu, J.-M. Pereira, A.M. Tang, Effect of clay content on the thermal conductivity of unfrozen and frozen sandy soils, International Journal of Heat and Mass Transfer 206 (2023).

C. Tabbiche, J.E.G. Roca, R. Sidi-Boulenouar, B. Maillet, J.-M. Pereira, B. Chabot, M. Bornert, P. Aimedieu, A.M. Tang, Magnetic Resonance Imaging as a tool for investigating frost heave dynamics: a new experimental setup and application, Can. Geotech. J. (2025).

Figures

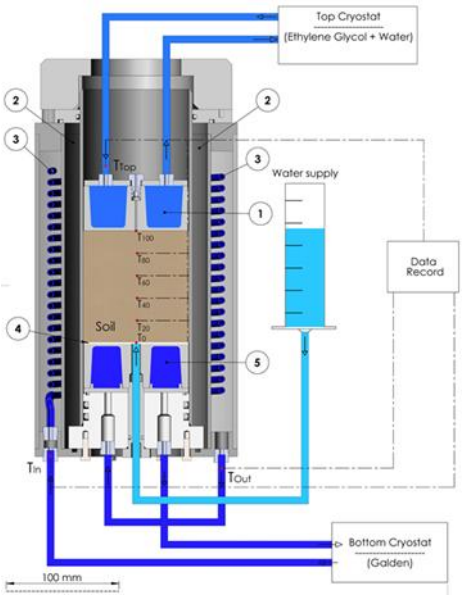

Figure 1 : *Experimental setup.*

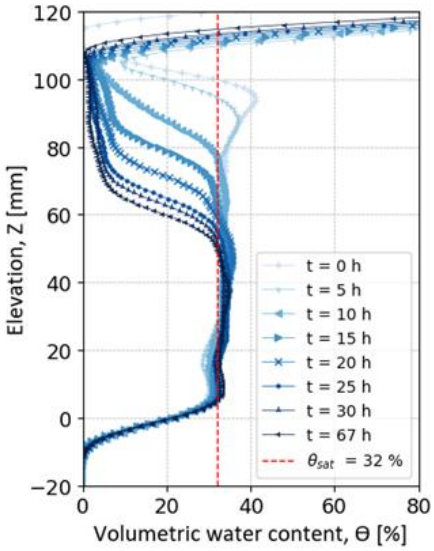

Figure 2: *Volumetric water content during freezing.*

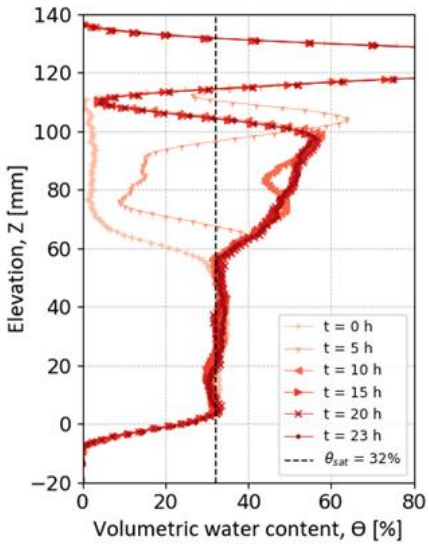

Figure 3: *Volumetric water content during thawing.*

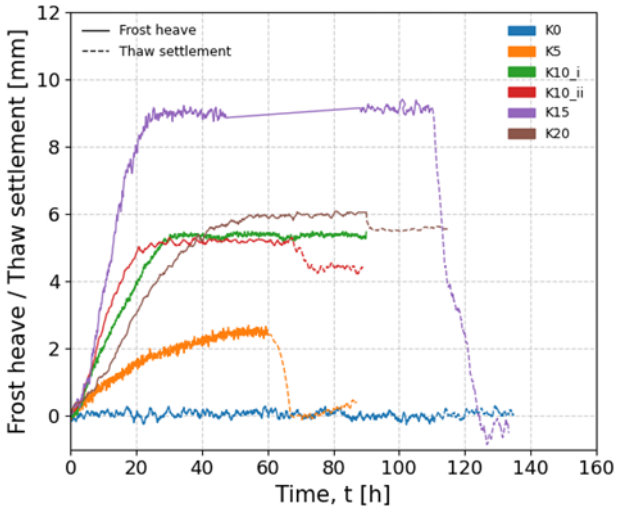

Figure 4: *Frost heave occurrence.*

Overcoming Mesh Dependence in Strain-Softening Problems via Cosserat Mechanics and the Particle Finite Element Method

Nathan Delpierre, Thomas Leyssens, Sandra Soares-Frazão, Hadrien Rattez

Institute of Mechanics, Materials and Civil Engineering, UCLouvain (Belgium)

nathan.delpierre@uclouvain.be

Keywords: PFEM, Cosserat Mechanics, Retrogressive landslide

Abstract

Landslide and slope failures are geomechanical phenomena characterized by the formation of distinct shear bands whose thickness is governed by the material's elasto-plastic constitutive behavior. While shear band characteristics can be determined through post-failure analysis, their accurate numerical prediction remains challenging due to constitutive model dependencies.

Retrogressive landslides in sensitive clays represent a particularly complex case, exhibiting pronounced strain-softening behavior that leads to progressive failure mechanisms. Numerical simulation of these phenomena using classical finite element methods typically suffers from pathological mesh dependence, where strain localizes within single elements and mesh refinement fails to provide convergent solutions.

Solutions exist to mitigate these technological issues. Non-local approaches are, for example, very popular since they are straightforward to implement. These approaches rely on averaging of the state variables around each quadrature point, based on an internal length that must be selected prior to the simulation.

In the present study, we address the strain localization issue through the implementation of Cosserat Mechanics. This physics inherently incorporates a physical internal length scale within its mathematical formulation, which can be directly related to characteristic microstructural dimensions such as grain size. Prior research conducted by Rattez et al (2018) has shown that Cosserat mechanics successfully achieves mesh-independent solutions for strain-softening material behavior.

This work focuses on the combined use of Cosserat Mechanics and of the Particle Finite Element Methods (PFEM) to simulate in a physical way phenomena such as retroactive failure.

Figure 1 illustrates the general framework of the PFEM algorithm. The methodology follows a straightforward procedure: beginning with an initial set of points, GMSH generates the physical domain mesh (Leyssens et al., 2024), upon which the displacement field is computed using a physical solver—in this case, the open-source MOOSE software. Finally, particle positions are updated and all state variables are transferred to the newly generated mesh.

In this work, we show how the general framework was applied to shear test benchmark (Figure 2). The parameters of the Cosserat mechanics and their effects on the failure pattern are also investigated in case of retrogressive failure pattern.

References

Hadrien Rattez, Ioannis Stefanou, Jean Sulem, Manolis Veveakis, Thomas Poulet, The importance of Thermo-Hydro-Mechanical couplings and microstructure to strain localization in 3D continua with application to seismic faults. Part II: Numerical implementation and post-bifurcation analysis, Journal of the Mechanics and Physics of Solids, Volume 115, 2018, Pages 1-29, ISSN 0022-5096, https://doi.org/10.1016/j.jmps.2018.03.003.

Leyssens, T., Henry, M., Lambrechts, J., & Remacle, J.-F. (2024, September). A Delaunay refinement algorithm for the particle finite element method applied to free surface flows. *International Journal for Numerical Methods in Engineering*, *125*(18), e7554. John Wiley & Sons, Ltd. https://doi.org/10.1002/nme.7554

Figures

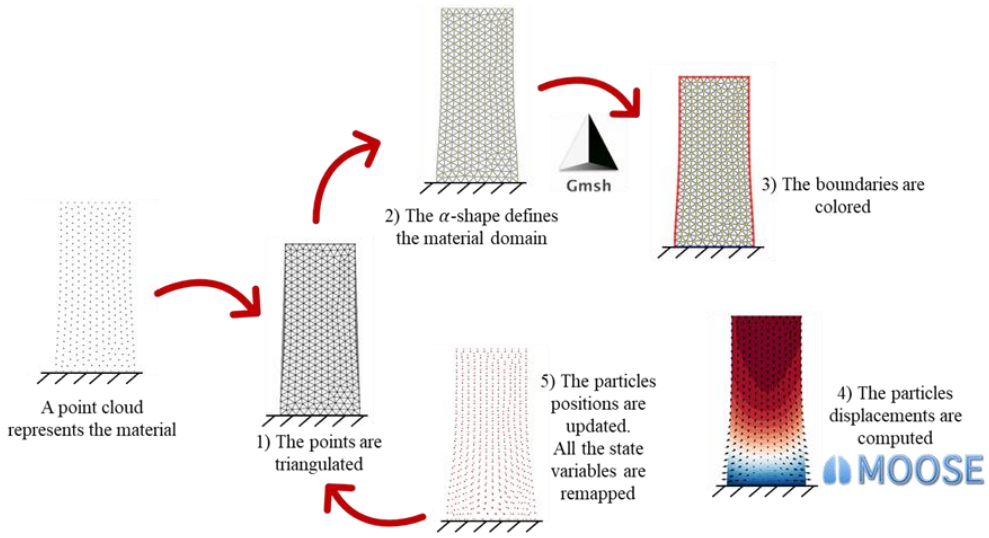

Figure 1: *Typical PFEM workflow.*

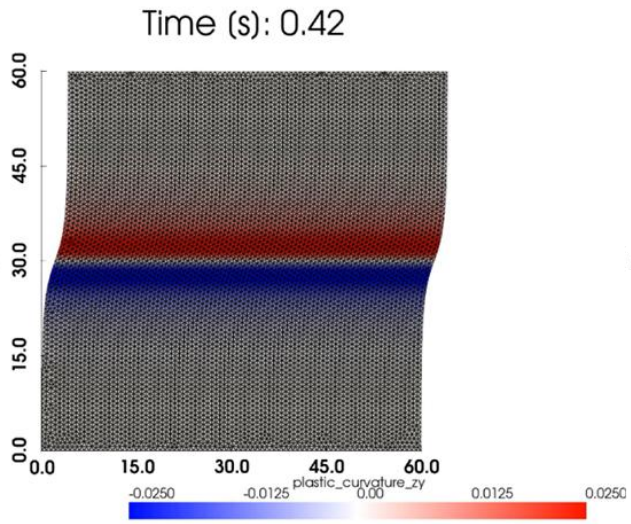

Figure 2*: Shear band localization arising at constant shear velocity.*

ReFrozen - Element tests at GUT RWTH Aachen

Nico Molls

Institute for Geomechanics and Underground Technology (GUT), RWTH Aachen, Germany

molls@gut.rwth-aachen.de

Keywords: frozen soils, sand clay mixtures, uniaxial compression test, triaxial compression tests

Abstract

This study investigates the thermo-hydro-mechanical (THM) behaviour of frozen soils through a comprehensive experimental and numerical approach. The experimental campaign focuses on element-scale testing conducted within the FrostLabor at RWTH Aachen (GUT lab), designed to capture the complex freezing and thawing behaviour of clayey sand mixtures under various boundary and loading conditions. The FrostLabor allows the sample preparation, freezing and testing all under constant freezing temperatures, therefore, avoiding spurious artifacts that arise from subjecting samples to different temperatures, even if for a short time.

The soils tested in the experimental program are reference sand-clay mixtures with controlled gradation and up to 20% kaolin content. These materials reflect natural soils found in alpine and high-latitude environments. The mechanical behaviour of the frozen soils was characterized through one-dimensional compression and triaxial compression tests, all performed at sub-zero temperatures ranging from –20 °C to –5 °C. The compression tests were conducted at different strain rates from 0.1 %/min to 10 %/min to capture the rate-dependent behaviour and highlight the role of ice-particle bonding in strength development and degradation. These tests revealed significant time- and temperature-dependent deformation mechanisms, particularly under slow loading rates and close to thawing conditions, which are of particular relevance to the prediction of climate-induced instabilities in permafrost soils (Fig. 1).

Complementary triaxial compression tests are performed on specimens at –20 °C, –10 °C and –5 °C evaluate shear strength parameters and the development of failure planes under different confining stresses. These tests allow the determination of the effective friction angle and cohesion of the frozen soils under undrained conditions (Fig. 2).

This work is part of a multi-national research initiative involving Ecole de Ponts et Chausses in Paris, France, and GUT, Aachen, Germany, and is financed by the French ANR and German DFG research funding agencies.

The project is called REFROZEN and all of the tests will be in the near future, available in a freely available database where researchers can sort, extract and plot the results using all of the variables used, such as temperature, clay content, loading rate, or results, like deformation or stress. The database includes pictures of all the samples – e.g., Fig. 3.

Figures

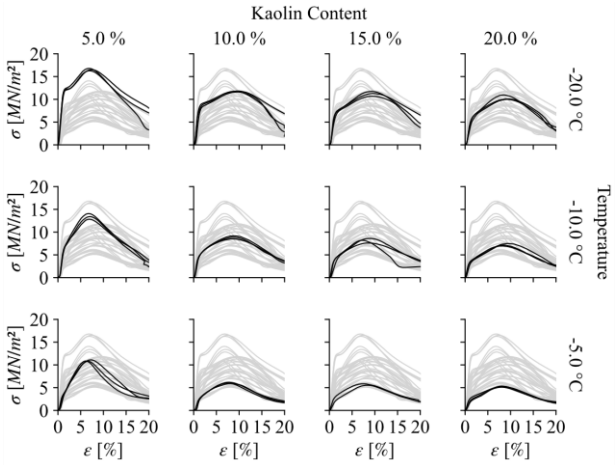

Figure 1: *Stress-Strain on unconfined compression tests at a strain rate of 1.0 %/min with different clay contents and temperatures.*

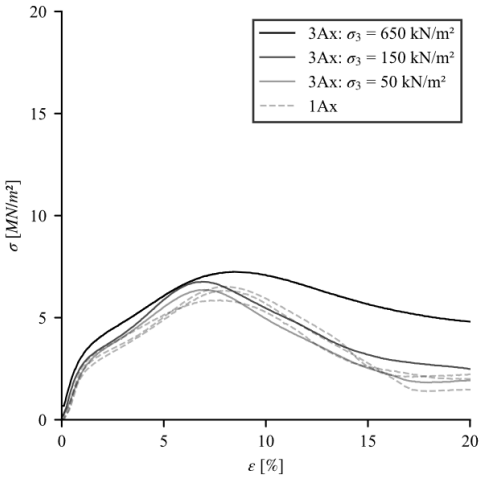

Figure 2: *Stress-Strain on triaxial compression tests at a strain rate of 0.1 %/min and 20 % clay with varying cell pressure compared to unconfined compression tests.*

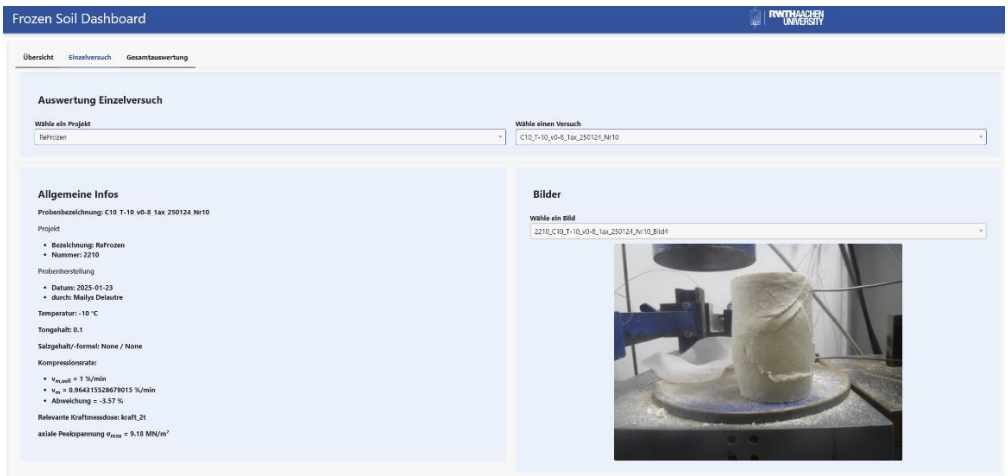

Figure 3: *Database example of unconfined tests at -10ºC, 10% clay content and 1%/min loading rate.*

The Elusive Concept of Soil Dilatancy

Merita Tafili[1], Mehdi Pouragha[2], Gertraud Medicus[3], Alexandros Petalas[4]

[1]Ruhr-Universität Bochum, Germany

[2]Carleton University, Canada

[3]University of Innsbruck, Austria

[4]Durham University, UK

Merita.Tafili@rub.de

Keywords: dilatancy, plastic strain, total strain, volume change

Abstract

Dilatancy is the tendency of soils to change volume during shear and it represents a defining feature that distinguishes (granular) soils from other materials. Despite its central role in constitutive modeling and soil mechanics at large, its precise definition remains a subject of ongoing debate. In this interactive poster, we revisit the various definitions and interpretations of dilatancy, critically examining their theoretical foundations, practical implications, and limitations. Visitors are invited to engage with the material and contribute their own perspectives to this still-unsettled question.

A central focus of the discussion lies in the choice of strain measure used to define dilatancy: total versus plastic strain rate. While total strain is directly measurable in laboratory experiments, definitions based on it are inherently dependent on boundary and loading conditions — for example, dilatancy in an undrained test would be zero. In contrast, plastic strain-based definitions, e.g. Pradhan et al. (1989), offer the appealing feature of being independent of external loading, making them more suitable as internal state variables in constitutive models. However, plastic strain components are notoriously difficult to measure — even in advanced numerical simulations such as the Discrete Element Method (DEM) — posing serious practical challenges for calibration and validation.

This poster further explores various theoretical origins and interpretations of dilatancy, particularly for granular soils, and critically assesses the extent to which dilatancy can be considered a meaningful and measurable state variable. The influence of key factors — such as relative density, confining pressure, and stress path — is illustrated to highlight the implications of dilatancy on key phenomena like shear strength, strain localization, and cyclic mobility.

To foster meaningful discussion and exchange, the poster includes interactive elements that allow attendees to contribute their own questions, comments, and insights (see for e.g. Figure 1). These inputs will help capture the diversity of views within the geotechnical community and promote dialogue across research areas, including constitutive modeling, experimental soil mechanics, and practical geotechnical engineering.

References

Pradhan, Tej BS, Fumio Tatsuoka, and Yasuhiko Sato. "Experimental stress-dilatancy relations of sand subjected to cyclic loading." Soils and Foundations 29.1 (1989): 45-64.

Figures

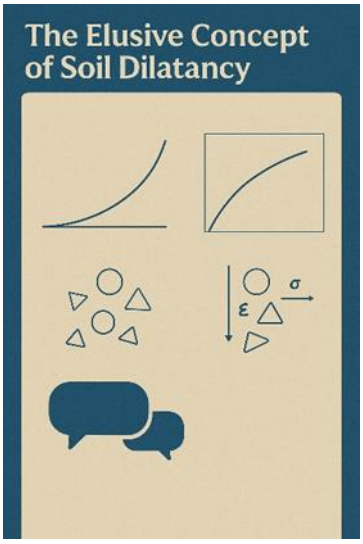

Figure 1: *Representation of the interactive nature of the poster*.

Towards sustainable decommissioning of offshore monopiles: a 1g experimental investigation

Pauline André[1 3], Luc Simonin[1], Stijn François[2], George Anoyatis[3], Hadrien Rattez[1]

[1]Department of Civil Engineering, Institute of Mechanics, Materials, and Civil Engineering (iMMC), UCLouvain, Louvain-la-Neuve, Belgium

[2]Department of Civil Engineering, Structural Mechanics Section, KU Leuven, Leuven, Belgium

[3]Department of Civil Engineering, KU Leuven, Bruges, Belgium

p.andre@uclouvain.be

Keywords: offshore geotechnics, offshore wind turbine foundations, decommissioning of monopiles, monopile vibratory extraction, 1g lab tests

Abstract

As the first offshore wind farms reach the end of their 25-year design life, the decommissioning of monopile foundations has become a pressing challenge (Shafiee et al., 2016). Current industry practice is to cut monopiles at seabed level, leaving thousands of tons of steel buried . This approach has major drawbacks: a substantial amount of buried steel (tens of thousands of tons per wind farms) remains in place, it complicates the future installation of larger piles at the same strategic locations and it is a risky operation due to the confined space, the water depth and the blindness of the process (Hinzmann et al., 2018). Full removal of monopiles offers a more sustainable alternative, yet it remains technically demanding in offshore environments. Vibratory extraction, using hammers like those employed for installation, is a promising method to reduce the required uplift force while minimizing noise and environmental disturbance(Jiang, 2021).

This study presents 1g scaled laboratory experiments investigating vibration-assisted extraction of monopiles in dry North Sea sand. A miniature vibro-hammer, illustrated in Figure 1, with counter-rotating eccentric masses was developed to apply vertical vibrations to a scaled monopile (6 cm diameter, 1.35 m length). A motor applied a constant pulling velocity, while extraction force was continuously measured. A scaling factor of 70 was used to represent early generation monopiles. A 1.1m diameter cylindrical container along with a pluviation system and vibrating needles were used to generate 80 cm deep North Sea sand sample with a relative density D_R=37 ±3%. The repeatability of the preparation technique was validated by cone penetration tests and further confirmed by analogous number of hammer blows (100 ±10, with a 1.2 kg ram dropping 30 cm) across impact installations of the pile to an embedment ratio of three diameters.

Results, presented in Figure 2, show that vibrations can reduce net extraction forces by up to 70 %. Without vibration, the maximum pull-out load was 85 N, whereas high-frequency vibrations (442–525 Hz) lowered it to about 45 N for a pile weighing 30 N. Two regimes were observed: modest reduction at lower frequencies (350–400 Hz) and substantial reduction at higher ones. An additional test revealed that interrupting vibration before full extraction increased resistance, likely due to a densification of the sand. These results are aligned with the ones of (Davidson et al., 2017) and complement them.

These findings demonstrate the potential of vibratory extraction for offshore monopile decommissioning. Further research will investigate the role of frequency, eccentric moment, and vibration duration, as well as tests in denser and saturated conditions to improve offshore representativeness.

References

Davidson, C., Brown, M., Brennan, A., & Knappett, J. (2017). Decommissioning of Offshore Piles Using Vibration.

Hinzmann, N., Stein, P., & Gattermann, J. (2018). Decommissioning of Offshore Monopiles, Occuring Problems and Alternative Solutions. Volume 9: Offshore Geotechnics; Honoring Symposium for Professor Bernard Molin on Marine and Offshore Hydrodynamics, V009T10A020. https://doi.org/10.1115/OMAE2018-78577

Jiang, Z. (2021). Installation of offshore wind turbines : A technical review. Renewable and Sustainable Energy Reviews, 139, 110576. https://doi.org/10.1016/j.rser.2020.110576

Shafiee, M., Brennan, F., & Espinosa, I. A. (2016). A parametric whole life cost model for offshore wind farms. The International Journal of Life Cycle Assessment, 21(7), 961-975. https://doi.org/10.1007/s11367-016-1075-z

Figures

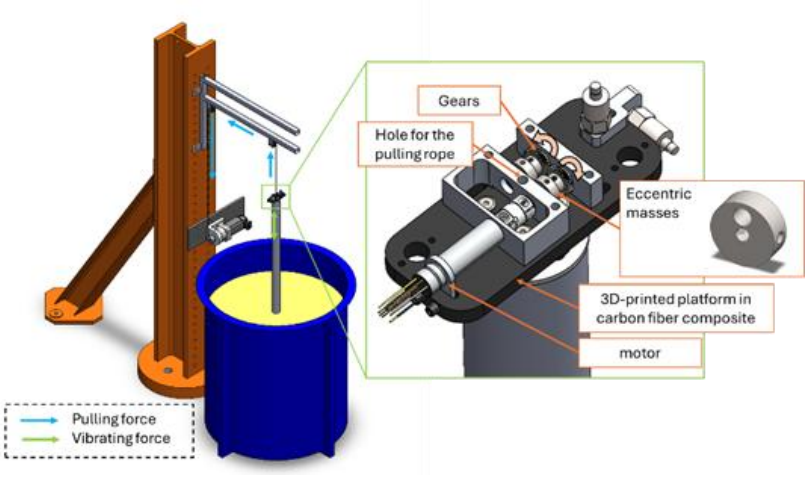

Figure 1: *Schematic of the mini vibro-extractor.*

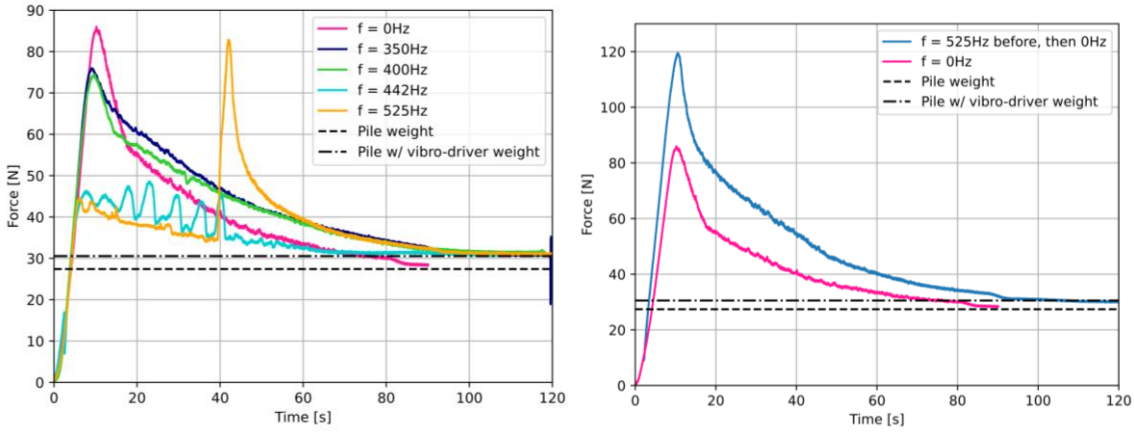

Figure 2: *(Left) Comparison of the extraction force at different frequencies. (Right) Comparison between simple extraction and vibration for 45 seconds then extraction.*

Multiphysics modeling of thermal cracks in multiphase porous materials

Zechao Chen[1], Laura De Lorenzis[2], Lorenzo Sanavia[3]

[1]Center of Studies and Activities for Space (CISAS) - "G. Colombo", University of Padova, Italy

[2]Department of Mechanical and Process Engineering, ETH Zurich, Switzerland

[3]Department of Civil, Environmental and Architectural Engineering, University of Padova, Italy

zechao.chen@phd.unipd.it, ldelorenzis@ethz.ch, lorenzo.sanavia@unipd.it

Keywords: Phase-field brittle fracture, Thermo-hydro-mechanical coupled problems, Finite element method, variably saturated porous media

Abstract

A thermo-hydro-mechanical crack phase-field model is developed to investigate initiation and propagation of fissures in multiphase porous media under thermal loading (e.g. Figure 1). While the coupled u-p_w-d framework in [1] addressed water flow, deformation, and fracture in variably saturated media, subsequent studies have highlighted the significant influence of gaseous phases, especially under temperature variations [2]. Based on the poromechanics theory developed in [3–4], the present work introduces a computational framework that integrates heat, water, and gas transport with fracture processes, providing a robust tool for simulating coupled thermo-hydro-mechanical cracking in variably saturated porous systems.

To validate the proposed model, several benchmark cases were carried out. First, the implemented framework was compared with the results of the Griphfith finite element code [5] in terms of phase-field solution and force–displacement response of a tensile solid mechanical test, showing a very good agreement (Figure 2). Then, validation for the thermo-mechanical implementation of the model was performed using a classical benchmark case [6–7], demonstrating consistent agreement between the numerical solution and the analytical one, Figure 3. Finally, a hydro-mechanical fracture problem was solved, in which the simulated vertical stress and pore-water pressure distributions during tensile fracture along a vertical sand column were compared with the reference results in [1], Figure 4. These benchmark studies confirm the accuracy and applicability of the proposed framework. Moreover, a simple thermal expansion simulation was conducted to further illustrate the model's capability in capturing thermally induced crack initiation and propagation. Further validation tests in non-isothermal variably saturated soils are ongoing.

References

[1] Cajuhi, T., Sanavia, L., & De Lorenzis, L. (2017). Phase-field modeling of fracture in variably saturated porous media. Computational Mechanics, 61(3), 299-318.

[2] Sanavia, L., Pesavento F., Schrefler, B.A. 2006, Finite element analysis of non-isothermal multiphase geomaterials with application to strain localisation simulation, Computational Mechanics, 37(4), 331-348[3].

[3] Lewis, R. W., Schrefler, B. A. 1998. The Finite Element Method in the Static and Dynamic Deformation and Consolidation of Porous Media (Second). Chichester, UK: John Wiley & Sons.

[4] William G. Gray, Cass T. Miller 2014. Introduction to the Thermodynamically Constrained Averaging Theory for Porous Medium Systems. Springer.

[5] Griphfith Code. Available at: https://gitlab.ethz.ch/compmech/GRIPHFiTH

[6] Mandal, T. K., Nguyen, V. P., Wu, J.-Y., Nguyen-Thanh, C., & de Vaucorbeil, A. (2021). Fracture of thermo-elastic solids: Phase-field modeling and new results with an efficient monolithic solver. Computer Methods in Applied Mechanics and Engineering, 376.
[7] Jiang, C. P., Wu, X. F., Li, J., Song, F., Shao, Y. F., Xu, X. H., & Yan, P. (2012). A study of the mechanism of formation and numerical simulations of crack patterns in ceramics subjected to thermal shock. Acta Materialia, 60(11), 4540-4550.

Figures

Figure 1: *Desiccation cracks in clayey soils.*

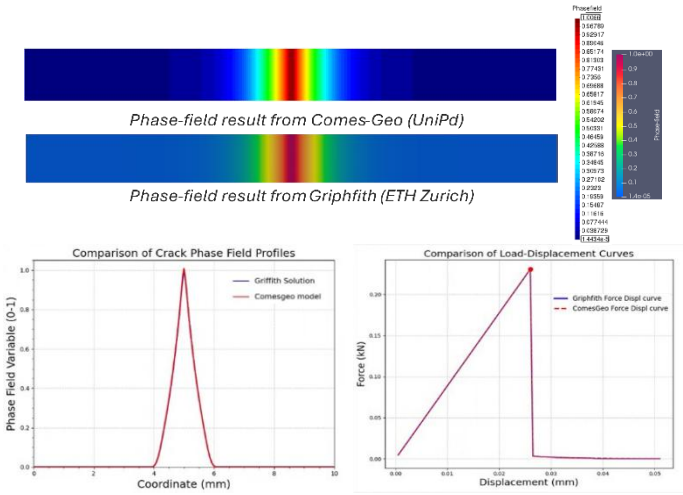

Figure 2: *Comparison of tensile fracture response with Griphfith code*

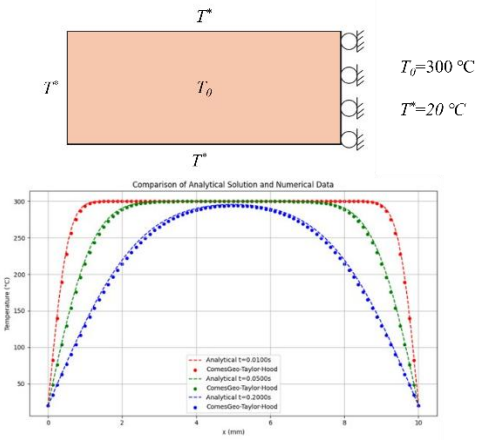

Figure 3: *Validation of the thermo-mechanical model*

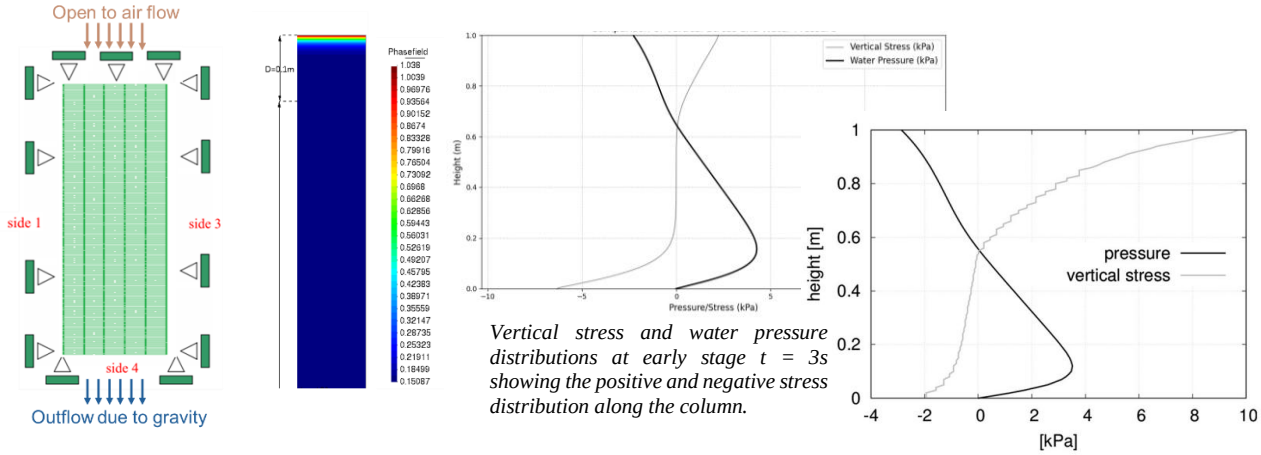

Vertical stress and water pressure distributions at early stage t = 3s showing the positive and negative stress distribution along the column.

Figure 4: *Induced seismicity minimization in an underground reservoir for energy production and storage.*

Particle shape effects on the texture and force transmission in randomly packed granular samples

Auwal Alhassan Musa, Farhang Radjai, Saeid Nezamabadi

Mechanics and Civil Engineering Laboratory (LMGC), CNRS, University of Montpellier

alhassan-musa.auwal@umontpellier.fr

Keywords: Particle shape, Isotropic compaction, Force transmission, Packing fraction, Coordination number, entanglement

Abstract

The relationship between the shapes of individual grains and the microstructural properties and mechanical behavior of granular materials is essential for many applications [1]. The microstructural parameters include local arrangement, connectivity, entanglements, and force transmission. These features control the mechanical strength and flow behaviour of granular materials [2]. In this work, particle dynamics simulation was employed to construct assemblies of nonconvex particles using the code Rockable, which implements the classical Discrete Element Method (DEM) [3]. The particles have a hexapod shape (composed of three mutually perpendicular cylindrical lobes) of varying aspect ratio α, defined as the ratio of the length of each lobe to its diameter, ranging from 1 to 15. Each sample is composed of 10648 mono-sized hexapods. The samples were subjected to isotropic compaction with zero friction between particles by applying a small isotropic pressure under periodic boundary conditions (PBCs) to avoid inherent wall boundary effects. The compaction process is stopped when the kinetic energy vanishes and a stable value of packing fraction is reached.

We observe a nonmonotonic evolution of the packing fraction with increasing aspect ratio, whereas the degree of interlocking shows a stable, monotonic increase with increasing aspect ratio. We also examine how the local coordination numbers (Number of contact neighbors per particle) and Z_c (Number of contacts per particle), both of which evolve to isostatic values. For ($\eta < 0.67$), Z remains nearly constant at a plateau of approximately 7, with the exception of the spherical particles case ($\eta = 0$), where both Z_c and Z stabilize at 6. Beyond this regime, Z increases with η, which can be attributed to the ability of elongated hexapods to establish contacts with their second-nearest neighbors. We see that, for all other hexapods, Z_c approaches a limiting value close to 12, consistent with the condition of perfectly rigid particles.

As the aspect ratio increases, the probability density function (PDF) of normal forces becomes broader: stronger forces appear, whereas the number of forces below the mean force increases. In all cases, the force PDF has a clear decreasing exponential shape in the range of strong forces. The PDFs can be accurately described by an analytical expression with a single free parameter, as shown in the inset of Figure 4.

These samples serve as initial states for shear simulations with friction to investigate the influence of particle shape on the stress-strain behaviour. Our preliminary results indicate that the shear strength increases with aspect ratio. These results will be presented in future work.

References

[1] Trieu-Duy Tran, Saeid Nezamabadi, Jean-Philippe Bayle, Lhassan Amarsid, Farhang Radjai, Effect of interlocking on the compressive strength of agglomerates composed of cohesive nonconvex particles, Advanced Powder Technology 36, (2) 2025, 104780, https://doi.org/10.1016/j.apt.2025.104780

[2] Trieu-Duy Tran, Saeid Nezamabadi, Jean-Philippe Bayle, Lhassan Amarsid, Farhang Radjai, Contact networks and force transmission in aggregates of hexapod-shaped particles Soft Matter, 20, 3411-3424, 2024, https://doi.org/10.1039/D3SM01762A

[3] Vincent Richefeu, Gaël Combe, Pascal Villard, Jean-Yves Delenne, Lhassan Amarsid, et al.. Rockable. 2025 ⟨hal-04933604⟩

Figures

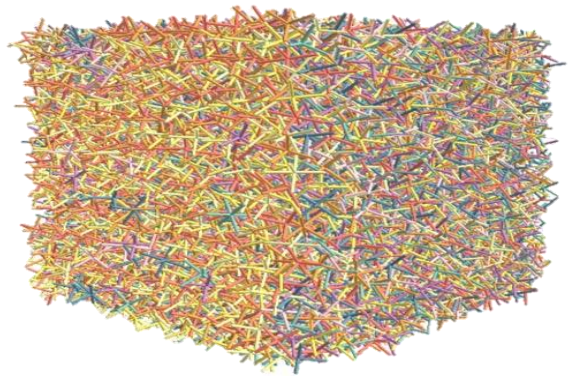

***Figure 1**: Isostatically compacted sample composed of mono-sized hexapods* ($\alpha = 13$)

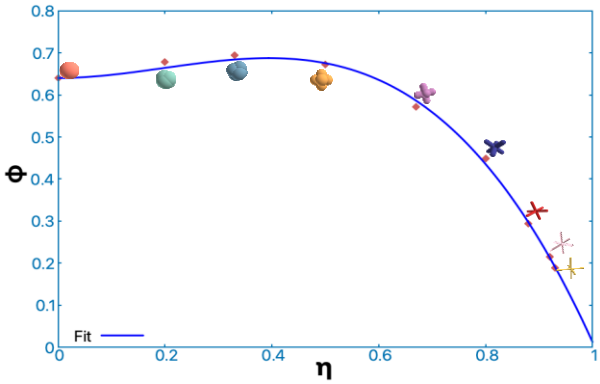

***Figure 2**: Evolution of packing fraction ϕ of all samples as a function of nonconvexity parameter.*

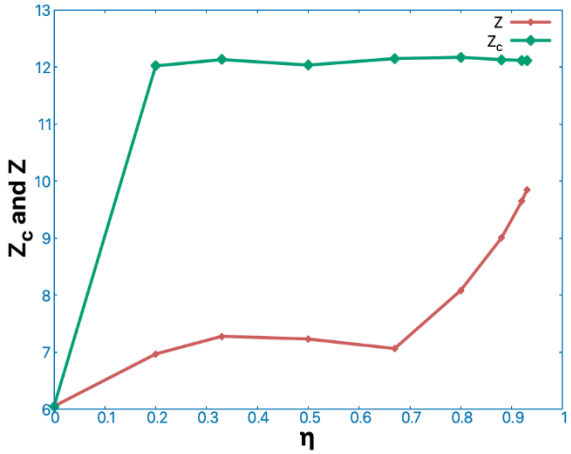

***Figure 3:** Local coordination numbers Z_c (number of contacts per particle) and Z (number of contact neighbors per particle).*

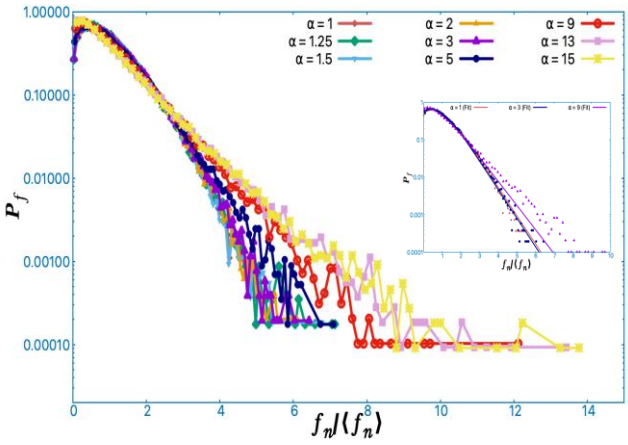

***Figure 4:** Probability density function of normal forces for different values of the aspect ratio α.*

Biomechanical properties and root associated microbiota in willows through indoor pot experiments for effective sand dune stabilization

Otim, G.I., Zhelezova, A., Sorrentino, G., Trapp, S., Rocchi, I.

DTU Sustain, Department of Environmental and Resource Engineering, Denmark

geot@dtu.dk

Keywords: Biomechanical properties, willows, rooted soil, microbiota, sequencing

Abstract

Vegetation is essential in implementing nature-based solutions, actively contributing to sustainability efforts aimed at mitigating natural hazards such as landslides and erosion (Fraccica et al., 2025). By doing so, it not only supports the ecological and hydrological health of watersheds but also contributes to the overall resilience of our natural environments. Vegetation growth is supported by symbiosis between the plant roots and microbial communities such that plants provide microbes with root exudates, and microbes provide essential nutrients (Lepinay et al., 2024; Xie et al., 2024; Zhelezova et al., 2024) of which Willows come with their own microbial communities. This study aimed to assess the contributions of biomechanical properties and root associated microbiota in the effectiveness of sand dune stabilization. Indoor pot experiments were used to cultivate willow (*Sallix sp.*) stakes 18 cm long and 10 - 14 mm diameter into customized PVC pots of diameter 100 mm and 200 mm height for the tensile strength, vertical pullout resistance and direct shear strength test respectively with each set of tests having four replicates. The willows were grown on sterile loose sand of median size 0.3 mm in light-controlled conditions, amended with fertilizers biweekly and with daily watering for 150 days. At the end of this age, the shoot was trimmed from the stake before performing each of the biomechanical tests. The direct shear test was performed using customized root soil shear apparatus (Sorrentino et al., 2025) with an effective shearing displacement of 27 mm at a strain rate of 1 mm / min along the pre-split PVC pipes. These laboratory measurements were complemented with the quantification of the root architectural features. At the end of each of the tests, the pots were disassembled for moisture content along the length of the pot for every 30 mm. Bacterial communities in root-affected sand and in aggregates were analyzed using qPCR and sequencing of 16S rRNA gene libraries. The mean shoot biomass and dry rooted density were 16.3 g and 1.96 kg/m^3 respectively. The average tensile strength, Young's modulus and vertical pullout resistance of the roots were 6.92 MPa, 112 MPa and 87.1 N respectively. The average direct shear strength was performed at four varying moisture contents of 4.9 %, 9.6 %, 17.5 % and 23.5% along the shearing plane and the shear strength generally decreased with an increase in moisture content while the controls had low strength compared to the rooted soils. The moisture content in all pots for the biomechanical tests generally decreased with an increase in depth of the pots. In addition, soil aggregates were unexpectedly observed within the pots, and these had a mean size ranging from 1.31 - 2.15 mm. Root penetration is achieved by roots releasing a complex mixture of organic compounds into the soil especially around its root tip and this supports microbial communities within the rhizosphere and in the soil farther from root (Otim et al., 2025). At day 150, bacteria were on average 2.15×10^8 gene copy numbers/g of soil, and on average 7.47×10^8 gene copy numbers/g of soil in aggregates. The predominant top three bacterial phyla in root-affected sand were Proteobacteria (44.8 %), Actinobacteriota (11.9%), Firmicutes-D (9.6 %). In

aggregates, the abundance of classes Proteobacteria and Bacteroidia increased, while Actinomycetia was less abundant, and class Bacilli represented less than 1%. This shows that the classes enriched in aggregates were involved more closely in processing of root-derived organic matter (not only exudates). While the classes that were more abundant in sand and not presented in aggregates are maybe less associated with plant-derived organic matter. This study highlighted the biomechanical properties in rooted sand substrates and their associated microbiota over a 150-day period, demonstrating the mutual benefits and resilience they provide to the ecosystem.

References

Fraccica, A., Romero, E., & Fourcaud, T. (2025). Effects of vegetation growth on soil microstructure and hydro-mechanical behaviour. Geotechnique, 75(3), 293–307. https://doi.org/10.1680/jgeot.23.00163

Lepinay, C., Větrovský, T., Chytrý, M., Dřevojan, P., Fajmon, K., Cajthaml, T., Kohout, P., & Baldrian, P. (2024). Effect of plant communities on bacterial and fungal communities in a Central European grassland. Environmental Microbiome, 19(42). https://doi.org/10.1186/s40793-024-00583-4

Otim, G. I., Zhelezova, A., Sorrentino, G., Trapp, S., & Rocchi, I. (2025). Hydraulic properties of rooted soils from Salix sp . pot experiments. E3S Web of Conferences (EUNSAT2025 + BGE), 06009. https://doi.org/10.1051/e3sconf/202564206009

Sorrentino, G., Otim, G. I., Zhelezova, A., & Rocchi, I. (2025). Rooted Soil Shear Apparatus: A low cost, direct shear apparatus for measuring the influence of plant roots on soil shear strength. SSRN. https://doi.org/10.2139/ssrn.5238170

Xie, H., Chai, Y., Liu, Z., Hao, W., & Gai, J. (2024). Community assembly of endophytic bacteria and fungi differs in soil-root continuum of Carex cepillacea. Applied Soil Ecology, 194, 105206. https://doi.org/10.1016/j.apsoil.2023.105206

Zhelezova, A., Sorrentino, G., Otim, G. I., & Rocchi, I. (2024). Soil is alive – how does soil biota influence soil mechanical properties? A perspective review. Biogeotechnics, BGTECH1001. https://doi.org/10.1016/j.bgtech.2025.100175

Figures

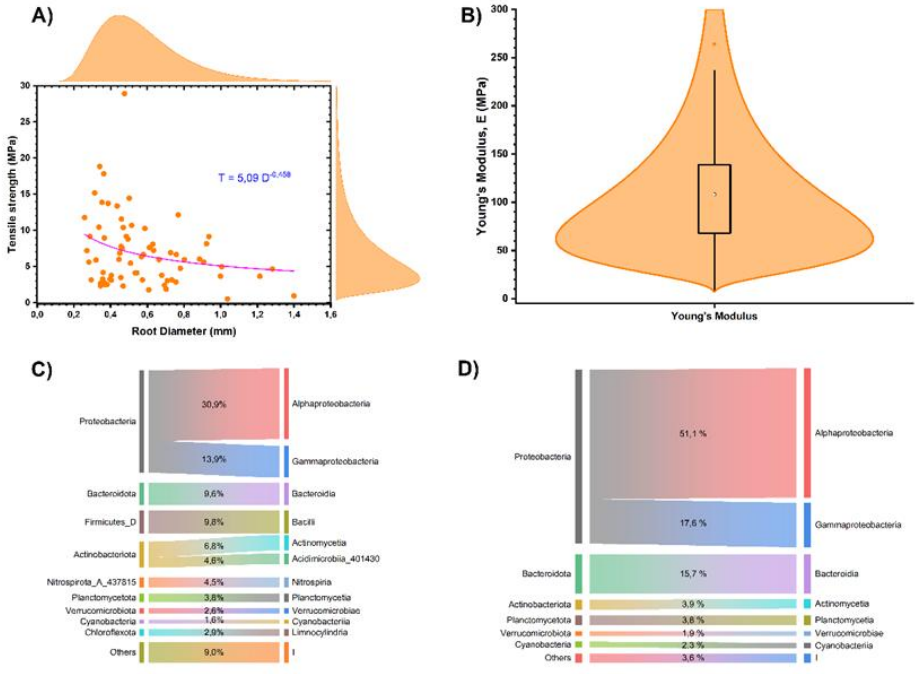

Figure 1: *A) Tensile properties, B) Young's modulus, (C) Microbial communities in rhizosphere and aggregates (D).*

DEM simulations of crack initiation and propagation in plant cell tissues

Frank Tsemo[1], Yohann Trivino[2], Jean-Yves Delenne[2], Antonio Pol[2], Vincent Richefeu[3], Farhang Radjaï[1]

[1]LMGC, Univ. Montpellier, CNRS, 34090 Montpellier, France

[2]IATE, Univ. Montpellier, INRAE, Institut Agro, Montpellier, France

[3]3SR, CNRS, University of Grenoble Alpes, Grenoble, France

frank-ulrich.tsemo-tayou@umontpellier.fr

Keywords: DEM, plant tissue, crack propagation, tensile test, mechanical parameters

Abstract

The fragmentation of plants to produce food, medicines, materials, or energy is a major challenge for the industrial sector. Fragmentation processes enable the separation of different compounds of interest through failure mechanisms [1]. In this study, relying on a DEM soft particle dynamics approach based on shape degrees of freedom [2], we focus on crack propagation in 2D plant tissues. In this approach, each cell is modeled as an articulated sphero-polyhedron, whose mechanical properties are defined by internal stiffness, the stiffness and length of the bars representing polyhedral edges, bending rigidity, and envelope stiffness (Fig. 1). The polyhedral vertices are treated as nodes with uniform mass, enabling an accurate description of the dynamic response of the cell. Four numerical tests were conducted: (i) compaction of a highly discretized circular particle (Fig. 2a), (ii) tensile loading of a hexagonal cell (Fig. 2b), (iii) tensile loading of two hexagonal cells connected by a cohesive interface (Fig. 2c), and (iv) tensile loading of a group of connected cells forming a tissue (Fig. 2d). The aim of these tests is to assess the impact of discretization, to clarify the role of mechanical parameters in crack initiation and propagation, and to identify parameter sets that reproduce consistent fracture behavior as the number of cells increases. These results constitute an initial step toward modeling plant tissue failure at the cellular scale and will provide a foundation for more detailed investigations into the effects of structural heterogeneities in plant tissues on failure and fragmentation.

Acknowledgment

The authors acknowledge the ANR – FRANCE (French National Research Agency) for its financial support of the PlantCom project n°ANR-23-CE51-0053.

References

[1] Mayer-Laigle, Claire, Nicolas Blanc, Rova Karine Rajaonarivony, and Xavier Rouau. "Comminution of dry lignocellulosic biomass, a review: Part I. from fundamental mechanisms to milling behaviour." *Bioengineering* 5, no. 2 (2018): 41.

[2] Yohann Trivino, Vincent Richefeu, Farhang Radjai, Komlanvi Lampoh, Jean-Yves Delenne, A soft particle dynamics method based on shape degrees of freedom for core-shell particles, submitted to Computer Physics Communications.

Figures

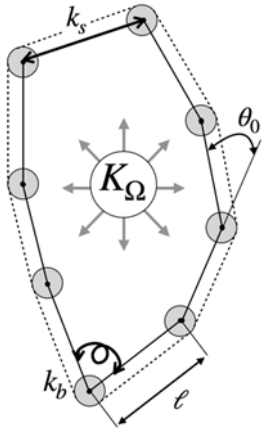

Figure 1: *Representation of a deformable cell composed of eight interconnected nodes, with the possibility of internal turgor pressure (controlled by the volumetric stiffness K_Ω).*

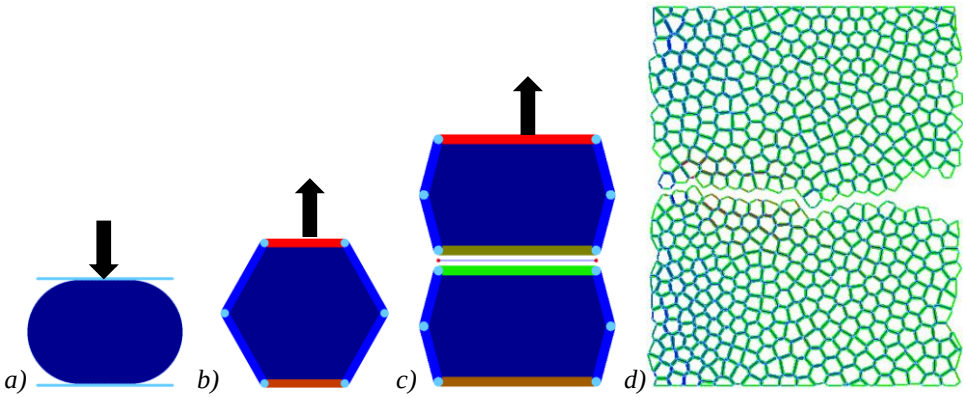

Figure 2: *Four test cases: a) compressed disk-shaped particle; b) tensile test on a hexagonal particle; c) tensile rupture of an adhesive interface; d) fracture of a pre-notched cell tissue.*

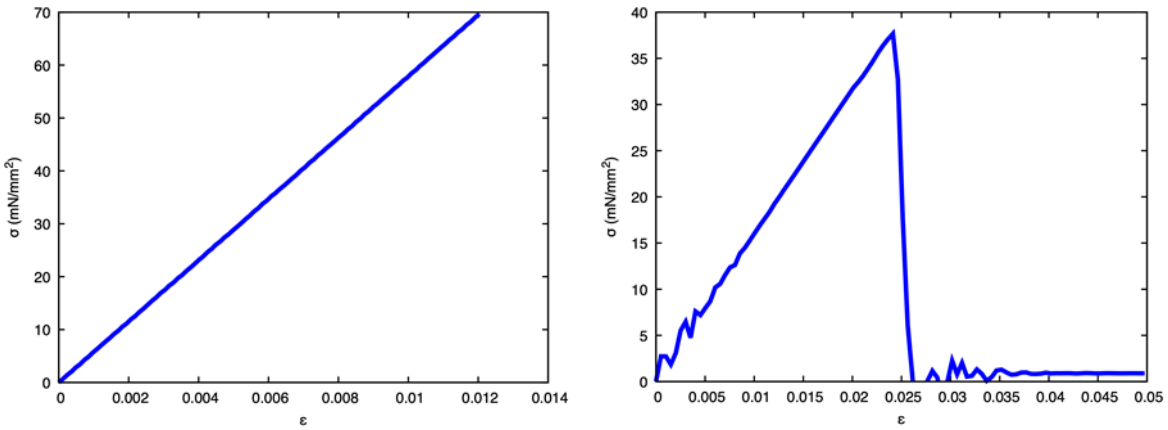

Figure 3: *a) Stress (force/initial diameter of the particle)-strain curve for Test 2 (Fig. 2b). b) Stress–strain curve for Test 4 up to failure (Fig. 2d).*

Multiphysics modelling of a catastrophic landslide prototype

Maria Lazari, Lorenzo Sanavia

Department of Civil, Environmental and Architectural Engineering, University of Padova, Padova, Italy

maria.lazari@unipd.it, lorenzo.sanavia@unipd.it

Keywords: Multiphase porous media, Finite element modelling, Temperature effects, Dynamics

Abstract

Catastrophic landslides are characterised by high velocity of the sliding mass with detrimental effects to the natural and built environment. The activated landmass induces significant vertical pressure in the sliding zone which triggers friction mechanisms between the sliding materials. The friction generates substantial heat, which can lead to various thermal effects on the response of the materials such as vaporization and thermal pressurization of the liquid water, that may contribute to the high acceleration and velocity of the landslide.

In this work a prototype of a catastrophic landslide has been developed as inspired by the works in [1-2] and has been analysed using the finite element code for non-isothermal multiphase geomaterials in dynamics Comes-Geo [3-4], enhanced with Taylor-Hood finite elements [5]. The geometry is shown in Fig. 1a and a constant acceleration of 1.0 m/s^2 is applied at the nodes of the top rigid block to trigger the failure. The model reaches a displacement of 60.5 m at the top at the end of the analysis as shown in Fig. 1b.

The numerical results show that the development of the plastic strain (Fig. 3) causes the temperature increase inside the frictional shear zone. This temperature occurs higher than the boiling temperature of liquid water close to the maximum displacement, with consequent formation of a water vapour cushion, desaturation (Fig. 4) and loss of shear strength in the shear band. This work highlights the possible importance of thermal effects in the evolution of rapid catastrophic landslides.

Acknowledgments

The authors wish to thank the Fondazione Cassa di Risparmio di Padova e Rovigo - CentRo studi sugli ImpatTi dei CambiAmenti cLmatici CRITICAL for financially supporting this work.

References

[1] Vardoulakis, I. 2000. “Catastrophic landslides due to frictional heating of the failure plane.” Mechanics of Cohesive-frictional Materials, 5, 443-467.

[2] Cecinato, F., Zervos, A., and Veveakis, E. 2011. “A thermo-mechanical model for the catastrophic collapse of large landslides.” International Journal for Numerical and Analytical Methods in Geomechanics, 35, 1507-1535.

[3] Lewis, R.W. and Schrefler, B.A. 1998. The Finite Element Method in the Static and Dynamic Deformation and Consolidation of Porous Media. John Wiley, New York.

[4] Cao, T. D., Sanavia, L., and Schrefler, B. A. 2016. “A thermo-hydro-mechanical model for multiphase geomaterials in dynamics with application to strain localization simulation.” International Journal of Numerical Methods in Engineering, 107: 312–337.

[5] Sanavia, L. and Cao, D.T. 2017. Modelling multiphase geomaterials at high temperatures in dynamics with application to strain localization and rapid catastrophic landslides. Poromechanics VI: Proceedings of the Sixth

Biot Conference on Poromechanics. July 9-13, 2017, Paris, (F). Edited by Matthieu Vandamme; Patrick Dangla; Jean-Michel Pereira and Siavash Ghabezloo. 1866-1875.

Figures

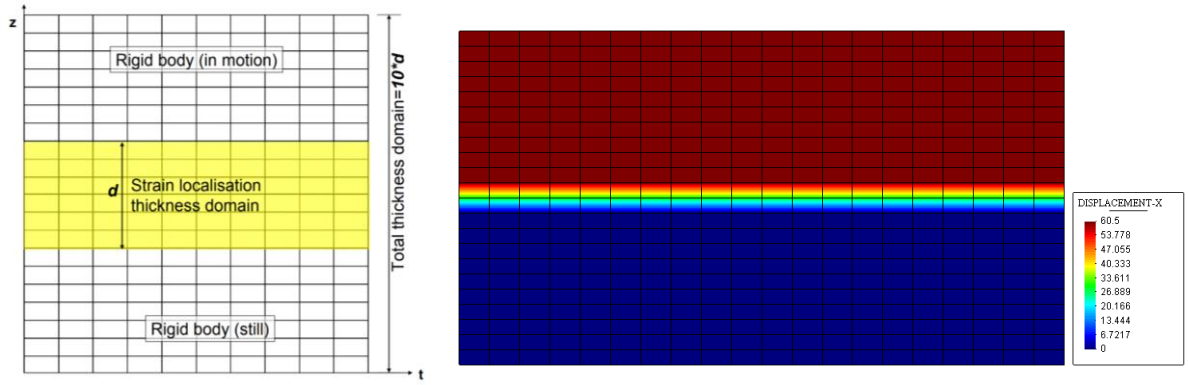

Figure 1: *(a) The shear band of thickness d embedded in a homogeneous soil of total thickness 10d, Cecinato et al. (2011) and (b) the horizontal displacement contour of the FEM simulation.*

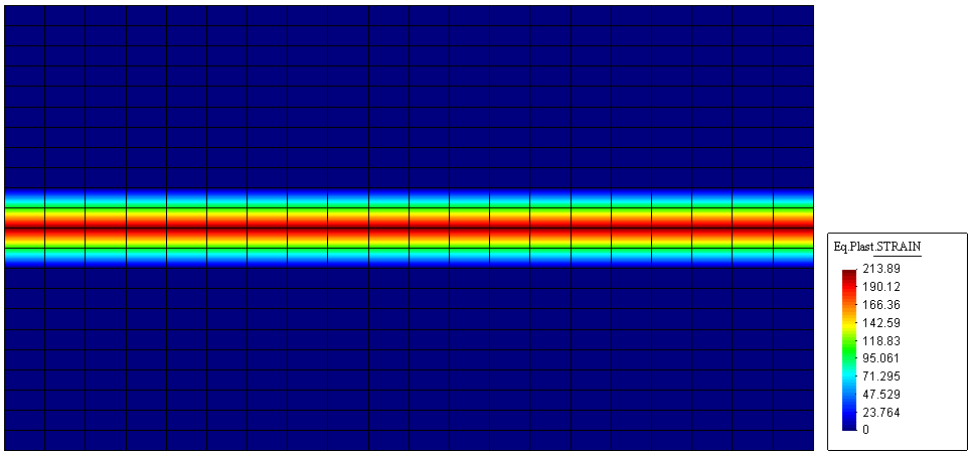

Figure 2: *Contour of equivalent plastic strain.*

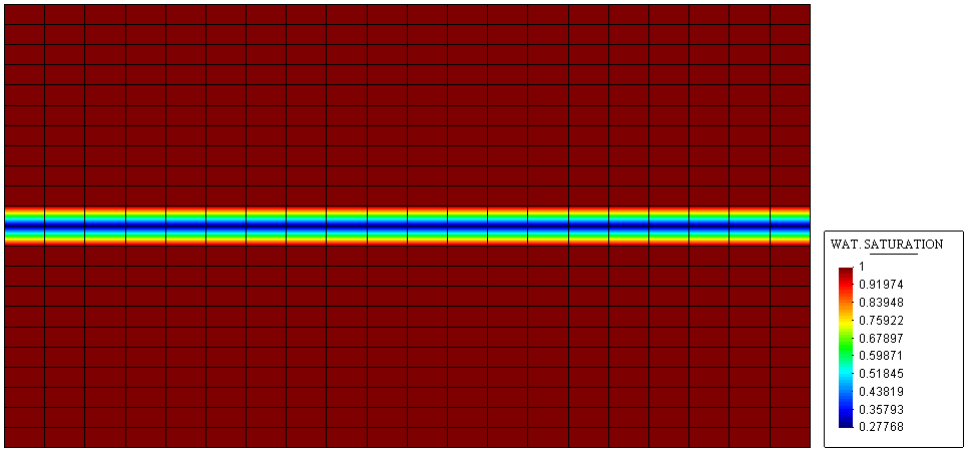

Figure 3: *Contour of water degree of saturation.*

On the automated calibration of the Hypoplastic Clay model: a machine learning approach

Phuong Chinh Do, Tomas Kadlicek

Charles University, Prague 140 00, Czech Republic

dophu@natur.cuni.cz

Keywords: Hypoplastic Clay, calibration, Machine Learning

Abstract

Advanced constitutive models such as the hypoplastic clay is a powerful tool for engineers to determine soils' responses for practical applications, but the model calibration is not an ease. Calibration of these such models can be addressed with several approaches, which are generally distinguished as stochastic or deterministic approaches. These approaches are to extract information from the experimental data, and then with optimisation process, the best combination will be chosen. These conventional approaches are integrated and combined to create the online automated calibration tools, for example, ExCalibre (Kadlíček et al., 2022a, 2022b). This paper presents a Machine Learning approach for automated calibration of the Hypoplastic Clay (Mašín, 2013) model's parameters that are: λ^*, κ^*, φ_c, ν and N. By using pairs of input experimental data and calibrated results performed by ExCalibre as training data, a Deep Neural Networks (DNNs) model is constructed to recognise how the experimental data can be used to derive asymptotic state parameters such as the slope and the interception of the Normal Compression Line (NCL), or the critical friction angle, and the optimised stiffness parameters. The training and testing data comprises of generated artificial data of compression (oedometer) and shear (undrained triaxial) test. The artificial data generation is created with the help of the cross-correlation between the Hypoplastic Clay model's parameters (Do et al., 2023), with deviation of +/-10% to prevent overfitting.

Three parameters which are well-correlated as shown in Figure 1, are λ^*, κ^* and N were selected. Then the NNs are constructed in the way that it received an oedometer test and three undrained triaxial tests as input, and then transfered the data and concatenated them to create an input layer, together with k neural layers and an output layer that has a length of number model parameters. Two scenarios were testing, in which the number of the output parameters are either single (scenario 1) or all five of the Hypoplastic Clay model's parameters (scenario 2). Finally, investigations on how the DNNs model recognise the asymptotic patterns, as well as its calibration results with scenario 2 will be presented, as shown in Figure 2. Figure 3 describes the much more accurate prediction and loss function with the output considering of only the friction angle.

References

Kadlíček, T., Janda, T., Šejnoha, M., Mašín, D., Najser, N., Beneš, Š.: Automated calibration of advanced soil constitutive models. Part I: Hypoplastic Sand. Acta Geotechnica 17, 3421–3438 (2022a)

Kadlíček, T., Janda, T., Šejnoha, M., Mašín, D., Najser, N., Beneš, Š.: Automated calibration of advanced soil constitutive models. Part II: Hypoplastic clay and modified Cam-Clay. Acta Geotechnica 17, 3439–3462 (2022b)

Mašín, D. Clay hypoplasticity with explicitly defined asymptotic states. Acta Geotech. 8, 481–496 (2013).

Do, P. C., Kadlíček, T., Mašín, D., & Najser, J. (2023). Correlation analysis of the hypoplastic clay parameters based on ExCalibre dataset database. Proceedings of the 10th European Conference on Numerical Methods in Geotechnical Engineering (NUMGE 2023)

Figures

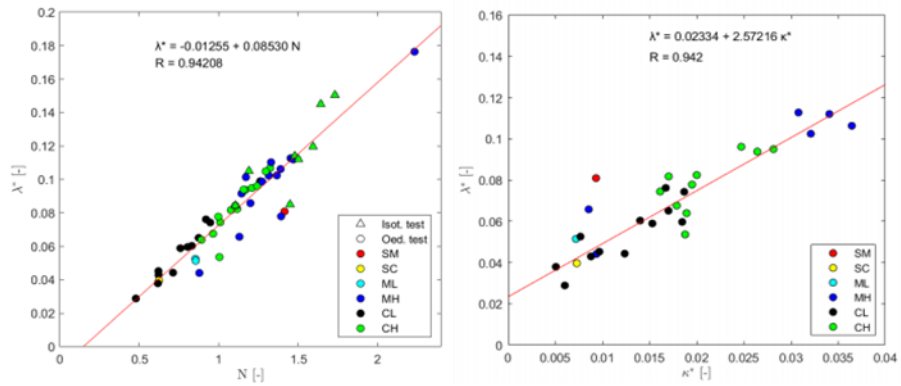

Figure 1: *Correlation of the Hypoplastic Clay parameters, reconstituted samples.*

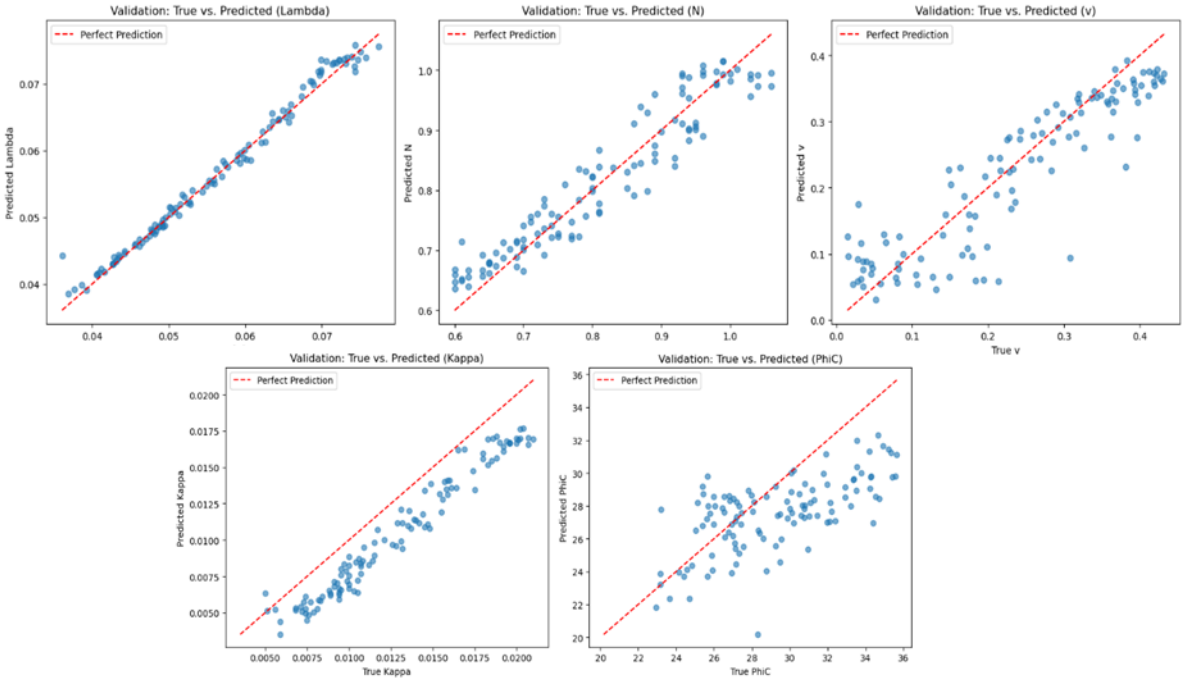

Figure 2: *Performance of the NNs with scenario 2.*

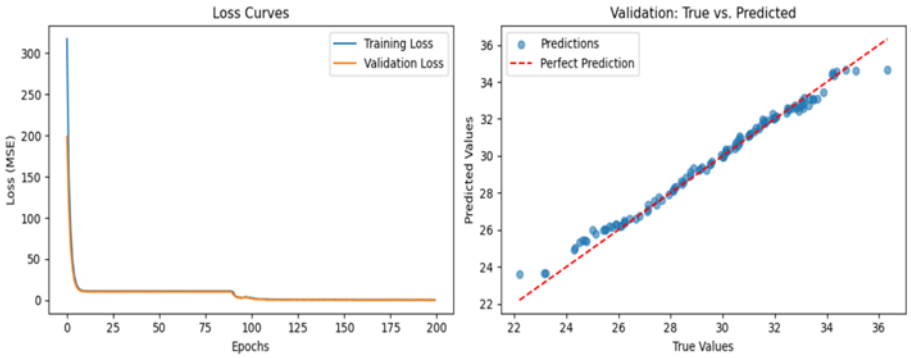

Figure 3: *Performance of the NNs with scenario 2.*

Friction in Complex Geometries with the Shifted Boundary Method

David Michael Riley*, Guglielmo Scovazzi+, Ioannis Stefanou*

**IMSIA (UMR 9219), CNRS, EDF, CEA, ENSTA Paris, Institut Polytechnique de Paris, Palaiseau, France*

+*Duke University, Raleigh, North Carolina, USA*

david.riley@ensta.fr, guglielmo.scovazzi@duke.edu, loannis.stefanou@ensta.fr

Keywords: Shifted Boundary Method; unfitted FEM; frictional interfaces; nonsmooth friction

Abstract

In geomechanics and rock mechanics often there are internal frictional interfaces, e.g., fractures and earthquake faults. These interfaces often have nontrivial geometries, making finite-element modelling challenging. To circumvent this, a range of unfitted finite-element methods, where the interface is embedded in a pre-existing background mesh, have been developed; however, many suffer from algorithmic complexity and ill-conditioning [1]. We use the shifted boundary method (SBM) [2], replacing the true crack with a mesh-conforming surrogate; boundary conditions are enforced on the surrogate and its values are corrected via Taylor expansions along the closest-point projection to the true interface as shown in Figure 1. By representing the interface on a surrogate and enforcing friction by variational inequalities [3], the approach preserves sharp slip/traction behaviour while reducing setup cost. Results indicate that this pairing accurately captures friction-dominated response and improves computational efficiency, enabling fast, reliable studies of cracks and faults where friction is the primary mechanism. Moreover, when paired with a nonsmooth Coulomb friction law, SBM enables accurate and computationally efficient simulations relevant to earthquake phenomena and opens the door to applications integrated with control theory [4].

References

[1] F. de Prenter *et al.*, "Stability and conditioning of immersed finite element methods: Analysis and remedies," *Archives of Computational Methods in Engineering*, vol. 30, no. 6, pp. 3617–3656, 2023.

[2] A. Main and G. Scovazzi, "The shifted boundary method for embedded domain computations. Part I: Poisson and Stokes problems," *Journal of Computational Physics*, vol. 372, pp. 972–995, 2018.

[3] V. Acary, M. Brémond, and O. Huber, "On solving contact problems with Coulomb friction: Formulations and numerical comparisons," in *Advanced Topics in Nonsmooth Dynamics: Transactions of the European Network for Nonsmooth Dynamics*. Cham: Springer International Publishing, 2018, pp. 375–457.

[4] D. Gutiérrez-Oribio, I. Stefanou, and F. Plestan, "Passivity-based control of underactuated mechanical systems with Coulomb friction: Application to earthquake prevention," *Automatica*, vol. 165, 2024, Art. no. 111661.

Figures

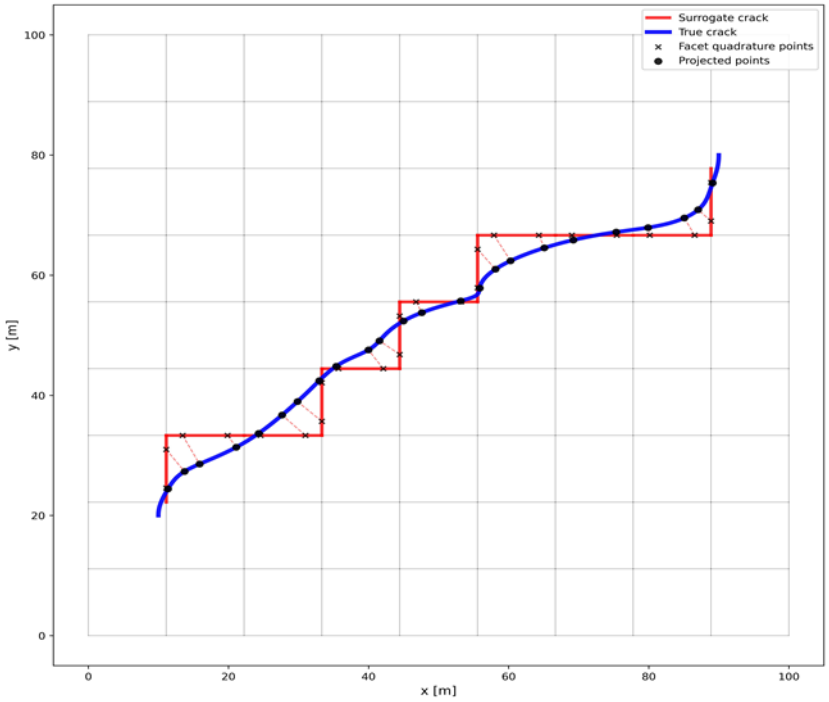

Figure 1: *True crack (blue) and mesh-aligned surrogate crack (red). Crosses are facet quadrature points on surrogate crack; dots are their closest-point projections onto the true crack; dashed lines show the projection vectors.*

ALERT Geomaterials

The Alliance of Laboratories in Europe for Education, Research and Technology